Investigating neuroregulation of sebaceous gland biology

A thesis submitted to the University of Manchester for the degree of Doctor of Philosophy in the Faculty of Biology, Medicine and Health

2019

Richard W. Clayton

School of Biological Sciences

Division of Musculoskeletal & Dermatological Sciences

Contents

List of figures 5
Frequently used abbreviations 8
Abstract 11
Declaration 12
Copyright statement 13
Acknowledgements 14
Chapter 1: Introduction 15
1.1 Sebaceous glands and the pilosebaceous unit 16
1.2 Sebum composition and function 19
1.3 Sebaceous gland development 21
1.4 Overview of the cell and molecular biology of sebaceous gland homeostasis 22
1.5 Acne and other sebaceous gland-associated dermatoses 28
1.6 The nervous system of the skin and pilosebaceous unit 31
1.7 Clinical indicators of sebaceous gland innervation 34
1.8 Aims and objectives 38
Chapter 2: Materials and methods 40
2.1 General animal handling 41
2.2 Waxing depilation 42
2.3 Surgical cutaneous denervation 43
2.4 Mouse genotyping 45
2.5 Genetically-inducible fate mapping (GIFM) 46
2.6 General tissue processing and microtomy 48
2.7 Immunostaining 48
2.8 Confocal fluorescent microscopy and image analysis 50
2.9 RNA in situ hybridisation 52
2.10 Electron microscopy 53
2.11 Statistics 53
2.12 Collection & general processing of human tissue 55
2.13 Silver methods for nerve fibres 55
2.14 Light microscopy of ultra-thin sections 56
Chapter 3: Characterising sebaceous gland neuroanatomy 58
3.1 Introduction 59
3.1.1 Previous attempts to identify and characterise sebaceous gland innervation 59

3.1.2 Experimental aims 60
3.2 Results 60
3.2.1 Re-examination of human sebaceous gland innervation 60
3.2.2 Investigation of hypothesised neuronal-sebocyte interactions via immunofluorescent confocal microscopy in mouse skin 65
3.2.3 Nerves constituting FNB contain synaptophysin and calcitonin gene-related peptide 67
3.2.4 Transmission electron microscopy of murine follicular nerve network B 70
3.3 Discussion 74
Chapter 4: Investigating the functional requirement of sebaceous glands for input from the peripheral nervous system 76
4.1 Introduction 77
4.1.1 Cutaneous denervation and phenotypes relevant to sebaceous homeostasis 77
4.1.2 Experimental aims 78
4.2 Results 79
4.2.1 Surgical denervation of mouse skin has no effect on SG volume during telogen, but results in smaller SGs in anagen skin 79
4.2.2 Denervation has a minimal effect on SGs in young mice undergoing synchronous hair cycling 84
4.2.3 Denervation results in attenuated SG enlargement throughout depilation-induced anagen 86
4.2.4 SGs in male and female mice exhibit differential responses to depilation and dependence on cutaneous innervation 89
4.2.5 Lipid intensity per SG is increased in female SGs following denervation 91
4.2.6 Denervation results in reduced proliferation in multiple compartments of the PSU during anagen 93
4.3 Discussion 95
4.3.1 Intact cutaneous innervation is required for sebaceous gland homeostasis during hair growth 95
4.3.2 The sebaceous gland exhibits cyclical fluctuation in homeostasis that is co-ordinated with the hair cycle 97
Chapter 5: Identifying the cell and molecular basis of neuro-regulation of sebaceous gland function 98
5.1 Introduction 99
5.1.1 Placing neuroregulation within models of sebaceous gland homeostasis 99
5.1.2 Nerve-derived substances and receptors implicated in regulation of sebaceous gland biology 100
5.1.3 Experimental aims 102
5.2 Results 103

5.2.1 Denervation results in reduced contribution of Lrig1-positive cells to the sebaceous gland 103
5.2.2 Isthmus Gli1 expression is lost after denervation, and Gli1-expressing cells in the upper bulge also express Lrig1 109
5.2.3 The CGRP receptor, but not the AMY_1 or substance P receptors, are expressed in the murine junctional zone and infundibulum 114
5.2.4 Mouse skin contains non-neuronal sources of acetylcholine, but nicotinic acetylcholine receptor α7 does not appear to be expressed in mouse SGs *in vivo* 117
5.2.5 Peripheral sebocytes express the glutamate transporter Slc1a3, but not the metabotropic glutamate receptor Grm5 121
5.3 Discussion 123
5.3.1 Neurons are required for proper contribution of intra-follicular progenitor cells to the SG 123
5.3.2 Nerve-derived sonic hedgehog as a niche factor for hair cycle-activated intra-follicular progenitors 125
5.3.3 The CGRP receptor, but not the Tacr1 substance P receptor, is expressed in the mouse PSU 126
5.3.4 Potential role of neuronal and non-neuronal acetylcholine in regulating sebaceous gland function 127
5.3.5 Potential role of glutamate in regulating sebaceous gland function 129
Chapter 6: General discussion 130
6.1 Murine sebaceous glands require intact cutaneous innervation in a hair cycle dependent context 131
6.2 Other unexplored aspects of sebaceous gland neuroregulation 133
6.2.1 Adrenaline 133
6.2.2 Neurotrophins 134
6.2.3 Endocannabinoids 136
6.3 Translational relevance of neuroregulation of sebaceous glands 140
6.4 Working hypotheses and future work 141
Chapter 7: References 144

Word count: 30958

List of figures

Figure 1.1. General anatomy of the pilosebaceous unit. 16

Figure. 1.2. The hair follicle cycle. 18

Figure 1.3. Histology of the human sebaceous gland. 23

Figure 1.4. Histology of the murine sebaceous gland. 24

Figure. 1.5. The structure and cellular homeostasis of sebaceous glands. 26

Figure 1.6. Molecular biology of processes underlying sebaceous gland homeostasis. 27

Figure 1.7. Primary histological differences between a normal human sebaceous follicle and an acne lesion (open comedo). 30

Figure 1.8. The comedo switch hypothesis of acne pathogenesis. 31

Figure 1.9 General neuroanatomy of murine pilosebaceous units. 34

Figure 2.1 Primary experimental methodologies used in mice. 44

Figure 2.2. Performing surgical cutaneous denervation of mouse dorsal skin. 47

Figure 2.3. Molecular basis of genetically inducible fate mapping of *Lrig1*-expressing cells. 47

Figure 2.4. Staining, imaging and three-dimensional reconstruction of murine sebaceous glands. 51

Figure 3.1. Silver-staining method reveals nerve fibres in the proximity of human sebaceous glands. 61

Figure 3.2. Nerve fibres and sebaceous glands in toluidine-blue-stained sections of occipital scalp skin. 62

Figure 3.3. β3-tubulin-expressing nerve fibres adjacent to human sebaceous gland stroma. 64

Figure 3.4. Innervation of the mouse pilosebaceous unit. 66

Figure 3.5. Longitudinal nerve fibres directly contact LRIG1+ cells in the junctional zone. 67

Figure 3.6. Nerve endings of follicular nerve network B contain synaptophysin. 68

Figure 3.7. Nerves of follicular nerve network B contain calcitonin gene-related peptide. 70

Figure 3.8. Follicular nerve network B and sebaceous glands in dorsal skin. 72

Figure 3.9. Follicular nerve network B and sebaceous glands in the mouse whisker pad. 72

Figure 3.10. Follicular nerve network B and sebaceous glands in the murine auricular skin. 73

Figure 4.1. Surgical cutaneous denervation results in progressive loss of PGP9.5 immunoreactive nerve fibres in mouse skin. 81

Figure 4.2. Cutaneous denervation results in reduced SG volume at 2 weeks PD, but not at 3 months PD. 83

Figure 4.3. Different hair cycle stages between mice at 14-17d PD versus 90d PD. 84

Figure 4.4. Denervation does not affect SG volume in spontaneous, synchronously-hair cycling mice, observed at p35. 85

Figure 4.5. Induction of hair growth via depilatory waxing. 87

Figure 4.6. Cutaneous denervation attenuates enlargement of SGs throughout depilation-induced anagen progression. 88

Figure 4.7. Male-female comparison of the effects of denervation on SGs throughout depilation-induced anagen. 90

Figure 4.8. Depilation increases SG lipid intensity, and denervation is associated with increased lipid intensity per SG in female mice. 92

Figure 4.9. Preliminary assessment of proliferation in denervated skin following depilatory waxing. 94

Figure 5.1. Differential effect of denervation on the degree of SG GFP-labelling between male and female *Lrig1-Cre:Rosa-mTmG* mice. 104

Figure 5.2. Categorisation of different patterns of SG and infundibular GFP-labelling following induction in *Lrig1-Cre:Rosa-mTmG* mice. 106

Figure 5.3. Preliminary quantification of patterns of GFP-labelling in denervated, depilated female mice. 108

Figure 5.4. Expression of mRNA for the sonic hedgehog effector protein *Gli1* is lost in the UB of the PSU following denervation. 111

Figure 5.5. *Lrig1* mRNA expression overlaps with *Gli1* mRNA expression in the JZ/UB, and *Gli1* expression is progressively lost following denervation in depilated mice. 112

Figure 5.5 continued. *Lrig1* mRNA expression overlaps with *Gli1* mRNA expression in the JZ/UB, and Gli1 expression is progressively lost following denervation in depilated mice. 113

Figure 5.6. Neither the substance P receptor (*Tacr1*) or CGRP receptor AMY1 (*Calcr*) are expressed in murine PSUs. 115

Figure 5.7. Reactivity for *Calcrl* mRNA in the JZ indicates expression of the CGRP receptor. 117

Figure 5.8. Incubation of mouse skin with GFP-conjugated α-Bungarotoxin (α-BTX) does not result in labelling of the PSU. 119

Figure 5.9. *Chrna7* mRNA is not detectable in adult mouse skin. 120

Figure 5.10. Choline acetyltransferase (*Chat*) mRNA is expressed in bulge keratinocytes, but metabotropic glutamate receptor 5 (*Grm5*) is not detectable in mouse skin. 121

Figure 5.11. The glutamate transporter *Slc1a3* is expressed in peripheral sebocytes of mouse SGs. 122

Figure 6. Regulation of sebaceous glands by cutaneous nerves: working hypotheses. 142

List of tables

Table 1. Primary antibodies and incubation conditions. 49

Frequently used abbreviations

ACh – Acetylcholine

Calcr – Calcitonin receptor

Calcrl – Calcitonin receptor-like receptor

CGRP – Calcitonin gene-related peptide

Chat – Choline acetyl transferase

Chrna7 – Nicotinic acetylcholine receptor α7

CNFs – Circular nerve fibres

CTS – Connective tissue sheath

FNA – Follicular nerve network A

FNB – Follicular nerve network B

GFP – Green fluorescent protein

GIFM – Genetically-inducible fate mapping

Gli1 – Zinc finger protein GLI1

Grm5 – Metabotropic glutamate receptor 5

HC – Hair cycle

HF – Hair follicle

JZ – Junctional zone

LDCV – Large dense core vesicle

LNFs – Longitudinal nerve fibres

Lrig1 – Leucine-rich repeats and immunoglobulin-like domains protein 1

mRNA – messenger ribonucleic acid

MZ – Maturation zone

NZ – Necrotic zone

PD – Post-denervation

PSU – Pilosebaceous unit

PZ – Peripheral zone

SCD – Surgical cutaneous denervation

SD – Standard deviation

SER – Sebum excretion rate

SG – Sebaceous gland

SHH – Sonic hedgehog

Slc1a3 – Solute carrier family 1, member 3

Tacr1 – Tachykinin receptor 1

TEM – Transmission electron microscopy

TRPV1 – Transient receptor potential cation channel subfamily V member 1

UB – Upper bulge

α-BTX – α-bungarotoxin

Abstract

Investigating neuroregulation of sebaceous gland biology

Richard William Clayton - Thesis submitted for Doctor of Philosophy (PhD)

University of Manchester, September 2019

This project seeks to tackle the hypothesis of neuroregulation of sebaceous glands (SGs). SGs are appendages of mammalian skin that synthesise and secrete sebum, and SG dysfunction is associated with many common dermatoses, such as acne vulgaris. Clinical evidence suggests that SGs may be regulated by the peripheral nervous system. For example, sebum secretion is reduced in cases of partial facial paresis and following botulinum toxin injections. By understanding the putative neuronal controls of SG function, potential mechanistic links may be uncovered that exist between the nervous system and SGs in cutaneous physiology and human skin disease. This project first sought to characterise the neuroanatomy of the human and mouse pilosebaceous unit at the level of the SG. While the SG is not directly innervated, nerve endings closely associate with *Lrig1*-expressing stem cells in the follicular epithelium of mouse pilosebaceous units. To investigate the potential functional role of nerves in regulation of SG homeostasis, a technique for surgical denervation of mouse skin was utilised. While nerves appear to be dispensable for base maintenance of SGs, hair cycle-dependent upregulation of SG size during active hair growth was attenuated following denervation. Lineage tracing of LRIG1+ stem cells in the pilosebaceous unit suggests that reduced SG size following denervation is a result of impaired contribution of intrafollicular progenitor cells to the SG.

Declaration

No portion of the work referred to in the thesis has been submitted in support of an application for another degree or qualification at this university or any other institute of learning.

Copyright statement

Acknowledgements

Firstly, I would like to thank my dear friends in the acne and sebaceous gland lab; Peiwen, Faith, Keith, Ivo, Klaus, Arnette, Melvin, Jason, Sophia, Carol, Alvin, Selwyn, Khek Chian, Junren, Shang Wei, Siang Yun, Daniel, and Mei Qi. My time with all of you in Singapore was wonderful and unforgettable.

To Maurice and Xinhong, it has been a pleasure working in your lab. Your large and active brains are an inspiration, and I have benefitted immensely from your instruction, supervision, and guidance. Thank you.

Thanks to all the members of the dermatology group in Manchester, especially Talveen, Alex, Matiss, Nathan, April, Derek and Eleanor. You brighten up the dreary corridors of the Stopford building!

To Ralf and David, I must thank you for your effective and diligent supervision. I certainly wouldn't have got to this point without you both.

Thanks to all co-authors and collaborators who have, at some point, been temporarily pulled into the orbit of this PhD project.

I would also like to thank Prof. Des Tobin, Prof. Mauro Picardo and Dr David Liebl for kindly hosting me in their respective labs at various points throughout this project.

Chapter 1: Introduction

1.1 Sebaceous glands and the pilosebaceous unit

Sebaceous glands (SGs) are cutaneous appendages that synthesise and secrete a mixture of lipids, known as sebum. The cells of the SG are termed sebocytes. The SG is connected to the proximal portion of the hair follicle (HF) via a keratinised duct through which sebum is released (Figure 1.1). Secreted sebum coats the hair shaft, pilary canal, and the surface of the skin. Pilosebaceous units (PSUs) consist of HFs and SG lobes arranged in close proximity along with an arrector pili muscle and, in regions of skin that contain them, an apocrine gland (AG) (Figure 1.1) (Hinde *et al.*, 2013; Schneider & Paus, 2014).

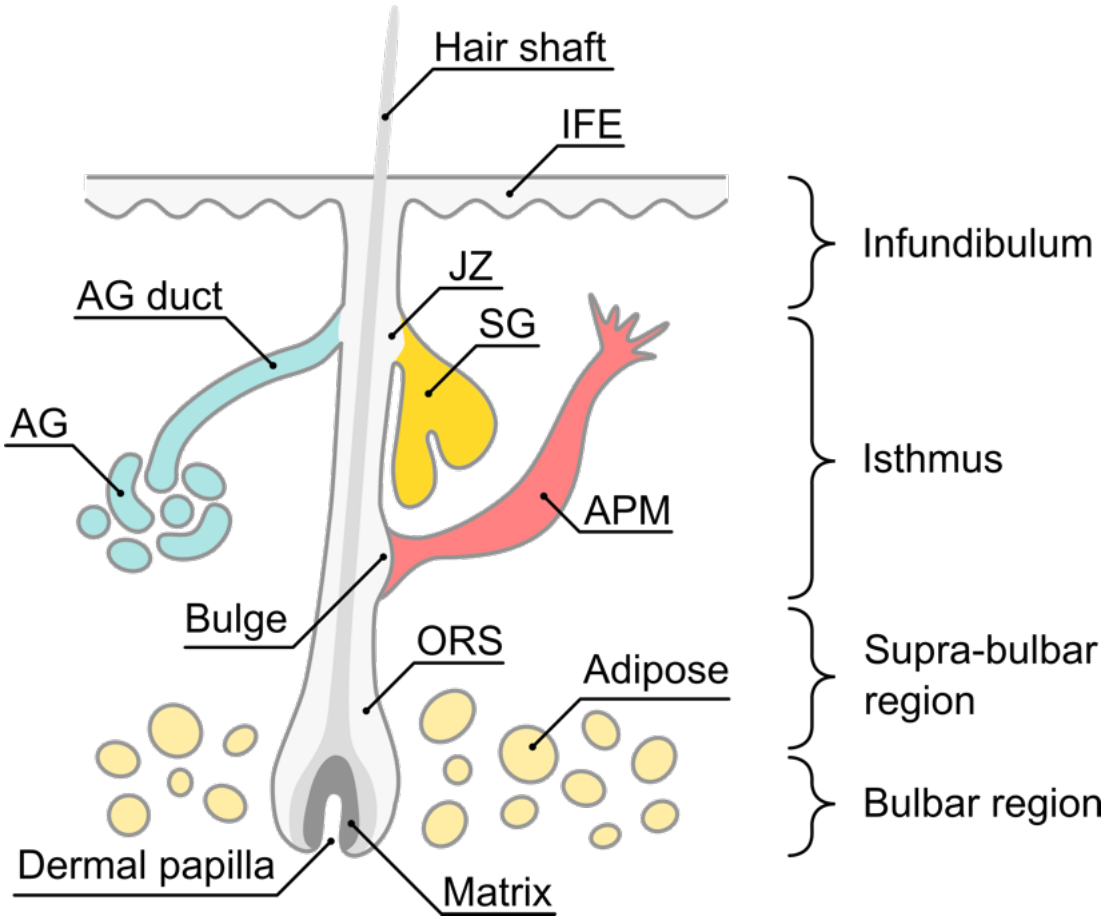

Figure 1.1. General anatomy of the pilosebaceous unit.

The pilosebaceous unit (PSU) is comprised of the hair follicle (HF), sebaceous gland (SG), and arrector pili muscle (APM). In humans, regions of skin that contain apocrine glands (AG) feature PSUs into which the AG duct also inserts. The basic arrangement of the HF, SG and APM is generally conserved between species, although the size of the PSU varies considerably. The PSU can be divided into four broad compartments. The distal portion that connects to the interfollicular epidermis (IFE) is referred to as the infundibulum. The isthmus contains the SG, junctional zone (JZ), APM, and the bulge, which contains follicular stem cells. The supra-bulbar regions bridge the isthmus to the bulbar region, which (in growing

HFs) contains the hair matrix and dermal papilla and is situated amongst dermal adipose. The outer root sheath (ORS) of the HF is contiguous with the SG epithelium and IFE. Figure created by the author and Dr Ivo de Vos. Figure now published in *Biological Reviews* (Clayton *et al.*, 2020).

Furthermore, in humans, the coil of an eccrine gland can also be found adjacent to the HF above the bulbar region, which is the most proximal part of the HF (Poblet, Jiménez, & Ortega, 2004). The region where the SG duct inserts into the pilary canal is referred to as the junctional zone (JZ). Distal to the JZ is the HF infundibulum, where the hair shaft separates from the follicular epithelium (Figure 1.1). The entire PSU is encapsulated by a connective tissue sheath (CTS), or stroma, made up of mesenchymal fibroblasts and collagen (Hinde *et al.*, 2013; Schneider & Paus, 2014). The HF goes through periodic phases of growth (anagen), subsequent regression (catagen) and rest (telogen) (Figure 1.2). This process is known as the hair cycle (HC) (Kligman, 1959). The formation and extrusion of the hair shaft occurs during the anagen phase of the HC. In mice, the first 6-7 weeks of life are associated with synchronous waves of hair growth throughout the dorsal skin (Müller-Röver *et al.*, 2001) (Figure 1.2), whereas in humans, hair follicles do not exhibit any synchronous cycling (Van Scott, Reinertson, & Steinmuller, 1957).

In humans, SGs are found throughout the skin, save for the palms and soles (Montagna & Parakkal, 1974c; Thody & Shuster, 1989). Facial SGs (also known as sebaceous follicles) are larger and more extensively branched than the SGs associated with terminal hairs of the scalp, and vellus body hairs. The scalp and face are the anatomical regions that are most densely populated by SGs, and this is reflected in their relatively high rates of sebum production (Kligman & Shelley, 1958; Montagna & Parakkal, 1974c).

It is worth noting here that the eyelid contains a specialised population of SGs called Meibomain glands (Montagna & Parakkal, 1974c). Meibomian glands are embedded within the tarsal plate of the eyelid, and therefore are also known as tarsal glands (Butovich, 2017). A substance comparable to sebum (meibum) is produced by

Meibomian gland meibocytes (similar to sebocytes). This meibum serves to prevent evaporation of the tear film that covers the eye (Butovich, 2017).

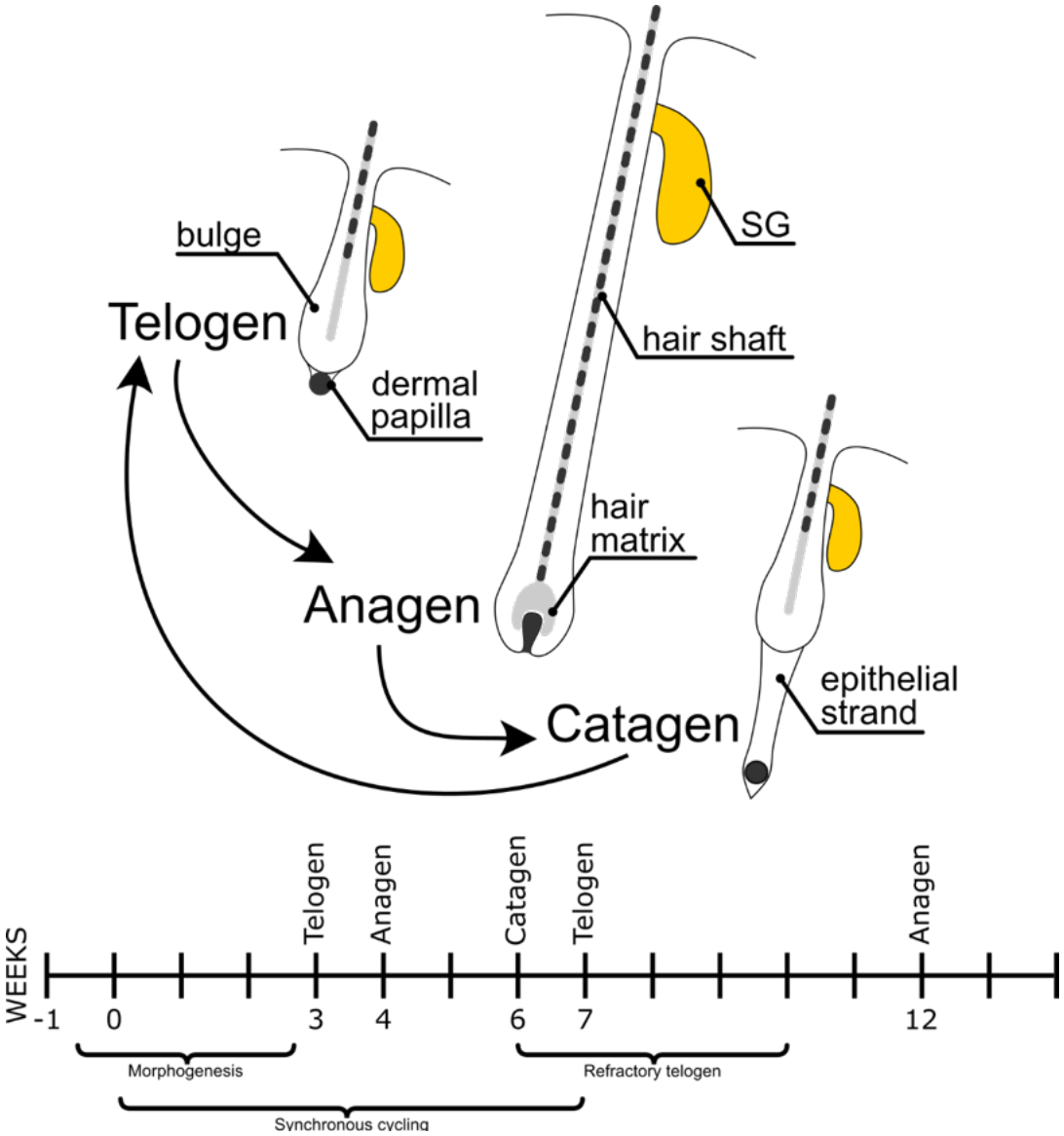

Figure. 1.2. The hair follicle cycle.

Hair follicles (HFs) go through cycles of growth (anagen), regression (catagen), and rest (telogen), known as the hair cycle (HC). Murine HFs are depicted here. The dermal papilla is a condensate of dermal cells that initiate hair growth, while the bulge contains follicular stem cells that generate the growing follicle. Anagen is associated with a lengthening of the hair follicle, formation of the highly proliferative hair matrix, and production of a pigmented hair shaft. During catagen, the HF regresses, and follicles in late catagen can be easily distinguished by the presence of the epithelial strand. Typically, the sebaceous gland (SG) is thought to reside within the non-cycling portion of the HF. In human skin, HFs cycle asynchronously. In mice, the first 6-7 weeks of life are associated with synchronised waves of HF cycling that proceed anterior-posterior through the dorsal skin. A period of refractory telogen, in which resting follicles are unable to be induced to grow by regions of adjacent anagen skin, precedes the onset of more asynchronous hair cycling in the adult mouse. Therefore, research conducted in the context of the HC is often conducted on younger mice within this period of synchronous hair cycling.

1.2 Sebum composition and function

Sebum consists of a diverse mixture of lipids (Picardo *et al.*, 2009; Camera *et al.*, 2010) and serves several important physiological functions that include: waterproofing of skin and fur (Chen *et al.*, 1997, 2002; Westerberg *et al.*, 2004; Dahlhoff *et al.*, 2016a), anti-microbial activity (Basta, Wilburg, & Heczko, 1980; Wille & Kydonieus, 2003; Drake *et al.*, 2008; Lee *et al.*, 2009; Nakatsuji *et al.*, 2010), maintenance of skin barrier function (Sundberg *et al.*, 2000; Fluhr *et al.*, 2003; Westerberg *et al.*, 2004; Man *et al.*, 2009), protection against ultraviolet radiation (Beadle & Burton, 1981; Ohsawa *et al.*, 1984; Passi *et al.*, 2002; Mudiyanselage *et al.*, 2003; Ryu *et al.*, 2009; Dahlhoff *et al.*, 2016a), immunomodulation (Georgel *et al.*, 2005; Cossette *et al.*, 2008; Lovászi *et al.*, 2017), and regulation of body temperature (Chen *et al.*, 1997, 2002; Sampath *et al.*, 2009; Dahlhoff *et al.*, 2016a).

The cutaneous phenotypes present in mice that are deficient for sebaceous lipids (Ehrmann & Schneider, 2016) have indicated many of these important functions of sebum, chiefly the loss of thermoregulation and waterproofing (Chen *et al.*, 1997, 2002; Dahlhoff *et al.*, 2016a), susceptibility to UV radiation (Dahlhoff *et al.*, 2016a), and reduced barrier function of skin (Westerberg *et al.*, 2004; Stoffel *et al.*, 2017). A role of sebaceous lipids in maintaining HF function and integrity can also be inferred from the hair growth defects and scarring alopecia present in mice that have no functional SGs (Zheng *et al.*, 1999; Sundberg *et al.*, 2000; Stenn, 2001; Sardella *et al.*, 2017; Stoffel *et al.*, 2017).

Sebum composition varies considerably between different species (Thody & Shuster, 1989; Smith & Thiboutot, 2008). In human sebum, triglycerides (TGs), squalene, and wax esters predominate, though cholesterol and cholesterol esters also constitute a small fraction (Summerly & Woodbury, 1971, 1972; Summerly *et al.*, 1976; Ridden, Ferguson,

& Kealey, 1990; Guy, Ridden, & Kealey, 1996; Picardo *et al.*, 2009). While sebum on the surface of the skin contains a significant proportion of free fatty acids (FFAs) (Downing, Strauss, & Pochi, 1969; Greene *et al.*, 1970; Nicolaides *et al.*, 1970), analysis of lipid composition from isolated SGs reveals that FFAs comprise only a comparatively small fraction of lipid synthesised in the SG (Summerly & Woodbury, 1971, 1972; Ridden *et al.*, 1990; Guy *et al.*, 1996). This discrepancy may be caused by lysis of TGs by commensal microorganisms including *Cutibacterium acne*s (*C. acnes*, formerly known as *Propionibacterium acnes)* and yeasts of the genus *Malassezia* (Marples, Downing, & Kligman, 1971; Puhvel, Reisner, & Sakamoto, 1975; Sommer *et al.*, 2016; Scholz & Kilian, 2016).

Human sebum is further characterised by the presence of unique lipids including squalene and Δ6 monounsaturated fatty acids like sapienic acid (Nicolaides, 1974; Thody & Shuster, 1989). Lipid droplet-associated proteins, such as perilipins, regulate the size and rate of formation of lipid droplets (Dahlhoff *et al.*, 2013b, 2015; Camera *et al.*, 2014; Schneider, 2015; Schneider, Zhang, & Li, 2016). Interestingly, sebum composition also varies by anatomical region, corresponding to differences in SG number (Ludovici *et al.*, 2018) and SG size (Summerly *et al.*, 1976). Moreover, sebum composition can be altered in diseased skin (Shi *et al.*, 2015). For example, in acne vulgaris there is a relatively increased presence of squalene, monounsaturated fatty acids, and diaglycerols (Cotterill *et al.*, 1972; Pappas *et al.*, 2009; Akaza *et al.*, 2014; Camera *et al.*, 2016), while psoriasis and atopic dermatitis both feature a reduction in total FFAs and FFA chain length (van Smeden *et al.*, 2014; Takahashi *et al.*, 2014). Altered sebum composition has also been associated with hypersensitive skin (Fan *et al.*, 2018). However, the direct functional importance of sebum composition remains untested and is incompletely understood.

1.3 Sebaceous gland development and progenitor cells

Human SGs appear around 3.5 months into the gestational period (Kligman & Strauss, 1956; Montagna & Parakkal, 1974c). Human SGs are active *in utero*, as part of the vernix caseosa of newborns is derived from sebaceous secretions (Rissmann *et al.*, 2006; Míková *et al.*, 2014). SGs are relatively inactive throughout childhood, then during adolescence SGs exhibit a dramatic increase in size and activity that then persists through adulthood (Pochi, Strauss, & Mescon, 1962; Cotterill *et al.*, 1972; Montagna & Parakkal, 1974c).

In mice, development of the PSU itself begins a few days prior to birth, however the first sebocytes emerge in the early-postnatal period during the 'bulbous peg stage' of PSU development, which occurs at 3-4 days post-partum in the C57BL/6J strain (Paus *et al.*, 1999; Frances & Niemann, 2012). Prior to the appearance of sebocytes, a population of cells that express both *Lrig1* (Leucine-rich repeats and immunoglobulin-like domains protein 1) and *Sox9* forms within the developing hair peg. As development of the PSU proceeds, two distinct groups of cells emerge that differentially express either *Lrig1* or *Sox9*, and which become restricted to the JZ and hair bulge compartments, respectively. The first sebocytes emerge from the *Lrig1*-expressing population in the JZ (Nowak *et al.*, 2008; Frances & Niemann, 2012; Schepeler, Page, & Jensen, 2014; Xu *et al.*, 2015; Ouspenskaia *et al.*, 2016).

Genetic lineage tracing techniques in adult mice has indicated that *Lrig1*-expressing cells in the HF generate both the SG and infundibulum, and act as a progenitor cell population for these compartments (Jensen *et al.*, 2009b; Page *et al.*, 2013) (Figure 1.5). Specific manipulation of beta-catenin signalling in *Lrig1*-expressing cells reveals that levels of wingless (Wnt) signalling dictate the lineage commitment decision of these cells (Kretzschmar *et al.*, 2016) (Figure 1.6). Leucine-rich repeat-containing G-protein coupled receptor 6 (*Lgr6*) has also been identified as a marker of a potential SG progenitor

population. *Lgr6*-expressing cells are long-lived and relatively quiescent, and intrasebaceous LGR6+ cells have been shown to contribute to the murine SG (Gong *et al.*, 2012; Page *et al.*, 2013; Liao & Nguyen, 2014; Kretzschmar *et al.*, 2016). Up until recently, the working model of SG homeostasis was that the SG was continually maintained by follicular *Lrig1*-expressing cells (Jensen *et al.*, 2009b; Page *et al.*, 2013). However, it was recently demonstrated using clonal lineage tracing methods, that under homeostatic conditions, that the SG is maintained entirely by progenitor cells within the SG (Andersen *et al.*, 2019). It remains unanswered however, whether maintenance of the SG under non-homeostatic conditions requires input from HF-resident stem cells.

1.4 Overview of the cell and molecular biology of sebaceous gland homeostasis

The SG has a layered structure that corresponds to different stages of sebocyte differentiation, which are the lipid-synthesising cells that comprise the SG (Figure 1.3; Figure 1.4; Figure 1.5). The outermost sebocytes make up the basal layer or peripheral zone (PZ), and are relatively undifferentiated and proliferative (Epstein & Epstein, 1966; Hamilton, 1974; Hamilton, Howard, & Potten, 1974) (Figure 1.5). Much of what is known about the factors that drive sebocyte mitosis and differentiation has been ascertained through treatment or genetic manipulation in rodent models (Ehrmann & Schneider, 2016; Clayton *et al.*, 2019), or through the extensive work undertaken on sebocyte cell lines (Schneider & Zouboulis, 2018). The SGs of mouse skin are smaller than their human counterparts and have only one or two lobes (Figure 1.4).

Sebocyte proliferation is promoted by multiple factors such as *Cmyc* (Horsley *et al.*, 2006; Jensen *et al.*, 2009b; Cottle *et al.*, 2013), androgens (Ebling, Ebling, & Skinner, 1969;

Petersen, Zone, & Krueger, 1984; Akamatsu, Zouboulis, & Orfanos, 1992; Fujie *et al.*, 1996; Rosignoli *et al.*, 2003), and receptor tyrosine kinases including *ErbB* family receptors (Bol *et al.*, 1998; Kiguchi *et al.*, 2000; Sato *et al.*, 2001; Akimoto *et al.*, 2002; Dahlhoff *et al.*, 2013a; Li *et al.*, 2016) and fibroblast growth factor receptor 2b (*Fgfr2b*) (Figure 1.6) (Danilenko *et al.*, 1995). Recently, caspase 3-mediated activation of yes-associated protein (*Yap*) was demonstrated to promote mitosis in murine tail SGs (Yosefzon *et al.*, 2018).

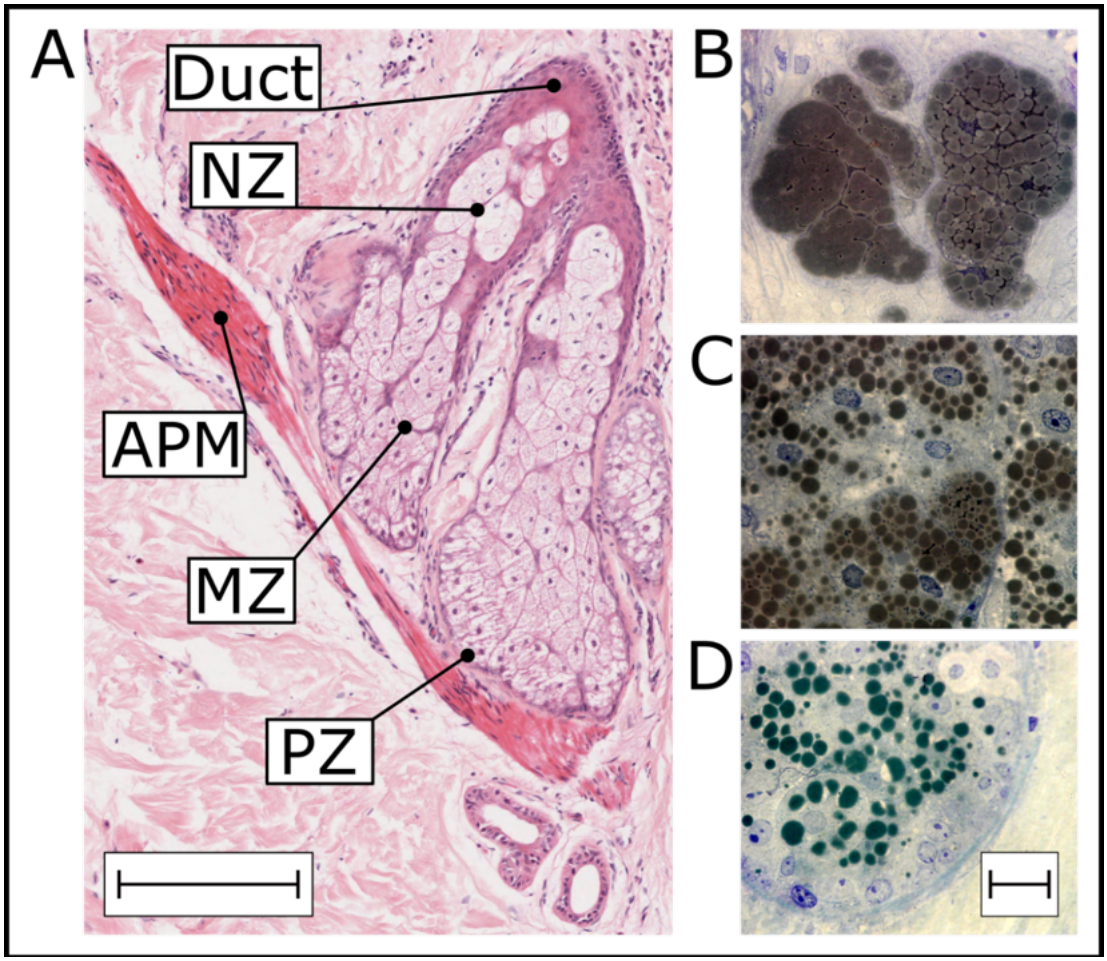

Figure 1.3. Histology of the human sebaceous gland.

(A) Photomicrograph of a haematoxylin and eosin-stained human sebaceous gland (SG), arrector pili muscle (APM), and surrounding stroma and dermis. Scale = 200 µm. **(B-D)** Photomicrographs of OsO4- and toluidine blue-stained SGs showing different stages of sebocyte differentiation. Scale = 20 µm. The peripheral zone (PZ) contains undifferentiated sebocytes. **(D)** The maturation zone (MZ) contains differentiating sebocytes, evident by lipid droplet accumulation **(C)**. Terminally differentiated sebocytes comprise the necrotic zone (NZ) where they undergo holocrine secretion **(B)**, releasing sebum into the SG duct. Figure now published in *Biological Reviews* (Clayton *et al.*, 2020).

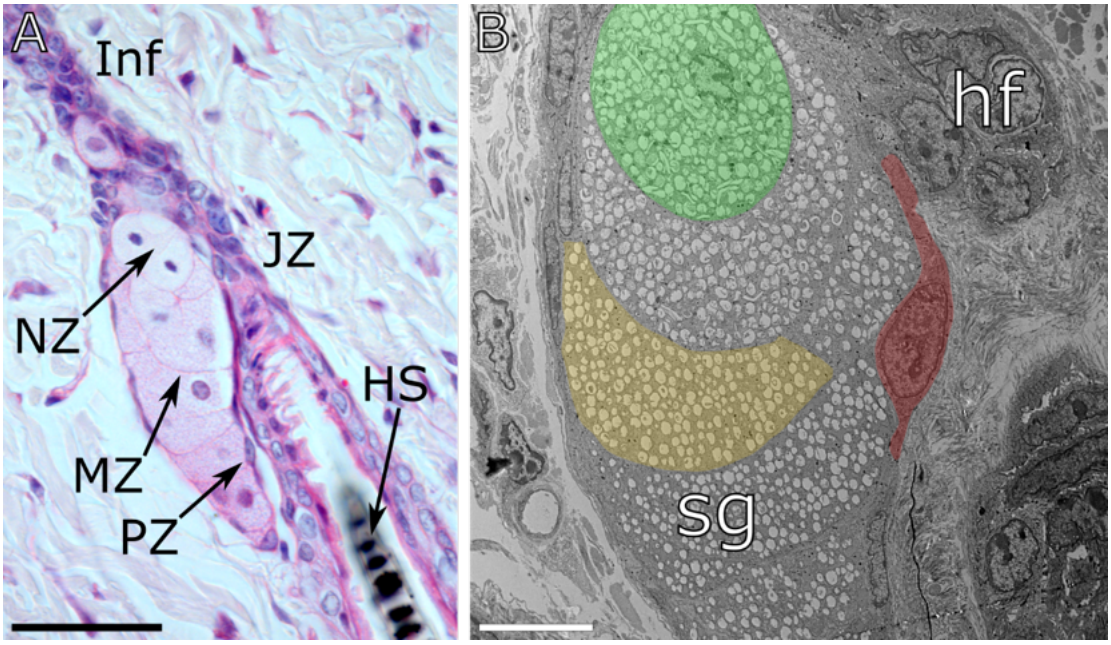

Figure 1.4. Histology of the murine sebaceous gland.

(A) Photomicrograph of a haematoxylin and eosin-stained sebaceous gland (SG) in mouse skin. The general structure of mouse SGs is similar to that of human SGs, although the pilosebaceous unit (PSU) is much smaller, overall. The peripheral zone (PZ), maturation zone (MZ) and necrotic zone (NZ) can be observed, containing proliferative, differentiating and apoptotic sebocytes, respectively. The junctional zone (JZ) refers to the region of the PSU where the SG attaches to the hair follicle (HF). Inf, infundibulum. HS, hair shaft. Scale = 50 μm. **(B)** Transmission electron micrograph of a mouse SG situated in whisker pad skin. The abundance of lipid droplets in maturing sebocytes can be appreciated. Red cell, undifferentiated peripheral sebocyte; yellow cell, maturing sebocyte; green cell, necrotic sebocyte with pyknotic nucleus; Scale = 10 μm.

Adjacent to the peripheral layer is the supra-basal layer, or maturation zone (MZ), which contains differentiating sebocytes (Figure 1.3; Figure 1.4; Figure 1.5). Differentiation is evident by the accumulation of lipid droplets in sebocytes within the MZ, and dramatically increased cell size compared to the PZ (Figure 1.3; Figure 1.4). Finally, the necrotic zone (NZ) is where terminally differentiated sebocytes release sebum by undergoing holocrine secretion; a process that shares key features with autophagic cell death (Brandes, Bertini, & Smith, 1965; Mesquita-Guimarães & Coimbra, 1976; Fischer *et al.*, 2017; Zouboulis, 2017; Rossiter *et al.*, 2018) (Figure 1.3; Figure 1.4). The time taken for an undifferentiated sebocyte in the peripheral layer to fully differentiate is around 7-14 days, which is comparable between human and rodent SGs (Epstein & Epstein, 1966; Hamilton, 1974; Hamilton *et al.*, 1974; Jung *et al.*, 2015).

Lipid synthesis is central to differentiation in the SG. This is reflected in the importance of transcription factors that promote the expression of lipogenic enzymes to sebocyte differentiation. Such transcription factors include PPARγ (peroxisome proliferator-activated receptor gamma) (Berger & Moller, 2002; Icre, Wahli, & Michalik, 2006) and CCAAT-enhancer-binding proteins (C/EBPs) (Chung *et al.*, 2012; Guo, Li, & Tang, 2015), both of which are required for sebum production and SG maintenance (Karnik *et al.*, 2009; House *et al.*, 2010; Sardella *et al.*, 2017). Androgens, through adrenoceptors (ARs), also promote sebocyte differentiation (Figure 1.6) (Ebling *et al.*, 1969; Petersen *et al.*, 1984; Rosignoli *et al.*, 2003; Cottle *et al.*, 2013). Broad manipulation of Wnt signalling throughout the murine PSU reveals that low levels of Wnt promote sebaceous differentiation (Gat *et al.*, 1998; Merrill *et al.*, 2001; Niemann *et al.*, 2002, 2007; Collins & Watt, 2008; Petersson *et al.*, 2011; Kakanj *et al.*, 2013; Lien *et al.*, 2014), while high levels of Wnt signalling result in SG loss and ectopic HF formation (Lo Celso, Prowse, & Watt, 2004; Kretzschmar *et al.*, 2016). Conversely, hedgehog signalling may act to promote sebocyte differentiation (Oro & Higgins, 2003; Allen *et al.*, 2003; Gu & Coulombe, 2008).

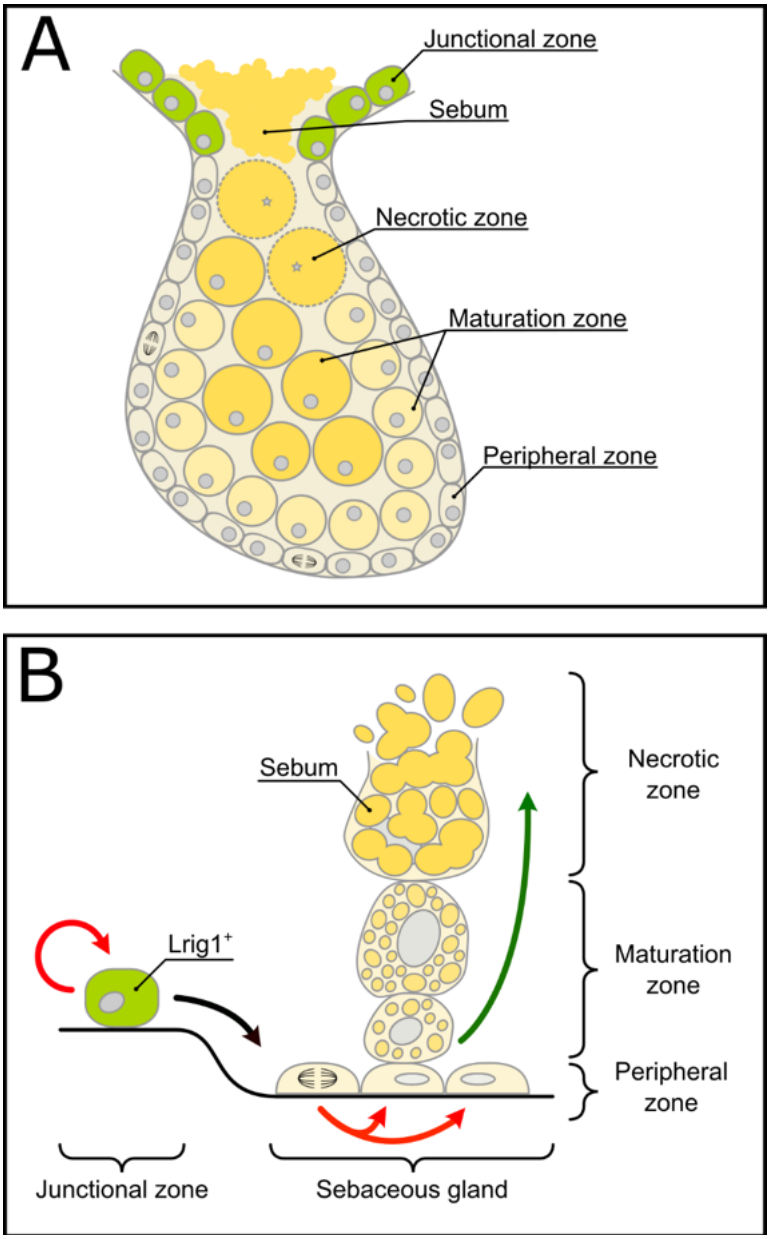

Figure. 1.5. The structure and cellular homeostasis of sebaceous glands.

(A) Diagrammatic representation of overall SG structure and compartmentalisation into zones corresponding to different stages of sebocyte differentiation. **(B)** Model of cellular homeostasis of SGs. Stem cells in the junctional zone that express leucine-rich repeats and immunoglobulin-like domains protein 1 (*Lrig1*) give rise to the SG. Proliferation occurs chiefly within the peripheral zone. Lipid synthesis and differentiation occur in the maturation zone. Terminal differentiation and cell death by holocrine secretion occurs in the necrotic zone. Red arrows indicate cell division. The black arrow indicates translocation of cells. The green arrow indicates differentiation. Panels were submitted as part of a figure now published in *Biological Reviews* (Clayton *et al.*, 2020).

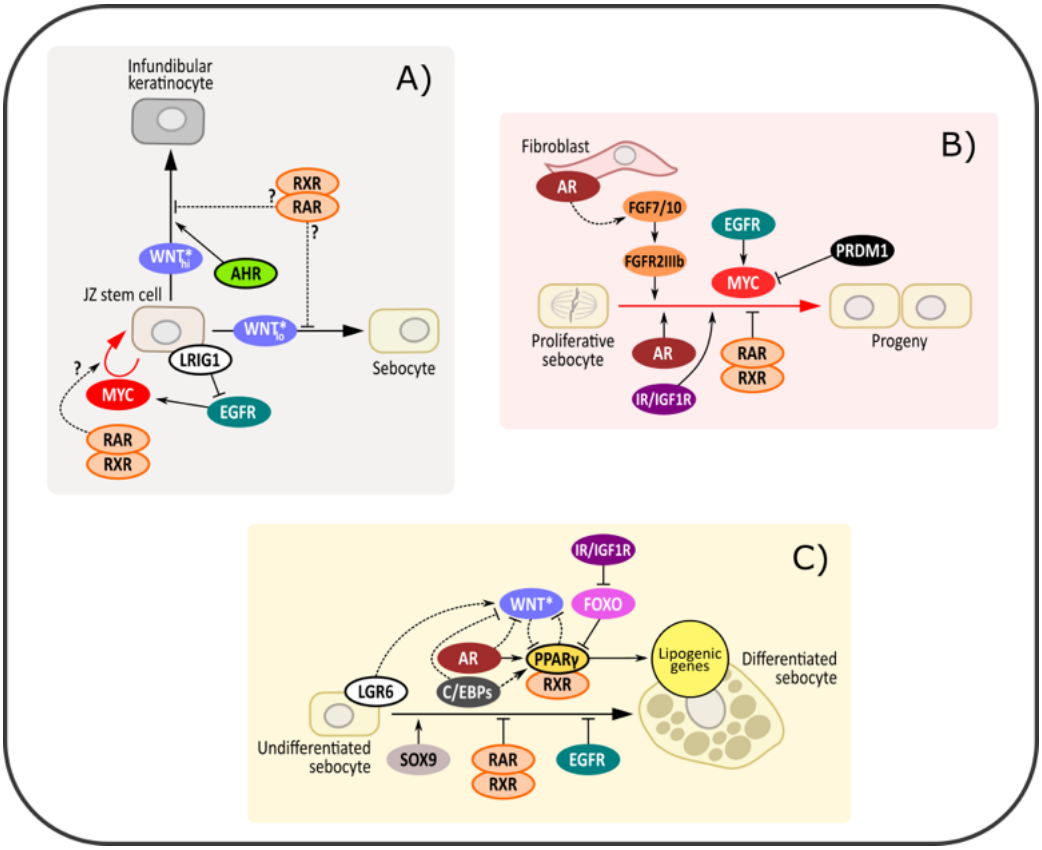

Figure 1.6. Molecular biology of processes underlying sebaceous gland homeostasis.

(A) Specification of sebocytes. Stem cells (SCs) in the junctional zone (JZ) give rise to either infundibular keratinocytes or sebocytes, dependent on high (WNThi) or low (WNTlo) levels of Wnt signalling, respectively. The aryl hydrocarbon receptor (AHR) appears to promote differentiation towards the infundibular fate. Proliferation in LRIG1+ cells is driven by MYC and EGFR. EGFR in turn is negatively regulated by LRIG1. Retinoids used as anti-acne therapeutics, acting through RARs, may either inhibit differentiation of JZ cells, or promote proliferation, resulting in stem cell exhaustion. **(B) Proliferation of undifferentiated pre-sebocytes.** Proliferation of basal sebocytes is driven by MYC, which in turn can be activated by epidermal growth factor receptor (EGFR). FGFR2b (Fibroblast growth factor receptor 2b) may also drive proliferation, responding to FGF7 and FGF10 released by stromal fibroblasts in response to androgens. Proliferation of basal sebocytes is also driven by AR and insulin receptor (IR) and insulin-like growth factor receptor 1 (IGF1R). Retinoids also appear to inhibit sebocyte proliferation. PRDM1 (also known as Blimp1), which is expressed in differentiated sebocytes, prevents further proliferation by interacting with and inhibiting MYC. **(C) Differentiation and lipid synthesis.** PPARγ promotes differentiation by upregulating expression of lipogenic genes. Retinoid X receptors (RXR) are obligate heterodimers for PPARγ. Premature differentiation is inhibited by WNT signalling and FOXO transcription factor, which suppress PPARγ expression. AR and C/EBPs suppress WNT and promote PPARγ expression, which in turn can further inhibit WNT, facilitating differentiation. LGR6, a marker for progenitor cells in the SG, may prevent premature differentiation by promoting WNT signalling. IR and IGF1R may also facilitate differentiation by downregulation of FOXO. SOX9 also appears to be required for differentiation. Red arrows indicate cell divisions. Thick black arrows indicate differentiation. Thin black arrows indicate stimulation (arrowheads) or inhibition (bars). *Indicates WNT pathway signalling. Figure is published in *British Journal of Dermatology* (Clayton et al., 2019).

1.5 Acne vulgaris

Acne vulgaris (acne) is an exceedingly common SG-associated skin disease (Tan & Bhate, 2015; Lynn *et al.*, 2016; Rocha & Bagatin, 2018), which is characterised by the formation of comedones (commonly called 'blackheads' or 'whiteheads') (Figure 1.7) (Kligman, 1974) and abnormally high sebum production (Cotterill, Cunliffe, & Williamson, 1971; Youn *et al.*, 2005b; Pappas *et al.*, 2009; Akaza *et al.*, 2014; Bilgiç *et al.*, 2015; Okoro, Bulus, & Zouboulis, 2016). Effective treatments for acne include various antibiotics and also retinoids, such as isotretinoin, which reduce the number of comedones, lower sebum secretion, and cause SG involution (Dahlhoff, Zouboulis, & Schneider, 2016b; Kosmadaki & Katsambas, 2017).

Several grading techniques exist for classifying acne severity (Thappa, Adityan, & Kumari, 2009). One of the most popular methods of grading acne is the Leeds system, where a qualitative assessment of acne severity is made (scale of 0-10), using a range of reference photographs. In addition, the number and type of acne lesions present are quantified (Cunliffe & Gould, 1979; Burke & Cunliffe, 1984; O'Brien, Lewis, & Cunliffe, 1998; Layton, 2014). Another common method is the global acne grading system (GAGS). A GAGS score is generated based on the number and type of comedo present in specific regions of the face and trunk (Doshi, Zaheer, & Stiller, 1997). Typically, acne can be graded as non-existent, physiological/minor, mild, or severe (Burke & Cunliffe, 1984; Doshi *et al.*, 1997). Inflammation, pain, and scarring are common complications of more severe acne (Kligman, 1974; Chuah & Goh, 2015).

Acne is by far most common during puberty and early adulthood. Prevalence during the teenage years has been estimated to be between 80-100% (Bloch, 1931; Burton *et al.*, 1971b; Rademaker, Garioch, & Simpson, 1989; Smithard, Glazebrook, & Williams, 2001; Tan *et al.*, 2007; Yahya, 2009; Ghodsi, Orawa, & Zouboulis, 2009; Law *et al.*,

2010). In 2009, an Iranian study involving 1002 randomly selected 12-20-year olds, found that only 6.8% had no acne at all. Mild acne was found in 79.1%, and more severe acne in 14% (Ghodsi *et al.*, 2009). In the same year, a Nigerian study found that in 167 randomly selected 17-19-year olds, none were acne free. 82.9% overall had mild acne while 10.8% had more severe acne (Yahya, 2009). In 2010, acne prevalence in Hong Kong late adolescents was determined to be 81.5%. Of the 389 randomly selected, mild acne was found in 58.4%, and more severe acne in 23.1% (Law *et al.*, 2010). For many however, acne is not an experience limited to the teenage years. While the incidence and severity of acne generally declines with advancing age, studies have shown that a significant portion of adults still suffer from acne (Cunliffe & Gould, 1979; Goulden, Stables, & Cunliffe, 1999; Schafer *et al.*, 2001; Poli, Dreno, & Verschoore, 2001; Collier *et al.*, 2008; Zeichner, 2017).

Acne is associated with a distinct histopathology of the PSU. As mentioned, acne is characterised by the formation of comedones, which are cystic dilations of the distal HF (infundibulum), and which are associated with atrophic SGs (Figure 1.7) (Kligman, 1974). A prevailing hypothesis with regards to acne pathogenesis is known as the comedo switch hypothesis, which postulates that comedones form via abnormal differentiation of the progenitor cells that generate both the SG and infundibulum (Figure 1.8) (Saurat, 2015; Clayton *et al.*, 2019). This hypothesis aligns with the observed histopathology of acne lesions (Figure 1.7). Moreover, retinoids appear to modulate differentiation of LRIG1+ progenitors (Jensen *et al.*, 2009b) which may explain their efficacy. Furthermore, a class of chlorinated hydrocarbons called dioxins, which cause an acne-like condition known as chloracne, also appear to act directly on LRIG1+ progenitor cells (Fontao *et al.*, 2017).

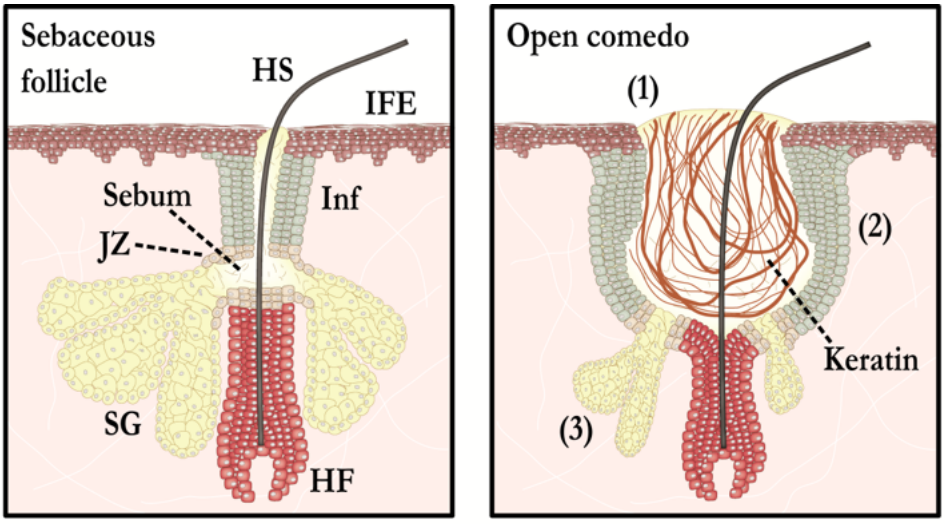

Figure 1.7. Primary histological differences between a normal human sebaceous follicle and an acne lesion (open comedo).

(Left panel). Healthy human sebaceous follicle with multi-lobular sebaceous gland (SG) and normal infundibulum (Inf). Cells of the junctional zone (JZ) give rise to the infundibulum and SG. (Right panel). An open comedo (or 'blackhead'). (1) The defining characteristic of the acne lesion is the formation of the comedo, which consists primarily of infundibular-derived keratins and sebum. Two other key histological features of the acne follicle are (2) hyperplasia and abnormal keratinisation of the infundibulum, and (3) atrophy of the associated SGs. HF, hair follicle; HS, hair shaft; IFE, interfollicular epidermis. Figure created by the author and Klaus Göbel, and published in *British Journal of Dermatology* (Clayton et al., 2019).

Finally, as mentioned previously, the composition of sebum in acne is also altered. Acne sebum is enriched for squalene, monounsaturated fatty acids, and diaglycerols (Cunliffe *et al.*, 1972; Pappas *et al.*, 2009; Akaza *et al.*, 2014; Camera *et al.*, 2016). No causal relationship between changes in sebum composition and comedo formation has been demonstrated in human skin. However, it has been hypothesised that the altered sebum of acne may induce infundibular hyperkeratinisation, facilitate bacterial growth, or even occlude the pillary canal (Kligman, 1974; Downing *et al.*, 1986; Mirshahpanah & Maibach, 2007; Tilles, 2014; Zouboulis, Jourdan, & Picardo, 2014). Interestingly, select sebaceous lipids, such as sapienic acid or oleic acid, can induce comedo formation in animal models (Kligman & Kwong, 1979; Motoyoshi, 1983).

While a high sebum production is characteristic of acne, it does not appear to be causative. Indeed, increased sebum secretion can occur independently of acne in other diseases (Burton *et al.*, 1973; Trivedi *et al.*, 2006; Borlu *et al.*, 2012). Furthermore, sebum

production in a given region of skin does not correlate with density of comedones in the same area (Youn *et al.*, 2005a; Kim *et al.*, 2015).

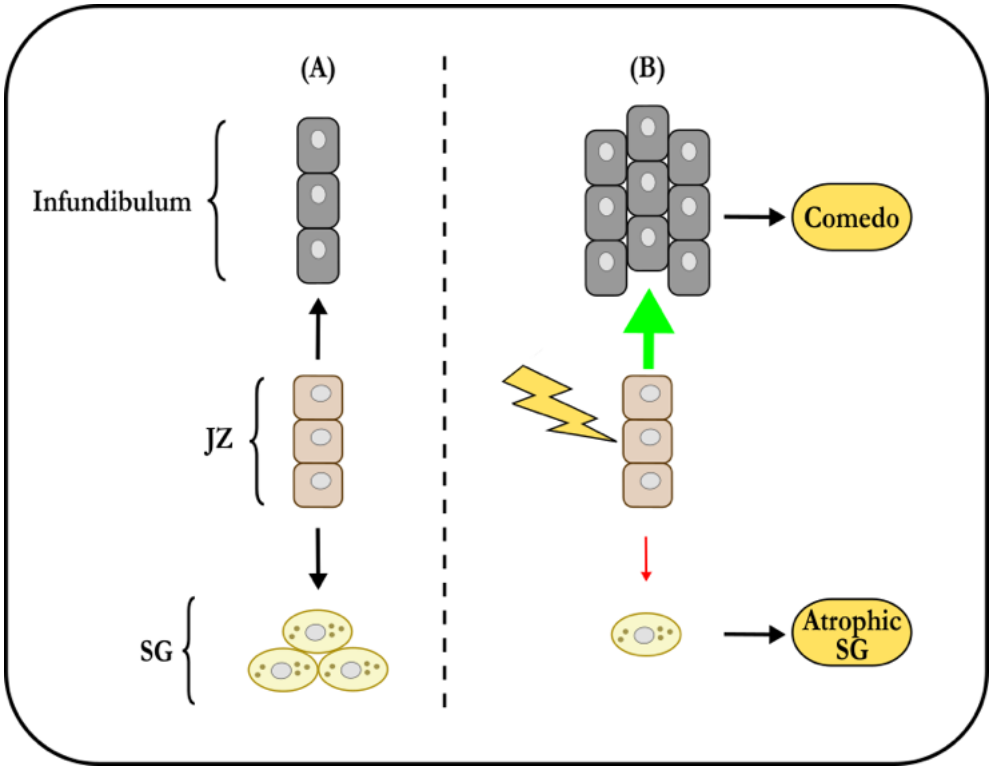

Figure 1.8. The comedo switch hypothesis of acne pathogenesis.

(A) In healthy pilosebaceous units, progenitor cells within the junctional zone (JZ) contribute to both the infundibulum and the sebaceous gland (SG). (B) In acne, a comedogenic stimulus acts on JZ cells, causing a switch in lineage determination that favours the infundibulum, resulting in the observed histopathology of acne lesions (comedo formation and SG atrophy). Green and red arrows indicate increased and decreased cellular contributions, respectively. Published in *British Journal of Dermatology* (Clayton et al., 2019).

1.6 Other SG-associated dermatoses

Acne aside, abnormal SGs can be found in several other cutaneous disorders (Shi *et al.*, 2015). Seborrheic dermatitis (SD), despite its name, does not feature seborrhoea (Burton & Pye, 1983). Rather, SD is named for its localisation to the SG-rich areas of the face and scalp (Shi *et al.*, 2015). In fact, SD shares many clinical features with psoriasis. For example, both SD and psoriasis manifest as patches of red, irritated skin that scale and become flaky (Park *et al.*, 2016). Psoriasis and SD may also be distinguished on the basis that psoriasis usually effects only the extremities, whereas SD is restricted to the face

(Dessinioti & Katsambas, 2013; Boehncke, 2015; Park *et al.*, 2016). Both SD and psoriasis feature epidermal hyperkeratosis and presence of an inflammatory cell infiltrate (Pinkus & Mehregan, 1966). The SGs of psoriatic skin are also hypotrophic, fewer in number, and exhibit dysfunctional differentiation (Werner, Brenner, & Böer, 2008; Rittié *et al.*, 2016; Liakou *et al.*, 2016). While no observation of SGs in the skin of SD patients has been made, the resemblance of SD to psoriasis would suggest that SGs in SD skin may also be hypotrophic. This is supported by the finding that sebum production is reduced in SD, particularly in women (Burton & Pye, 1983). Atopic dermatitis (AD) and eczema have also been found to feature hypotrophic SGs (Prose, 1965; Wheatley, 1965; Wirth, Gloor, & Stoika, 1981).

Furthermore, disturbances in cutaneous lipid composition are noted for many of these SG-associated skin conditions. In SD and AD for example, the reduction in total FFA levels and in FFA chain length correlates with increasing trans-epidermal water loss (van Smeden *et al.*, 2014; Takahashi *et al.*, 2014). Squalene and wax esters are also reduced in AD (Wirth *et al.*, 1981). Similar to acne, it is not known whether changes in sebum composition of SG function contributes to the aetiology of these dermatoses.

However, loss of SGs in mice has however been found to result in skin changes that recapitulate some aspects of human skin disease. Hypotrophy of dorsal SGs observed in *Dgat1* -/- mice (Chen *et al.*, 2002), and in mice treated with *Dgat1* inhibitors, is associated with epidermal hyperkeratosis (Floettmann *et al.*, 2015). Furthermore, both *Dgat1* -/- and *Scd3*-DTA mice exhibit impaired thermoregulation (Chen *et al.*, 2002; Dahlhoff *et al.*, 2016a); a characteristic shared with psoriatic lesions (Warshaw, 1973).

Finally, neoplasms can arise from the SG. Sebaceous carcinoma (SC), while relatively uncommon, is associated with a high rate of metastasis and recurrence following surgical excision. Peri-orbital SC is particularly metastatic (Dores *et al.*, 2008; Kyllo, Brady, & Hurst, 2015). SCs are evident histologically from their clear sebaceous differentiation,

but a range of immunohistochemical markers can be used in diagnosis, including adipophilin (PLIN2), epithelial membrane antigen (EMA/MUC1), and squalene synthase (SQS) (Ansai, 2017). Over-expression of *LRIG1* is also characteristic of SC (Pünchera, Barnes, & Kaya, 2016). Tumours of the SG can be indicative of Muir-Torre syndrome (MTS), a rare genetic disease of autosomal dominant inheritance (Torre, 1968; Abbas & Mahalingam, 2009; Jessup *et al.*, 2016). Those with MTS develop body-wide malignancies, but most frequently in the urogenital system, colon, and skin. In the skin, both sebaceous neoplasms and keratoacanthomas can be found. MTS is caused by mutations in the MLH genes (most commonly *MSH-2* and *MLH-1*), which are involved in DNA-mismatch repair (Abbas & Mahalingam, 2009).

1.7 Neuroanatomy of the pilosebaceous unit

The skin is a densely innervated organ. Neuropeptides and neurotransmitters released from cutaneous nerve fibres control many important processes in the skin, such as epidermal proliferation and apoptosis, wound healing, inflammation, and melanogenesis (Buckley *et al.*, 2012; Lebonvallet *et al.*, 2012; Cheret *et al.*, 2014; Blais *et al.*, 2014). Most skin appendages have a well-described nerve supply, such as the eccrine gland and HF (Montagna & Parakkal, 1974a, 1974b; Botchkarev *et al.*, 1997; Schulze *et al.*, 1997; Botchkarev *et al.*, 1999).

In the PSU, at the level of the bulge, a ‘basket-like’ structure of parallel running nerve fibres can be observed. Just below the level of the SG, a peri-follicular ‘ring’ of fibres is found, which run perpendicular to the length of the HF. In mouse skin, this network of nerve fibres is referred to as follicular nerve network B (FNB) (Figure 1.9) (Botchkarev *et al.*, 1997). The infundibulum is innervated by a less well-defined collection of nerve

endings which, in mice, is referred to as follicular nerve network A (FNA) (Botchkarev *et al.*, 1997) (Figure 1.9).

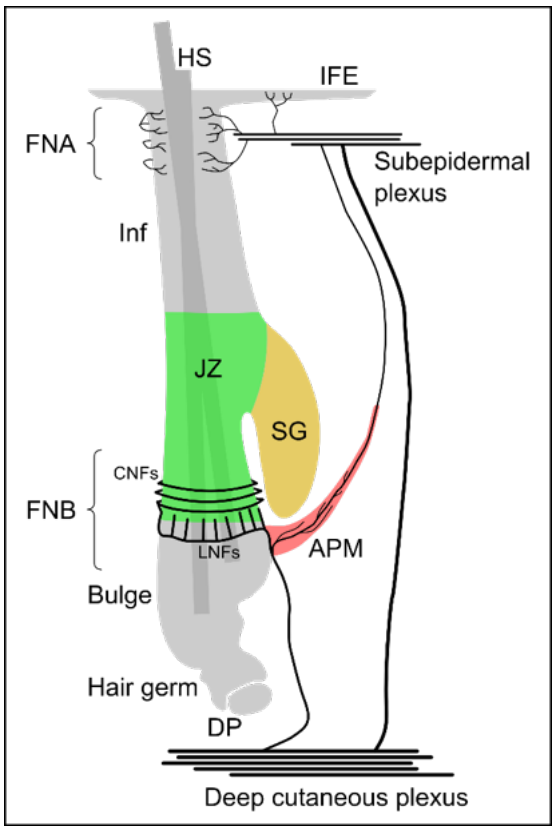

Figure 1.9 General neuroanatomy of murine pilosebaceous units.

The nerve supply to the mouse pilosebaceous unit (PSU) can be divided into two networks, follicular nerve network A (FNA) and follicular nerve network B (FNB). FNA is comprised of a loose collection of free nerve endings that supply the infundibulum (Inf). Comparatively, FNB represents a more structured arrangement of nerve endings that resides at the level of the bulge. Longitudinal nerve fibres (LNFs) and circular nerve fibres (CNFs), comprise FNB and run perpendicularly to each other. The primary function of LNFs is thought to be mechanosensation, while CNFs are nociceptors. HS, hair shaft. IFE, interfollicular epidermis; JZ, junctional zone; SG, sebaceous gland; APM, arrector pili muscle; DP, dermal papilla.

1.8 Principles of neuronal signalling

Neurons communicate to other cell types via the release of neurotransmitters: chemical substances that bind and modulate receptors on afferent cells (Bear, Connors, & Paradiso, 2007a). In the central nervous system (CNS), neuron-to-neuron communication is the principal form of neurocommunication (Connors, 2009), but many different types of cell can be innervated by neurons. In the skin alone, nerves are known to contact and

communicate with smooth muscle cells (Peters *et al.*, 2001), melanocytes (Zhang *et al.*, 2020), Langerhans cells (Gaudillere *et al.*, 1996), Merkel cells (Xiao *et al.*, 2015; Jenkins *et al.*, 2019), mast cells (Morellini *et al.*, 2018), keratinocytes (Talagas *et al.*, 2018), and sweat gland cells (Zhang *et al.*, 2018). Tight temporal coupling of neurotransmitter release to response of the target cells (for example, in the CNS or neuromuscular junction) requires close association of the neuron and target cell membranes and clustering of neurotransmitter receptors (synapse) (Bear, Connors, & Paradiso, 2007b; Connors, 2009). However, more diffuse and slow-acting types of neurocommunication also occur that do not require extensive synaptic specialisation (Goyal & Chaudhury, 2013).

There are various different types of neurotransmitter, which can be categorised according to their different characteristics. Many neurotransmitters are relatively small chemical compounds that are synthesised enzymatically (non-peptidergic; acetylcholine (ACh) or adrenaline), while others are gene products (peptidergic; i.e. calcitonin gene-related peptide (CGRP) or substance P) (Bear *et al.*, 2007a; Connors, 2009). Most neurotransmitters are packaged into discrete vesicles (vesicular) while others can diffuse through the presynaptic membrane or through membrane channels to signal to target cells (non-vesicular, such as adenosine triphosphate or nitric oxide) (Connors, 2009). The effect of any particular neurotransmitter is dependent on its cognate receptors expressed by the target cell, and the coupling of downstream effector proteins. For example, adrenaline can have opposing effects with regards to downstream adenylate cyclase and cAMP signalling, depending on whether the target cell expresses α_2 or $\beta_{1\text{-}3}$ adrenoreceptors (Richerson, 2009).

Secretion of vesicular neurotransmitters requires fusion of synaptic vesicles with the pre-synaptic neuronal membrane. This process is chiefly dependent on SNARE proteins, which are calcium-dependent proteins that facilitate membrane fusion (Bear *et al.*, 2007b; Ahnert-Hilger, Münster-Wandowski, & Höltje, 2013). The arrival of an action potential

depolarises the voltage across the cell membrane in the pre-synapse, causing an influx of extracellular calcium through voltage-gated calcium channels, which in turn stimulates SNARE proteins to fuse membrane-bound vesicles with the presynaptic membrane, releasing neurotransmitters into the extracellular space (Bear *et al.*, 2007b; Connors, 2009).

1.9 Neuroregulation of stem cells

Importantly, when considering the homeostasis and function of tissues, there is now an appreciation for a role of neurocommunication in the regulation of stem cells and stem cell niches. For example, sonic hedgehog (SHH)-secreting sensory nerves drive continual growth of the mouse incisor by acting on *Gli1*-expressing mesenchymal stem cells in the periarterial niche (Zhao *et al.*, 2014). In mouse skin, cutaneous nerves form niches for stem cells in the HF bulge (Brownell *et al.*, 2012; Cheng *et al.*, 2018) and in touch domes, which are special sensory structures of the epidermis comprised of Merkel cells (Xiao *et al.*, 2015). Again, both of these niches are characterised by the presence of innervated, *Gli1*-expressing stem cells that are dependent on nerve-derived SHH. Denervation leads to loss of *Gli1* expression and a loss of the functionality of innervated stem cell populations (Brownell *et al.*, 2012; Xiao *et al.*, 2015).

Recently, it has been demonstrated in mouse HFs, that the behaviour of melanocyte stem cells is modulated by adrenergic cutaneous nerve fibres, and hyperactivity of adrenaline signalling results in melanocyte depletion and hair greying (Zhang *et al.*, 2020). Furthermore, neuroregulated stem cells in skin also dictate the pattern of innervation through secretion of extracellular matrix components and neuron guidance cues (Füllgrabe *et al.*, 2015; Cheng *et al.*, 2018).

Other examples of innervated stem cell niches can include skeletal muscle, where transection of the sciatic nerve in rats results in depletion of supporting satellite cells in hindlimb muscle (Jejurikar, Marcelo, & Kuzon, 2002). Both development and homeostasis of the salivary gland is dependent on innervation of salivary gland stem cells. During salivary gland organogenesis in the mouse, cholinergic parasympathetic innervation is required to maintain K5+ progenitor cells in an undifferentiated state, and loss of innervation results in impaired development (Knox *et al.*, 2010). It has been subsequently shown in adult salivary glands that nerve-derived ACh is required to maintain SOX2+ acinar progenitor cells, which are required for continued homeostasis of salivary gland acini and functional secretion (Emmerson *et al.*, 2017, 2018).

It remains to be seen whether the progenitor cells that generate and maintain the SG are dependent on intact cutaneous innervation, or indeed, whether neurotransmitters might be able to affect sebocyte function directly.

1.10 Clinical indicators of functional sebaceous gland innervation

It has not yet been conclusively demonstrated whether SGs and sebocytes are innervated. Moreover, it is not known whether SGs are functionally dependent on the peripheral nervous system. The existence of neuronal control over SG function is, however, indicated by both historical as well as more recent clinical observations. In patients with partial facial paralysis, variations in the rate of sebum secretion can be observed between the normal and neurologically impaired halves of the face (Burton *et al.*, 1971a; Summerly, Woodbury, & Boddie, 1971). Unilateral facial acne has also been observed following partial facial paralysis (Tagami, 1983; Sudy & Urbina, 2018). Sebum secretion from the thighs of paraplegic patients is significantly higher than that in non-paraplegic controls, while the sebum excretion rate is unchanged above the level of spinal injury

(Thomas *et al.*, 1985). Furthermore, a significant decrease in sebum secretion can be achieved using topical anti-muscarinic agents (Cartlidge, Burton, & Shuster, 1972), and botulinum toxin-A ('Botox'), which prevents synaptic transmission via inhibition of SNARE proteins (Ahnert-Hilger *et al.*, 2013), has been used to effectively reduce acne severity and sebum secretion in humans (Jankovic & Diamond, 2006; Shah, 2008; Li *et al.*, 2013b; Min *et al.*, 2015). Together, these observations suggest that functional neurotransmission is required for maintaining normal levels of sebum secretion in humans. However, it remains to be seen whether SGs *in vivo* are indeed innervated or dependent on input from the peripheral nervous system.

1.11 Aims and objectives

The broad aims of this thesis are to establish whether SGs are functionally dependent on neurobiological input and, if so, to identify the cell and molecular mechanisms that underpin such dependence.

In order to fulfil these aims, the following questions are addressed:

1) Are sebaceous glands directly innervated?
2) Do sebaceous glands require intact cutaneous innervation?
3) Do sebaceous glands or known sebaceous progenitor cells express receptors for candidate nerve-derived substances?

To investigate, nerve fibres in both human and mouse skin were localised and mapped with relation to SGs and PSU through use of a combination of histochemical stains, immunofluorescence and electron microscopy. By identifying where nerve fibres terminate in relation to the SG, or regions of the HF that are thought to contain

intrafollicular progenitors, indications as to which cell biological mechanisms might be regulated by nerves were ascertained.

In parallel, the requirement of SGs for input from the peripheral nervous system was assessed in mice by means of unilateral surgical cutaneous denervation. Assessing the requirement of SGs for nerves *in vivo* in mice allows for better control of potential confounding factors such as age, hair cycle stage, and anatomical location. Moreover, unilateral denervation permitted for paired comparisons of denervated and intact SGs within the same animal, thus limiting the confounding effects of inter-individual variability on the observations.

To further characterise the mechanisms underlying neuronal control of SG homeostasis, transgenic reporter mice were used in conjunction with the method for cutaneous denervation, in order to perform lineage tracing of sebaceous gland progenitor cells. Finally, further mechanistic insight into any resulting denervated SG phenotype was derived by probing mouse skin for receptors for putative nerve-derived substances, via immunofluorescence and *in situ* hybridisation.

Chapter 2: Materials and methods

2.1 General animal handling

Wild-type (WT) C57BL/6J mice (Jackson), *Lrig1-Cre* (Jackson) (Powell *et al.*, 2012; Wang, Poulin, & Coffey, 2013) and *Rosa-mTmG* mice *(Gt(ROSA)26Sor$^{tm4(ACTB-tdTomato,-EGFP)Luo}$)* (Muzumdar *et al.*, 2007) were purchased from JAX® and housed according to Institutional Animal Care and Use Committee (IACUC) requirements associated with the Biological Resource Centre, Department 3 (BRC3), Singapore. Where required, animals were euthanised via CO_2 inhalation for at least 5 minutes, until breathing was no longer observable, followed by cervical dislocation. For the generation of *Lrig1-Cre* reporter mice used in lineage tracing experiments, heterozygous *Lrig1-Cre:Rosa-mTmG* mice were bred out to WT C57BL/6J mice.

2.2 Mouse genotyping

Mouse genotypes were confirmed from tail clippings and subsequent PCR and gel electrophoresis of extracted DNA. A small, 1-2 mm long piece of the distal tail was removed using surgical scissors for purposes of DNA extraction. While use of tail clippings is in line with approved IACUC protocols, according to Singapore Bioethics Council guidelines, it should be noted that ear punches/ear clipping represents a more refined and efficient method and can combine genotyping with animal identification purposes. Tail clippings were immediately immersed in hydrogen peroxide (H_2O_2) solution and incubated at ~100°C for 20 minutes with agitation. H_2O_2 was neutralised using TRIS-EDTA buffer. Tail lysates were then stored at 4°C prior to use for PCR. *Lrig1-Cre* and *Rosa-mTmG* mice were crossed to generate reporter mice. Genotypes were confirmed via PCR and subsequent gel electrophoresis.

The following primers were used:

Lrig1 3 - GACTTCACGAGGCACACTCGAT
Lrig1 5 - TCATCGCATTCCTTGCAAAAGT

Mtmg 1 - TCAATGGGCGGGGGTCGTT
Mtmg 2 - CTCTGCTGCCTCCTGGCTTCT
Mtmg 3 - CGAGGGGGATCACAAGCAATA

PCR reactions were prepared as follows:

5X MyTaq Red Reaction buffer – 2.5 µl

MyTaq DNA Polymerase – 0.063 µl

Template DNA – 1 µl

1 µM primer cocktail – 2.5 µl

Nuclease-free water – 3.93 µl

The following cycling conditions were used:

1. 95 °C 2 min
2. 95 °C 30 sec
3. 58 °C 30 sec
4. 72 °C 45 sec

Go to 2, repeat 35x

5. 72 °C 5 min
6. 4 °C hold

2.3 Waxing depilation

Anagen-induction by waxing depilation was performed via the following procedure, which was an amendment to existing IACUC protocols approved by the A*STAR Animal Care and Use Committee, according to Singapore Bioethics Council guidelines. The

method was based on a previously established protocol (Paus et al. 1997). A 1:1 mixture of Paraplast (Biomed Diagnostics, 39601006) and gum rosin (mixture referred to hereafter as 'depilatory wax' or 'wax') was heated to 60°C and mixed, before being cooled and stored as solid blocks for later use.

Before the procedure, adult (7-13 weeks old) mice were anaesthetised by isoflurane inhalation and the dorsal skin was shaved using electrical clippers (Wahl). The desired amount of depilatory wax was prepared by re-melting within heat-resistant glass or plastic containers placed on a benchtop hotplate. The melted wax was then allowed to cool until it became visibly opaque but still liquid. A small amount was applied to the back of a gloved hand to ensure the mixture had cooled sufficiently so as to not elicit pain. This cooled, melted wax was then applied liberally to the dorsal skin of the mouse using a metal or glass rod, against the direction of hair growth. Great care was taken to ensure, where applicable, that the wax did not touch any incision site from previous procedures. After the depilatory wax had cooled, it was peeled gently from the skin in the posterior-anterior direction. This procedure could be repeated up to 3 times on the same site, to ensure the complete removal of hair shafts.

2.4 Surgical cutaneous denervation

Cutaneous denervation was performed via the following procedure, which was an amendment to existing IACUC protocols approved by the A*STAR Animal Care and Use Committee, according to Singapore Bioethics Council guidelines. The technique for surgical cutaneous denervation of mouse dorsal skin was based heavily on previously established methods (Maurer *et al.*, 1998; Peterson, Brownell, & Wong, 2016). Where applicable, either WT C57BL/6J mice and *Lrig1-Cre:Rosa-mTmG* mice underwent the

cutaneous denervation procedure (Figure 2.1; Figure 2.2). Young (p21-24) or adult (7-13 weeks old) mice were anaesthetised by isoflurane inhalation and then administered meloxicam (analgesic), injected either subcutaneously or via intraperitoneal route. The fur was removed using electrical clippers (Wahl). Depilatory cream (e.g. Veet) can be used to completely remove all fur prior to surgery (1-2 minutes application), but this is not advisable for studies conducted in the context of the hair cycle, given the potential for inadvertent anagen-induction (Peterson *et al.*, 2016). Immediately prior to making the incision, the skin was cleaned and sterilised using a 1:4 Betadine solution diluted in sterile phosphate-buffered saline (PBS). Ophthalmic gel was applied to the eyes after fur removal to prevent excessive ocular dehydration.

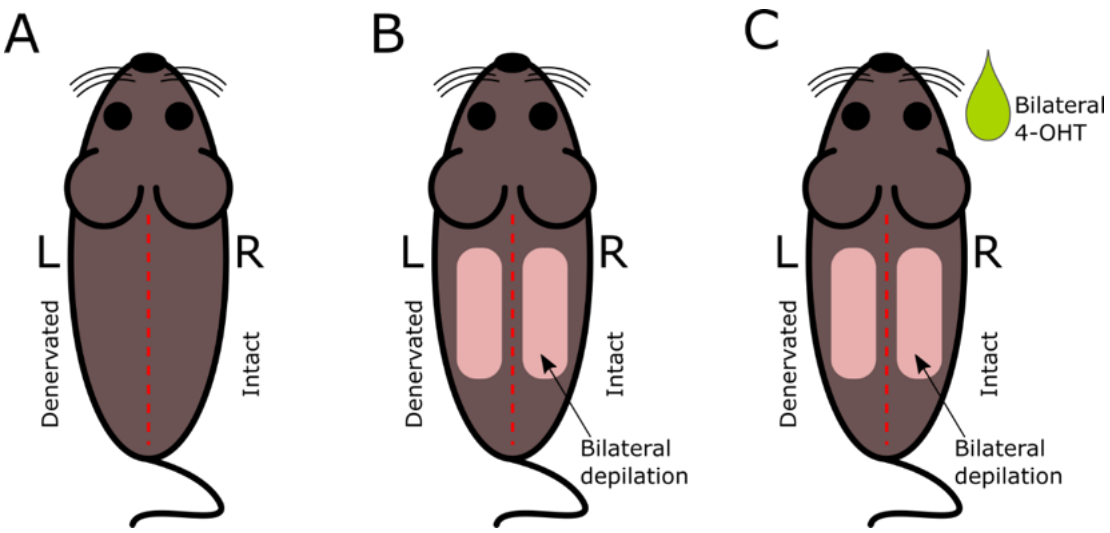

Figure 2.1 Primary experimental methodologies used in mice.

(A) Surgical cutaneous denervation (SCD) of mouse dorsal skin. Denervation is performed unilaterally (left flank) while the opposing (right) flank is left intact as a sham-operated control flank. An incision is made along the midline of the dorsal skin, and the skin is reflected to expose the underlying dorsal cutaneous nerves (DCNs), which can be removed by plucking. (B) Combination of SCD with waxing depilation for the induction of hair growth (anagen). After 5 days post-denervation, the incision from SCD is sufficiently healed to allow for depilation. A 1:1 mixture of paraffin:gum rosin is applied bilaterally, remaining at least 0.5 cm from the incision site. The hardened mixture is peeled off in the posterior-anterior direction, resulting in the removal of hair shafts. This procedure can be repeated up to three times to ensure the removal of all hair shafts. (C) Induction of Cre-recombinase-mediated lineage tracing in denervated/depilated mice by 4-hydroxy tamoxifen (4-OHT) application. Topical 4-OHT, suspended in acetone, is applied to the depilated skin.

An incision was made along the midline of the dorsal skin, beginning approximately 1-2 cm behind the ears and ending approximately 1-2 cm above the tail (Figure 2.1; Figure 2.2)). The dorsal skin of each flank was then gently reflected using blunt forceps. Throughout the procedure, the wound site was regularly moistened and flushed using sterile PBS. The dorsal cutaneous nerves were transected using fine forceps, at the point of exit from the trunk wall and at point of entry to the skin. The intervening segment of nerve was then removed (Figure 2.2). Particular attention was paid to ensure transection of nerves only, and not any adjacent vasculature. The incision was closed using non-continuous sutures placed approximately every 0.5 cm along the incision, and secured by application of cotton gauze, self-adhesive bandage, and surgical tape, all cut-to-size. The blunt end of a surgical tool (bandage scissors or scalpel handle) was passed beneath the bandage, to ensure the tightness of the bandage did not unacceptably restrict breathing.

Mice were monitored until recovery from anaesthesia and observed for manifest signs of pain and discomfort. For at least 3 days post-operation, mice were watered using bottled water containing enrofloxacin (antibiotic) and were administered daily doses of analgesic. After 3-5 days, the bandage was carefully removed using surgical scissors. Mice were then monitored for another 1-2 days to ensure continued integrity of the incision and progression of proper healing. In any instances of unacceptable pain, inflammation, or re-opening of the incision, mice were euthanised via the method described above. Successful denervation can be clarified by comparing the response of mice to being touched between the left and right flanks. Shuddering and turning of the head indicate the presence of functional sensation (Peterson *et al.*, 2016).

2.5 Genetically-inducible fate mapping (GIFM)

Recombination and subsequent lineage tracing of *Lirg1*-expressing cells in *Lrig1-Cre:Rosa-mTmG* mice was achieved via single topical application of 4-hydroxytamoxifen (4-OHT, Sigma Aldrich, H6278) in acetone. 50ul of 4-OHT solution at concentrations of either 15mg/ml, 0.75mg/ml, or 0.015mg/ml was applied to each flank of dorsal skin. In order to avoid potential systemic side effects induced by oestrogenic inhibition of sebotrophic hormones, such as androgens (Clayton *et al.*, 2019), 4-OHT was topically administered at end-point concentrations of 1.5mg/animal, 0.075mg/animal or 0.015mg/animal (Figure 2.1; Figure 2.3). A range of concentrations were selected as it was not known which concentrations would be sufficient to induce recombination, or at what concentration labelling would saturate. The chosen concentrations were based on preliminary data from Dr Sia Junren, ascertained through intraperitoneal 4-OHT injections of *Lrig1-Cre:Rosa-mTmG* mice.

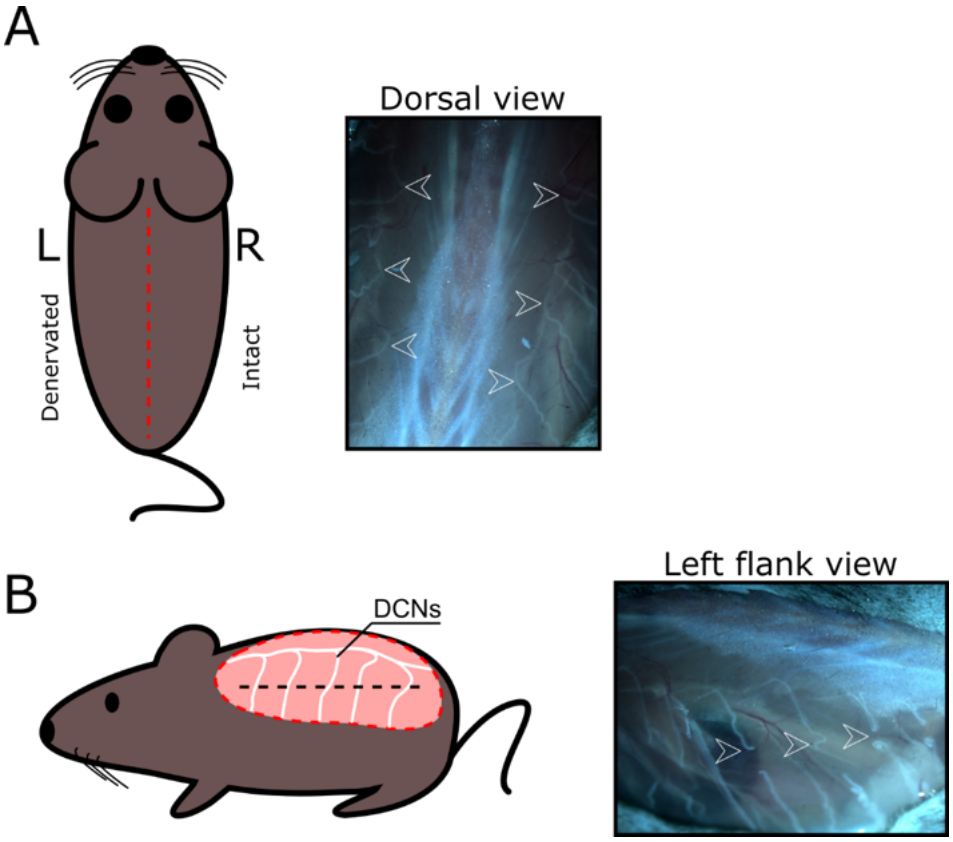

Figure 2.2. Performing surgical cutaneous denervation of mouse dorsal skin.

(A) Surgical cutaneous denervation is performed in mice, resulting in unilateral loss of nerve endings in dorsal skin (Peterson et al., 2016). Mice are anaesthetised and shaved. An incision is made along the dorsal midline, from roughly 1 cm below the ears and 1 cm above the tail. Both the left and right flanks are gently reflected to reveal the underlying fascia and trunk wall. **(B)** The dorsal cutaneous nerves (DCNs), which supply the dorsal skin, are superficially located and are easily spotted (arrowheads). On the left flank only, all of the visible DCNs that exist between the scapula and hind limb brown adipose tissue are removed by plucking with sharp forceps. These nerves correspond approximately to vertebrae T3-T12. Care must be taken to avoid damaging associated blood vessels. After removal of the DCNs, the incision is closed with sutures. Successful denervation can be tested behaviourally using a pin-prick test (Peterson et al., 2016).

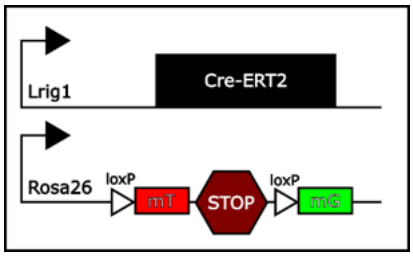

Figure 2.3. Molecular basis of genetically inducible fate mapping of *Lrig1*-expressing cells.

Lineage tracing of *Lrig1*-expressing cells can be achieved using *Lrig1-Cre:Rosa-mTmG* transgenic mice. Inducible Cre recombinase is expressed downstream of the *Lrig1* promoter. Concurrently, the *mTmG* reporter transgene is expressed downstream of the ubiquitous promoter, rosa26, resulting in widespread red fluorescence prior to induction. Induction of Cre-ERT2 activity via treatment with oestrogenic compounds (tamoxifen or 4-OHT) results in activation of Cre-recombinase. The arrangement of loxP sites within the *mTmG* transgene sites results in excision of mTomato and the STOP sequence by Cre recombinase, allowing for expression of EGFP exclusively in *Lrig1*-expressing cells.

2.6 General tissue processing and microtomy

Harvested mouse tissues were fixed for either paraffin or optimal cutting temperature (OCT) compound-embedding by first fixing in either 4% methanol-free formaldehyde (Pierce, 28906) for 24 hours at room temperature, or in 4% paraformaldehyde (Merck, 30525-89-4) for 18-24 hours at 4°C. Formalin-fixed tissues were dehydrated and embedded in Paraplast (Biomed Diagnostics, 39601006) and stored at room temperature. Paraformaldehyde-fixed tissues were washed in PBS before incubating for 3-5 days in 30% sucrose w/v in PBS at 4°C. The use of sucrose is intended to displace water and limit formation of ice crystals during the freezing process, which can have a disruptive effect on tissue histology and make cryo-sectioning more difficult. Tissues were then embedded in OCT, frozen on dry ice, and stored at -80°C. OCT-embedded tissue was sectioned (7-30 μm for general immunofluorescence, or >100 μm for free-floating stains; see below) using a cryo-microtome and stored at -80°C prior to use.

2.7 Immunostaining

The primary antibodies used, and their incubation conditions are detailed in Table 1. Where needed, appropriate Alexa Fluor-conjugated secondary antibodies were used at concentrations of 1:500/1:1000 either at room temperature for 1 hour, overnight at 4°C, or 24 hours at 4°C, depending on the application. Staining of thicker sections requires reduced antibody concentration over a longer incubation in order to balance penetration with a sufficiently low background signal.

Table 1. Primary antibodies and incubation conditions.				
Antibody	**Labelling**	**Manufacturer**	**Concentration**	**Conditions**
Rabbit anti-PGP9.5	All nerve fibres	Abcam, ab108986	1:100*	1hr, RT
Rabbit anti-Ki67	Proliferative cells	Abcam, ab16667	1:50	1hr, RT
Guinea-pig anti-synaptophysin 1	Synaptic vesicles	Synaptic Systems, 101004	1:500	O/N, 4℃
Goat anti-CGRP	C-fibres/nociceptor neurons	Abcam, ab36001	1:500	O/N, 4℃
Mouse anti-LRIG1 Alexa Fluor® 488-conjugated	SG progenitors in JZ	R&D Systems, FAB3688G	1:20	1hr, RT
Guinea-pig anti-adipophilin	Sebocytes/adipocytes	Fitzgerald, 20R-AP002	1:100	O/N, 4℃
Mouse anti-embigin-APC	Mouse sebocyte membrane	Miltenyi Biotec, 130-117-527	1:100	1hr, RT
Alpha bungarotoxin Alexa488-conjugated	Neuromuscular junctions	LifeTech, B13422	1:100	O/N, 4℃
Rabbit Neuro-Mark Pan Neuronal Marker Cy3-conjugated	All nerve fibres	NeuroChrom, Merck, ABN2300C3	1:100	1hr, RT
Rabbit anti-VR1	Thermoreceptors/nociceptor neurons	Abcam, ab31895	1:500	O/N, 4℃
Rabbit anti-beta III Tubulin	Larger diameter nerves	Abcam, ab18207	1:100*	1hr, RT
Rabbit anti-MUC1 antibody	Human sebocyte cytoplasm	Abcam, ab15481	1:200	O/N, 4℃

Footnotes: RT, room temperature; O/N, overnight; *concentrations down to 1:1000 can be used for free-floating stains for incubations over 1-3 days at 4℃.

For labelling of mouse SG cell nuclei, the following reagents were used: Vectashield mounting media with DAPI (Vectashield, H-1200), NucBlue Live Cell Stain 6 (ThermoFisher, R37605), NucBlue Fixed Cell Stain 6 (ThermoFisher, R37606), TO-PRO-3 Iodide (ThermoFisher, T3605). Murine sebaceous lipids were labelled in situ using: HCS LipidTOX Green Neutral Lipid Stain (ThermoFisher, H34475), HCS LipidTOX Red Neutral Lipid Stain (ThermoFisher, H34476), HCS LipidTOX DeepRed Neutral Lipid Stain (ThermoFisher, H34477).

Cryo-sections were air-dried then permeabilised in 0.1% Triton X-100 in Tris-buffered saline (TBS). For the antibody incubation buffer, a solution of 2% bovine serum albumin, 0.3M glycine, 0.1% Tween 20, and 1% dimethyl sulfoxide (DMSO) in TBS was used. The composition of this buffer, including the incorporation of DMSO, was intended to facilitate antibody penetration in thick sections (Sorrells *et al.*, 2013) and could also be

used for standard-thickness sections (5-30 μm). The antibody buffer was supplemented with serum corresponding to secondary antibody host species. 0.05% Tween 20 w/v in TBS served as general wash buffer (TBST).

For floating immunostaining of thick sections (>100 μm), tissues were pre-treated with 20μg/ml proteinase K (Thermo Scientific, EO0491) in 0.1% Triton-X-100 in TBS or 0.5% saponin (Santa Cruz, sc-280079A) for 1-2 hours at room temperature. Sections were then washed for 3x15 minutes in TBST or 0.5% w/v saponin before primary incubation. Floating sections were incubated in primary and secondary antibodies for at least 24 hours each. Thick sections were optically cleared before imaging and mounted using RapiClear 1.47 (SunjinLab, RC147002) according to the manufacturer's instructions.

Sections of paraffin-embedded tissues were cleared before staining using the following protocol: Immerse slides in xylene for 3 minutes, then in fresh xylene for a further 3 minutes. Immerse slides in 100% ethanol for 3 minutes, then 90%, 80% and 70% ethanol for 3 minutes each. Finally, immerse slides in distilled water for 3 minutes.

2.8 Confocal fluorescent microscopy and image analysis

Fluorescent tissues were imaged using Olympus FV3000 and FV3000 RS confocal laser scanning microscopes, using 405 nm, 488 nm, 561 nm, and 640 nm laser lines and high sensitivity spectral detectors. Lenses used were 20X, 40X, and for imaging of thick, floating-stained tissues, 30X silicon lens. Confocal stacks were loaded into Imaris (version 9.2, Bitplane) for three-dimensional projection (Figure 2.4). SGs were manually delineated based on LipidTox or embigin staining. SG volume was quantified using the 'Generate surface' function which generates a 3D volume render of a region of relatively high signal within a manually segmented region of interest (based on staining of SG lipid).

SG cell number was quantified using the 'Detect dots' function which identifies and counts the number of spheres of a given radius (up to 4-5 μm), again within a manually segmented region of interest (based on DAPI or TO-PRO-3 Iodide staining).

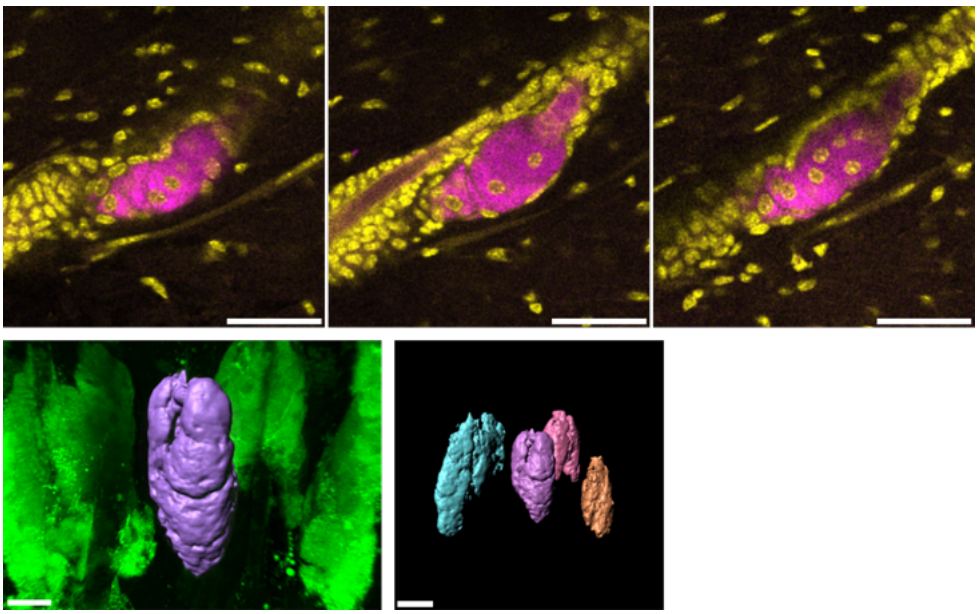

Figure 2.4. Staining, imaging and three-dimensional reconstruction of murine sebaceous glands.

Whole sebaceous glands (SGs) in mouse skin can be readily visualised by staining thick (~100 μm) sections of skin with lipophilic dyes (HCS LipidTOX Green Neutral Lipid Stain shown). Nuclei can also be visualised using DAPI or, as in the above panels, TO-PRO™-3 Iodide. Tissues can be optically cleared and imaged by confocal microscopy (three optical sections of the same SG shown in the top panels). Sebaceous lipids, magenta; Nuclei; yellow. Confocal stacks can then be imported into software for three-dimensional reconstruction, and the extraction of SG volume, cell number, and other parameters. Renders of entire mouse SGs shown in the bottom panels (pastel colours). Scale bars = 50 μm.

Lipid intensity analysis and quantification of proliferation were performed using Fiji ImageJ. The number of Ki67+ nuclei was counted manually and expressed as a percentage of overall detected nuclei. For lipid intensity, SG were delineated using the 'adjust threshold' function, which arbitrarily assigns pixels below a certain threshold to have a grey value of zero, effectively isolating SGs according to their relatively high staining intensity. The remaining signal was then converted to binary and SG outlines were extracted by using the 'analyse particles' function, which isolate particles over a certain size. The detected SGs were then overlaid onto the original image and the lipid signal (raw integrated density) was measured. The measured raw integrated density was

then normalised for SG area. Hair follicle staging was conducted using previously published guidelines (Müller-Röver et al. 2001).

2.9 RNA in situ hybridisation

Sections (5-7 μm) of paraffin embedded mouse tissue were cut and dried at 60 °C for 1 hour and stored in a humidity-proof dry cabinet before use. Sections were cleared using the protocol outlined above (Section 2.7). All probes and reagents were provided by ACDBio. Sections were then processed for detection of RNA in situ using either RNAscope 2.5 HD Reagent Kit-Red (322350) or RNAscope 2.5 HD Duplex Reagent Kit (322430) following the manufacturer's instructions.

The following probes were used: Mm-Lrig1 (310521); Mm-Gli1 (311001); Mm-Gli1-C2 (311001-C2); Mm-Chrna (465161); Mm-Calcr (494071); Mm-Calcrl (452281), Mm-Tacr1 (428781); Mm-Grm5 (423631), Mm-Chat (408731), and Mm-Slc1a3 (430781). Mm-Polr2a (312471) and *Dapb* (310043) were used in single-plex experiments as positive and negative control probes respectively. For duplex RNAscope, a positive control mixture of probes for *Ppib* and *Pol2ra* (321651) was used, while the negative control mixture is proprietary (320751).

For each paraffin block of tissue, positive and negative control probes were used to ensure presence and proper preservation of mRNA and lack of background signal. Where appropriate, positive control tissues that are known to express the gene of interest were also used to check for probe functionality.

2.10 Electron microscopy

Mouse whisker pad, auricular, and dorsal skin samples were fixed overnight in 4% formaldehyde and 2% glutaraldehyde (Electron Microscopy Sciences-EMS, USA) in 0.1 M sodium cacodylate buffer (pH 7.4) containing 2 mM calcium chloride.

The following was performed at the electron microscopy facility within the A*STAR microscopy platform (AMU).

After fixation samples were trimmed into 2x3 mm rectangular blocks and post-fixed in a mixture of 1% osmium tetroxide (EMS) and 1.5% potassium ferrocyanide for 3h. Fixed tissues were rinsed in distilled water and processed in parallel for embedding in either Durcupan (Sigma) or Epon (Serva) resins as follows: (1) dehydrated in ethanol series followed by propylenoxide infiltrated end embedded in Epon and polymerised at 65℃ for 48 hrs; (2) dehydrated in acetone series, infiltrated and embedded in Durcupan and polymerised at 80°C for 48 hrs. Ultrathin sections for imaging were cut with a diamond knife (Diatome, Switzerland) on a Leica Ultracut EM UC7 ultramicrotome (Leica Microsystems, Germany) and collected onto copper slot grids (EMS). Sections on grids were then counterstained with 4% aqueous uranyl acetate followed by Reynold's lead citrate. Imaging was conducted on a JEM-1010 Jeol transmission electron microscope (JEOL Ltd., Japan) operating at 80 kV.

2.11 Statistics

Throughout the thesis, means are reported along with 1 standard deviation (SD). Where given, individual data points (n) represent the mean value for a given animal, or individual measurements. The number of biological replicates and the number of individual measurements is reported in each figure legend, where appropriate.

Different statistical tests were used according to the type of data and comparison being made. For comparison of means which represent different experimental conditions within the same animals (e.g. denervated and non-denervated means from mouse #1, denervated and non-denervated means from mouse #2, etc.), t-test for paired samples was used. For multiple comparisons of paired samples, significance was determined using Repeated Measures one-way analysis of variance (ANOVA) with Sidak's correction. Single comparisons of independent data were made using unpaired t-test with Welch's correction for uneven variance. Multiple comparisons of independent data were performed using Welch's ANOVA with Dunnet's correction. For comparison of multiple data sets comprised of pooled, individual measurements from multiple biological replicates, Kruskal-Wallis one-way ANOVA was used with Dunn's correction.

Statistical significance was accepted if $P<0.05$ and indicated in figures with the attributable P value, or alternatively, the following placeholders: * = $P<0.05$; ** = $P<0.01$; *** = $P<0.001$; **** = $P<0.0001$. Graphing and statistical analyses of data were performed using GraphPad Prism®.

It should be noted that for some datasets, chiefly those based on experiments conducted in *Lrig1-Cre:Rosa-mTmG* mice and later resolved on the basis of gender, a low animal 'n' is sometimes reported (e.g. n = 1). This is due to the lack of control over litter composition and genotype, meaning that some experiments only had a small number of useable animals. The number of animals and number of individual SG measurements are detailed in the figure legends. Power calculations were not performed.

2.12 Collection & general processing of human tissue

Scalp and abdominal skin were supplied by Bradford Hospital or Salford Royal Hospital. Isolated follicular units were kindly supplied by the Crown Cosma Clinic and Farjo Clinic, Manchester. All tissue samples were kept registered, stored and tracked under the Manchester Skin Health Biobank following Human Tissue Act (HTA) guidelines in HTA licenced storage, with patient consent.

Fixation for paraffin embedding involved placing tissue in 10% formalin for 24 hours. After this, tissue was placed directly into cassettes, either between filter papers or in fine-netted processing bags and stored in 70% ethanol at room temperature before embedding in paraffin wax. For frozen samples, the tissue was placed in OCT and snap frozen in liquid nitrogen.

2.13 Silver methods for nerve fibres

Winkleman-Schmidt method: Frozen sections were placed in 20% silver nitrate (weight/volume) in distilled water for 20-30 minutes. Sections were then rinsed in three changes of distilled water, placed in a developer mixture containing 0.2% hydroquinone and 1% sodium sulphite solution for 10 minutes, and then rinsed in two changes of distilled water and toned in 0.2% gold chloride for 2 minutes. Sections were then washed in distilled water and then placed in 5% sodium thiosulfate. After a final rinse in distilled water, the sections were mounted using an aqueous mounting media, or cleared in xylene for 10 mins and mounted in Eukitt (Merck, 05393) (for paraffin sections). Sections stained by this method are almost entirely unstained save for nerve fibres and melanocytes, which are stained black/brown.

2.14 Light microscopy of ultra-thin sections

The following was performed with the guidance of Professor Desmond Tobin at the University of Bradford.

Freshly micro-dissected follicular units with SGs (Crown Cosma Clinic) were washed briefly in PBS and then fixed in half-strength 'Karnovsky's fixative' at pH 7.4 overnight at 4°C. The fixative was made by the procedure detailed below. After fixation the units were washed in three changes of 0.1 M sodium cacodylate buffer, and where convenient, were stored in the final wash at 4°C prior to post-fixation. Sodium cacodylate buffers were made by adding the appropriate amount of sodium cacodylate to distilled water and adjusted to pH 7.4 with 1 M HCl. The fixed follicular units were then incubated in a 2% solution of OsO_4 as post-fixative for 1 hr at room temperature, and then washed in three changes of distilled water before storage in 70% ethanol. The follicular units were held in 70% ethanol at this stage for between 1-2 months at 4°C.

Immediately prior to embedding, the units were removed from 70% ethanol and moved to 95% ethanol at 4°C for 20 minutes, followed by three consecutive 20 minute incubations in 100% ethanol, firstly refrigerated (4°C) and then at room temperature. This stage is crucial as it ensures full removal of water from the tissue before adding the resin. The araldite-based resin was made via the procedure detailed below. The resin was mixed with propylene oxide (PO) and the follicular units were placed in the following mixtures at room temperature: 2:1 PO:resin for 1hr, 1:1 PO:resin for 3hrs, 2:1 PO:resin overnight. After the final mixture, the units were left in 100% resin for 24 hours before being placed into pill moulds with fresh resin. The resin pills containing the units were allowed to polymerise at 60°C for around 3 days.

Before sectioning, the pills were trimmed down by hand using razors. Glass knives were prepared on a Reichert-Jung knife maker. Using a Reichert Ultracut E Ultramicrotome, semi-thin sections were cut at a thickness of between 0.5 μm-1 μm and floated onto water in knife boats. Sections were moved to slides using an inoculation loop and dried.

Staining & Imaging: Slides were stained with Toluidine Blue O solution for 30 seconds and rinsed with cool tap water before mounting. Bright field images were taken on a Keyence all-in-one microscope using 20-60X lenses.

Half-strength Karnovsky's fixative was prepared via the following protocol:

1. (Solution A) Add 2 g EM-grade paraformaldehyde to 20ml distilled H_2O and stir at 60-70.C for 40 minutes to 1 hour. Slowly drop in 1M NaOH until the solution clears.

2. (Solution B) To 20ml of 0.2M sodium cacodylate buffer add 10ml EM-grade glutaraldehyde (25%) and 25 mg $CaCl_2$.

3. Mix the solutions A and B. Add 50ml of 0.1M sodium cacodylate buffer to make 100ml of a 1:1 dilution. This is the half-strength 'Karnovsky fixative'.

Araldite resin was prepared via the following protocol:

1. For ~50ml of resin, heat separately 25 ml of araldite and 25 ml of dodecenyl succinic anhydride (DDSA) at 60°C for around 10 minutes.

2. Add the DDSA to the araldite and stir gently for 10 minutes. Avoid bubbles.

3. Add the accelerator, benzyl dimethylamide (BDMA) and continue to stir for another 10 minutes. When thoroughly mixed, leave to settle for around 1-2 hours.

Chapter 3: Characterising sebaceous gland neuroanatomy

3.1 Introduction

3.1.1 Previous attempts to identify and characterise sebaceous gland innervation

Earlier works that have attempted to demonstrate the putative nerve supply to the SG have relied primarily on the use of histochemical stains, such as silver nitrate deposition, or enzymatic staining using modified cholinesterase substrates, which indicates the presence of ACh-secreting nerve fibres (Champy, Coujard, & Coujard-Champy, 1945; Winkelmann & Schmit, 1959; Hashimoto, Ogawa, & Lever, 1963; Pawlowski & Weddell, 1967). However, no study has yet been able to accurately map the extent of sebaceous nerve fibres, nor determine where these nerve fibres terminate. Using the cholinesterase technique, some authors have claimed that cholinesterase-reactive nerve fibres can be seen in proximity to SGs (Montagna & Ellis, 1957a), while others have claimed there is no such innervation of the SG (Hurley, Shelley, & Koelle, 1953; Hellmann, 1955).

Isolated ultrastructural evidence of nerves in the SG connective tissue has been reported in rat (Pawlowski & Weddell, 1967; Dugan, 1974) and camel skin (Taha, 1988). The most recent report regarding sebaceous innervation has described nerve fibres in the stroma of human SGs that contain neuropeptide substance P, yet only in acne lesion-associated glands (Toyoda *et al.*, 2002a). Taken together, these findings paint a somewhat confusing image of SG innervation and raise the possibility that nervous input to human SGs might only exist, or become manifest, in the context of SG dysfunction. This may explain the historical difficulty in identifying and accurately mapping sebaceous neuroanatomy. A further, as yet unexplored possibility is that nerve fibres control the SG not by direct innervation, but by acting on sebaceous progenitors within the HF (Füllgrabe *et al.*, 2015; Barnes, Saurat, & Kaya, 2017).

3.1.2 Experimental aims

Here, the innervation status of human and mouse SGs was evaluated, using a combination of histochemical and immunological staining methods, as well as transmission electron microscopy (TEM).

The key experimental aims were as follows:

- Identify whether nerve fibres can be observed entering the SG mesenchyme and contacting the SG epithelium.
- Map nerve endings in relation to markers for SG progenitor cells labelled by expression of *Lrig1*.
- Quantify the frequency of neuronal-sebocyte contacts and the proximity of nerve endings to the SG.
- Identify whether nerves in proximity to the SG contain secretable substances that could act on sebocytes.

The resin embedding and toluidine-blue-staining of human tissues was performed in collaboration with Prof. Desmond Tobin at the University of Bradford. TEM was carried out in collaboration with Dr David Liebl at the A*STAR Microscopy Unit (AMU).

3.2 Results

3.2.1 Re-examination of human sebaceous gland innervation

The Winkleman-Schmidt method for silver-staining of nerve fibres was used on 30-50 μm thick sections of frozen human scalp skin. This method produces a high contrast stain,

with the formation of brown/black silver deposition on cutaneous nerve fibres (Figure 3.1). The SG is readily recognised by the 'foamy' appearance of sebaceous lipid droplets. While nerve fibres can be observed to approach the SG and pass through the CTS surrounding the SG (Figure 3.1), it is difficult to discern whether the SG is directly innervated without a method for definitively delineating the SG epithelium, or a method of extracting discrete focal planes from images of thick sections.

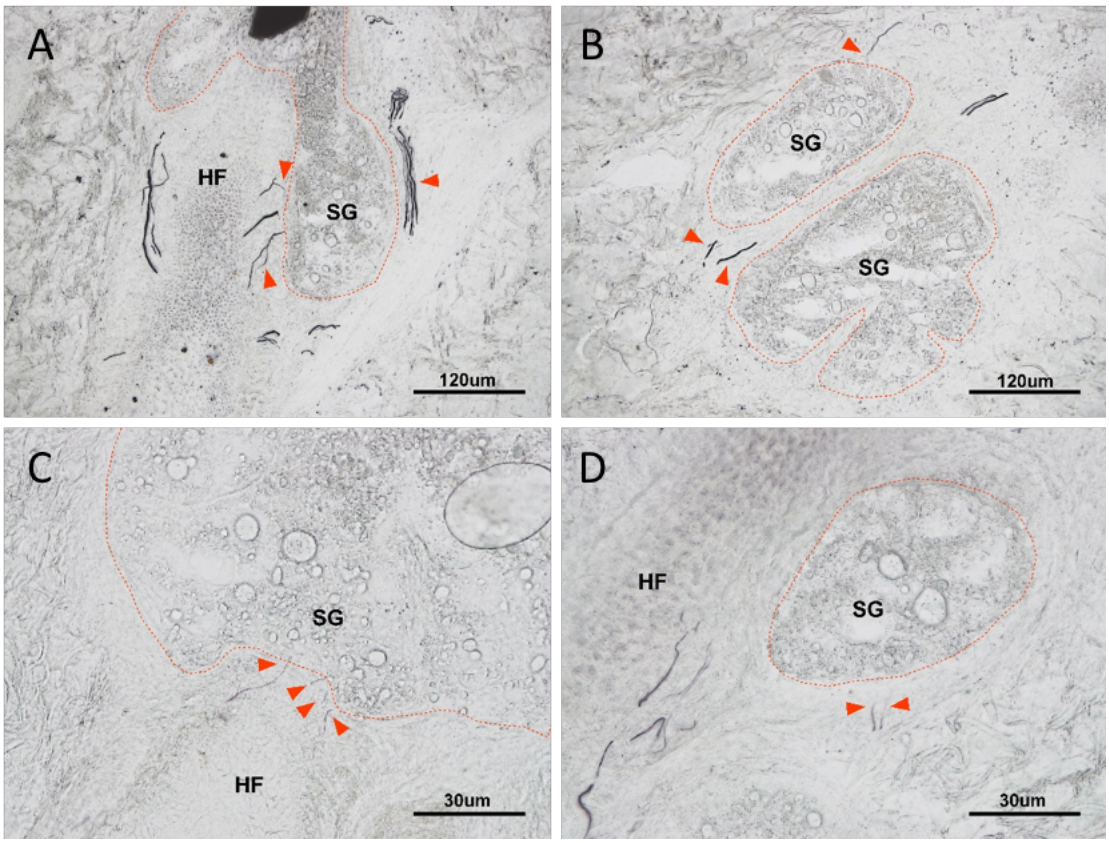

Figure 3.1. Silver-staining method reveals nerve fibres in the proximity of human sebaceous glands.

Brightfield images showing nerve fibres in relation to sebaceous glands (SGs) in occipital scalp skin, stained using the Winkleman & Schmidt method for silver impregnation of peripheral nerve fibres. Orange lines delineate SG lobes. In A, C-D, nerves constituting the peri-follicular nerve network can also be observed. Arrows indicate silver nitrate-stained nerve fibres. All images are derived from minimum intensity projections of consecutive images at different focal planes of the same field of view. SGs are recognisable by their foamy appearance. HF, hair follicle. Scale indicated in each panel.

Therefore, ultra-thin sections (0.5 µm) of resin-embedded human scalp SGs were stained with toluidine blue to more closely examine nerves in relation to the SG epithelium (Figure 3.2). At least two SGs each from three separate patients were examined.

Myelinated nerve fibres are evident from the peripheral blue/teal colouration. As was observed using the sliver method, nerves can be observed within the mesenchyme around the SG, and in the intervening space between the SG and follicular epithelia (Figure 3.2). However, no nerves were observed in contact with the sebaceous epithelium.

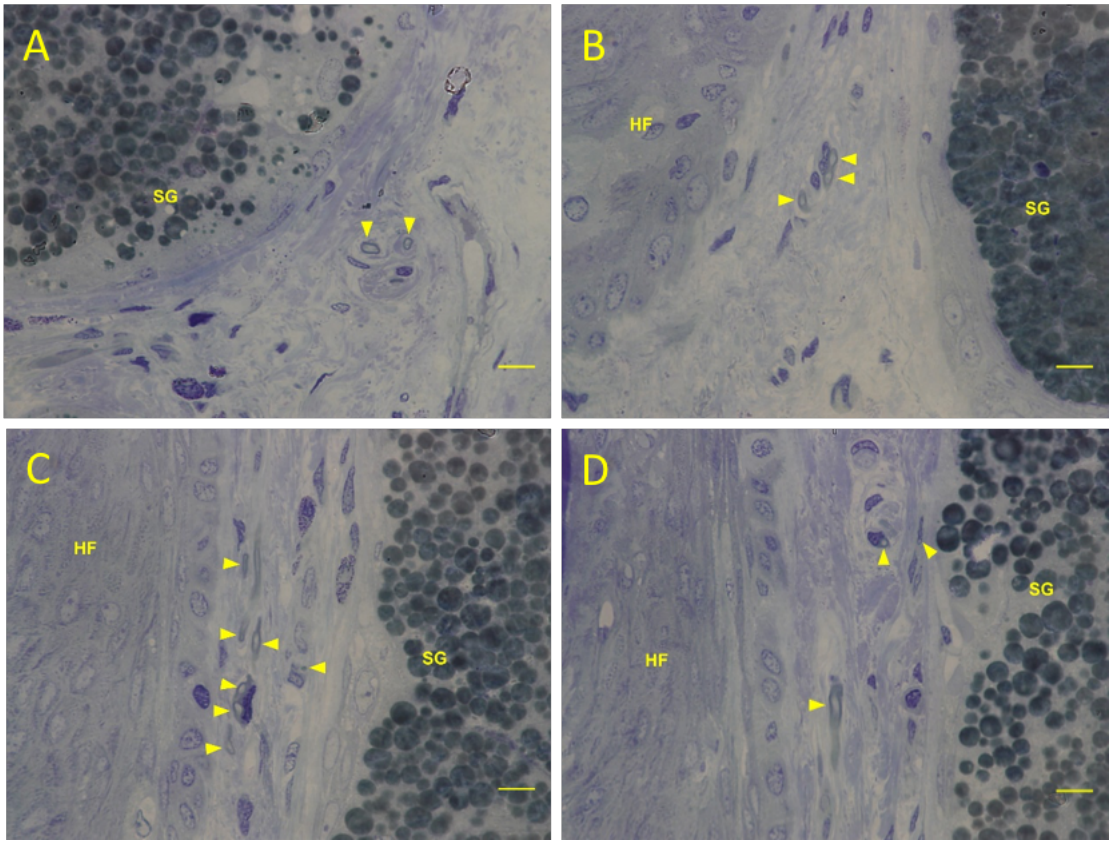

Figure 3.2. Nerve fibres and sebaceous glands in toluidine-blue-stained sections of occipital scalp skin.

Resin embedded human scalp tissue was cut at a thickness of 0.5 µm and stained with toluidine blue. Myelinated nerve fibres can be observed in cross-section. **(A)** Peripheral nerves can be observed approaching the sebaceous gland (SG) connective tissue sheath, but are rarely observed in proximity to the SG epithelium. **(B-D)** Nerves can regularly be observed in the intervening space between SGs and the hair follicle (HF) epithelium, which likely form part of the peri-follicular nerve network. Putative nerves indicated by yellow arrowheads. Scale bars = 10 µm.

For immunofluorescent detection of nerve fibres in human skin, an antibody specific for beta-3-tubulin (TUBB3) was used, which is considered a broad-spectrum nerve fibre marker (Ferreira & Caceres, 1992; Schulze *et al.*, 1997). TUBB3+ nerves fibres were observed in relation to the SG epithelium by labelling SGs with an anti-mucin 1 (MUC1)

antibody. A series of serial sections (7 μm thick) through scalp skin from one patient was examined. As with the silver-method and toluidine-blue staining, both TUBB3+ nerve fibre bundles and isolated nerve fibres can be observed in proximity to the SG (Figure 3.3). The isolated fibres are often concentrated to the lower lobes, where the APM can be found, but they can also be seen within the inter-lobular CTS or scattered about the SG periphery (Figure 3.3). No superposition of TUBB3+ staining with MUC1 was evident, suggesting that the human SG epithelium is not directly innervated.

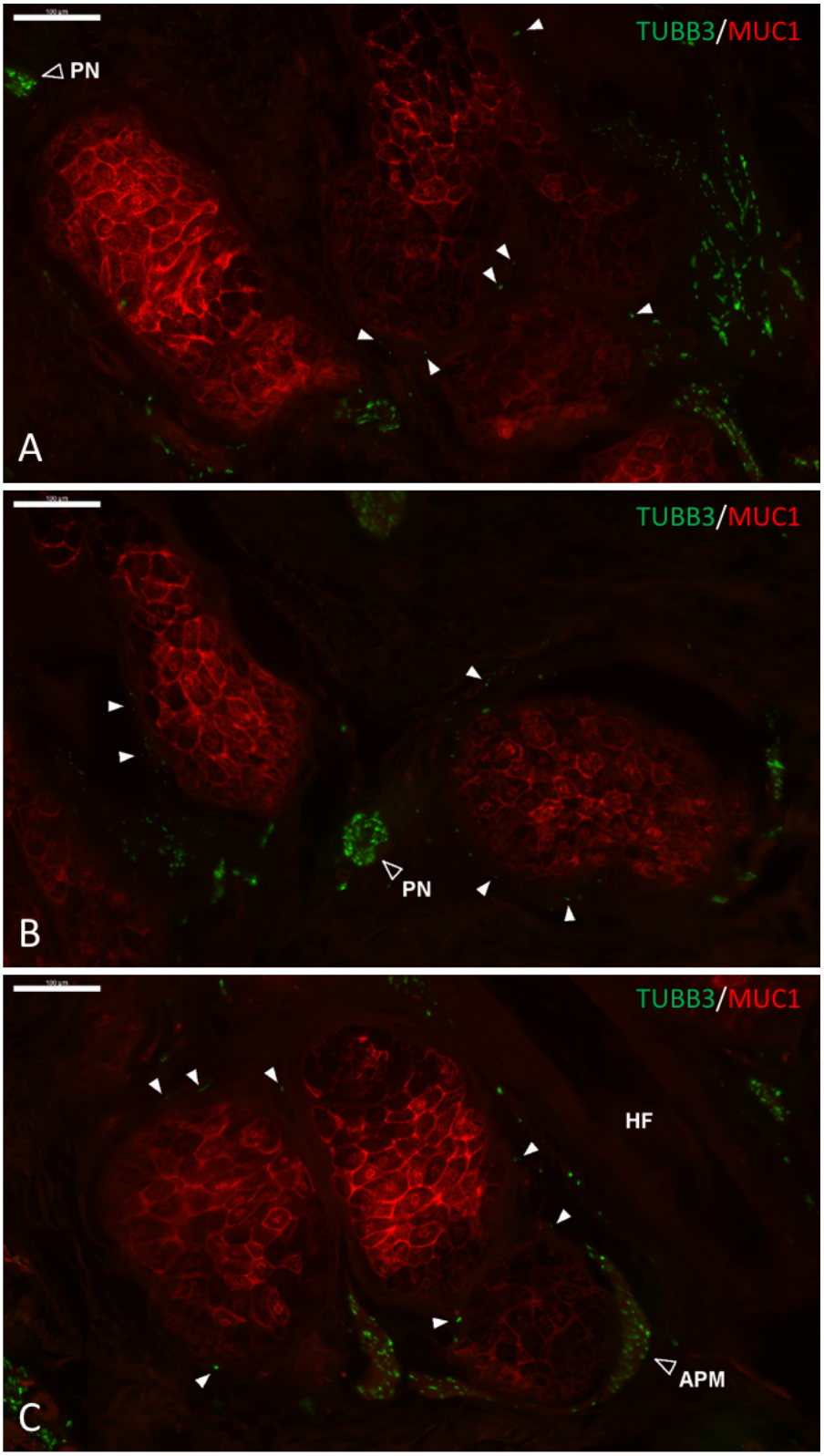

Figure 3.3. β3-tubulin-expressing nerve fibres adjacent to human sebaceous gland stroma.

Paraffin-embedded human occipital scalp skin incubated with anti-β3-tubulin (TUBB3) antibody (green). Sebaceous glands (SGs) labelled with anti-mucin (MUC1) antibody (red). TUBB3+ nerves can be observed approaching/entering the SG connective tissue sheath, (CTS), or stroma (white arrowheads). However, no innervation of the SG epithelium appears to occur. HF, hair follicle; APM, arrector pili muscle; PN, peripheral nerve. Scale bars = 100 μm.

3.2.2 Investigation of hypothesised neuronal-sebocyte interactions via immunofluorescent confocal microscopy in mouse skin

Next, the neuroanatomy of murine PSUs was examined in relation to SGs. Given their smaller size relative to human SGs, intact murine SGs can be visualized in thick, optically cleared sections of mouse skin, allowing for more complete visualisation of the surrounding neuroanatomy. Nerve fibres in dorsal skin were labelled with an antibody targeting the broad spectrum nerve fibre marker protein gene-product 9.5 (PGP9.5) (Maklad *et al.*, 2009; Nolano *et al.*, 2013). As reported previously, two distinct follicular nerve networks can be observed in mouse PSUs (Figure 3.4) (Botchkarev *et al.*, 1997; Peters *et al.*, 2002). Follicular nerve network B (FNB) is comprised of a network of circular and longitudinal nerve fibres (CNFs and LNFs) surrounding the HF at the level of the bulge and SG (Figure 3.4A). A more loosely structured collection of nerve endings supplies the distal infundibulum, known as follicular nerve network A (FNA). The APM also receives its own supply of PGP9.5+ nerve fibres (Figure 3.4A).

Interactions between nerves comprising FNB and the SG epithelium were then more closely examined, with the SG being effectively delineated by staining for the lipid-droplet associated protein, adipophilin (Figure 3.4B). While the CNFs and APM nerve supply can be seen in close proximity to the SG no superposition of PGP9.5 staining with the SG epithelium was observed, suggesting that the murine SG is not directly innervated (Figure 3.4B). Comparatively, LNFs are closely associated with the HF epithelium at the level of the SG and appear to directly contact follicular keratinocytes (Figure 3.4B).

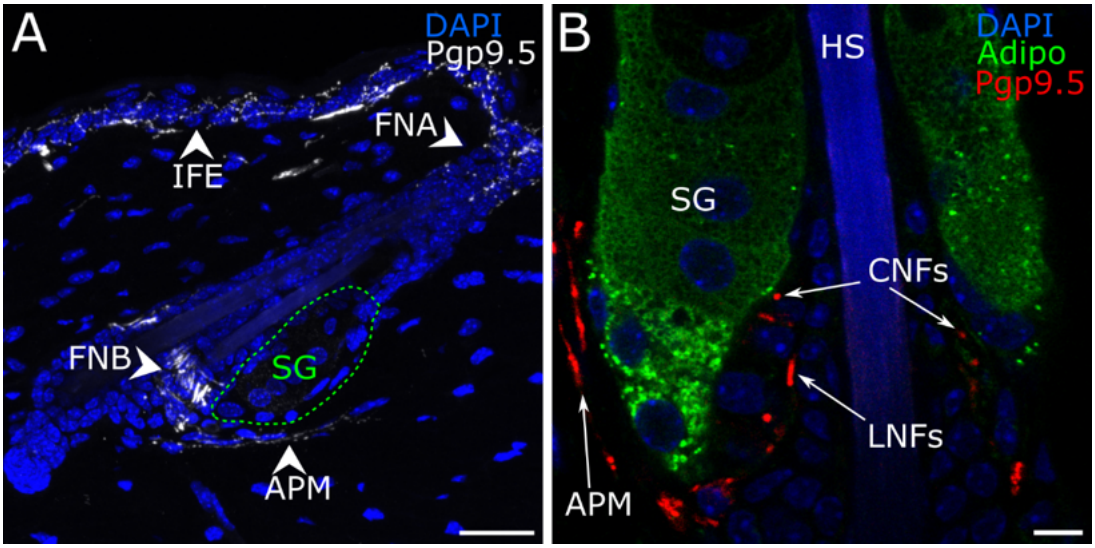

Figure 3.4. Innervation of the mouse pilosebaceous unit.

(A) Immunostaining for the broad-spectrum nerve fibre marker protein gene-product 9.5 (PGP9.5) in mouse skin. As reported in published work, two distinct networks of nerves supply the hair follicle. Follicular nerve network B (FNB) can be observed around the upper bulge and at the level of the sebaceous gland (SG). A less ordered network of nerves supplies the distal infundibulum and is known as follicular nerve network A (FNA). The arrector pili muscle (APM) and interfollicular epidermis (IFE) also receive their own nerve supply. Scale = 30 µm. **(B)** PGP9.5+ nerve fibres of FNB in relation to the SG, labelled with adipophilin (green). CNFs and nerves supplying the APM can be seen close to the sebaceous epithelium but do not appear to make direct contact. Scale = 7 µm.

As there is evidence indicating the existence of intrafollicular progenitors for the SG in the JZ (Page *et al.*, 2013), it was hypothesised that SG function could be controlled via direct innervation of these progenitor cells in the follicle. These intrafollicular progenitors express *Lrig1* (Jensen *et al.*, 2009b; Page *et al.*, 2013). Therefore, the interaction between PGP9.5+ nerves fibres and the LRIG1+ JZ keratinocytes was examined, using an antibody against LRIG1 in mouse dorsal skin (Figure 3.5). The SG was also delineated using an antibody against embigin, a cell surface protein which has been identified as a specific sebocyte marker (Joost *et al.*, 2016). While most of the JZ is not innervated, it was observed that the proximal portion of the LRIG1+ compartment is directly contacted by LNFs (Figure 3.5C). Again, CNFs represent the population of nerves that most closely approach the SG, but sebocytes themselves do not appear to be innervated (Figure 3.5A, B).

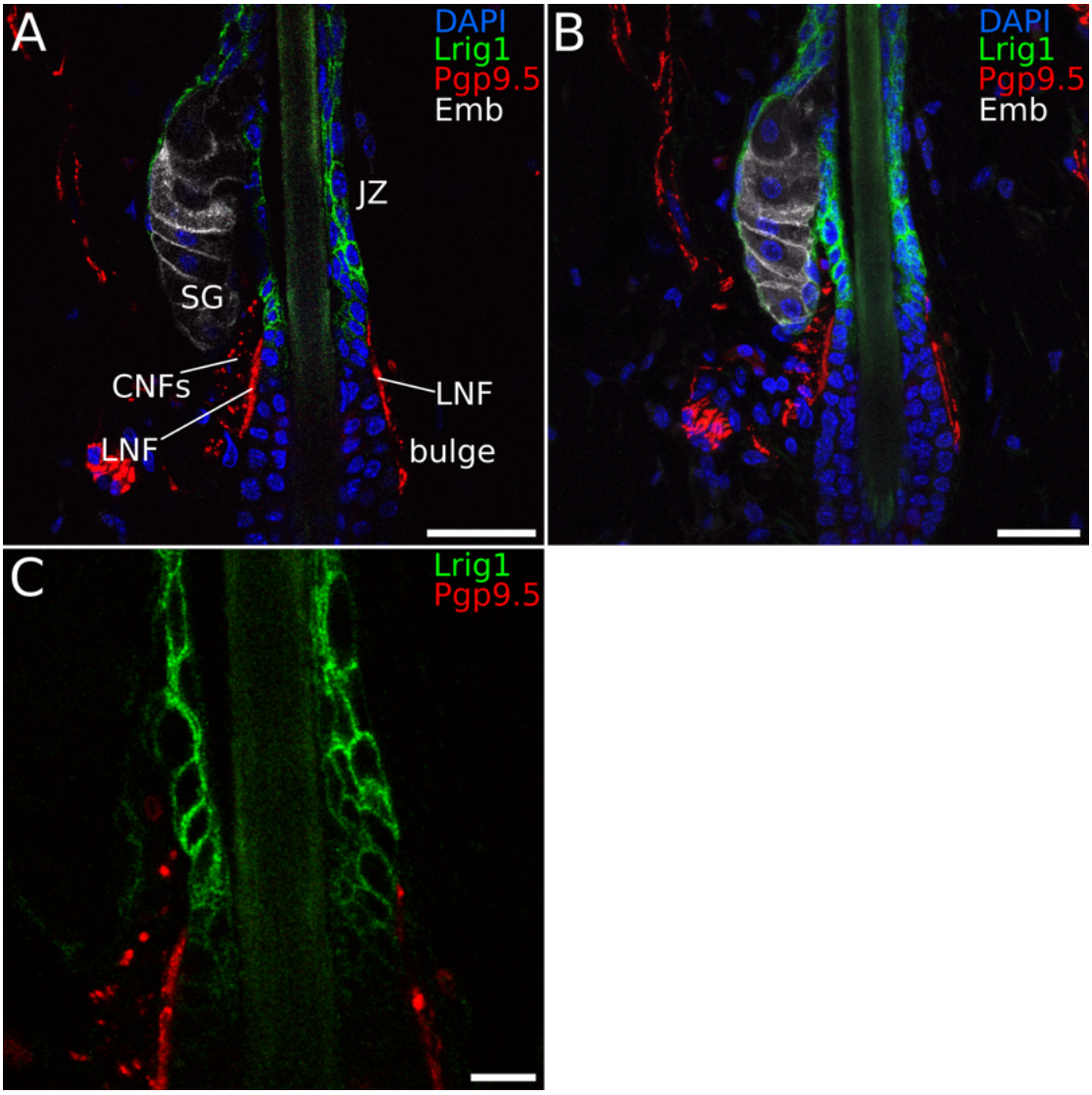

Figure 3.5. Longitudinal nerve fibres directly contact LRIG1+ cells in the junctional zone.

(A) Single confocal plane of a telogen pilosebaceous unit (PSU) in dorsal skin. Scale bar = 30 μm. **(B)** Z-projection of confocal stack of the same follicle shown in (A). The junctional zone (JZ) expresses Leucine-rich repeats and immunoglobulin-like domains protein 1 (*Lrig1*, shown in green), which is considered a marker for intrafollicular progenitors for the sebaceous gland (SG, labelled with embigin in white). PGP9.5+ (red) longitudinal nerve fibres (LNFs) directly contact the proximal portion of the LRIG1+ JZ. The SG does not appear to be directly contacted by either LNFs or the more closely located circular nerve fibres (CNFs). Scale bar = 30 μm. **(C)** Single confocal plane showing PGP9.5+ nerve endings in relation to LRIG1+ cells in the JZ. Scale bar = 10 μm.

3.2.3 Nerves constituting FNB contain synaptophysin and calcitonin gene-related peptide

The nerves that comprise FNB are typically considered to be mechanosensory and nociceptive nerve fibres (Li & Ginty, 2014). To support the hypothesis of a functional

role of innervation in biology of the SG, it was examined whether CNFs and LNFs exhibit a neurosecretory phenotype, by probing for the expression of markers of synaptic vesicles. Mouse skin was incubated with an antibody against synaptophysin, which is a marker for synaptic vesicles (Calhoun *et al.*, 1996; Dejanovic *et al.*, 2018). All of the nerves constituting FNB, as well as the APM innervation, were positive for synaptophysin (Figure 3.6 A-C). Mouse brain was used as a positive control tissue, and immunofluorescence for synaptophysin reveals sites of accumulations of synaptic vesicles along neuronal processes and cell bodies (Figure 3.6D). A similar pattern of synaptophysin-positive 'beads' indicates sites of synaptic vesicles along cutaneous nerves in mice (Figure 3.6A-C, E).

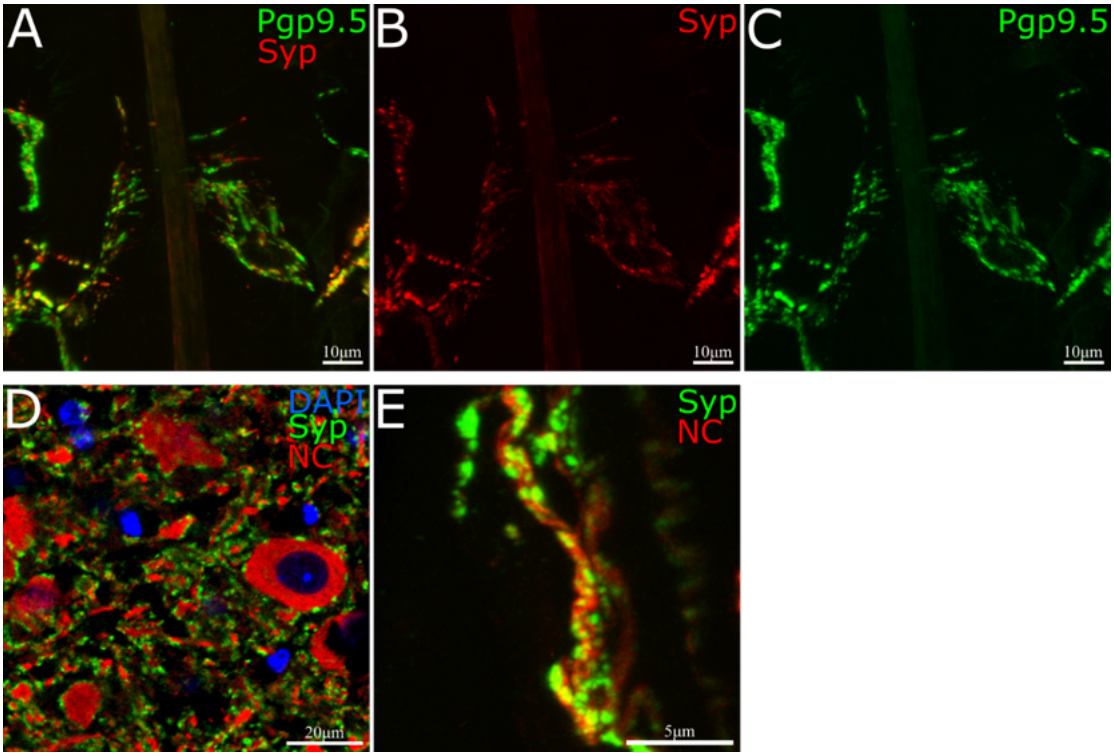

Figure 3.6. Nerve endings of follicular nerve network B contain synaptophysin.

(A-C) Z-projections of follicular nerve network B. Both longitudinal and circular nerve fibres are positive for the synaptic vesicle marker, synaptophysin (Syp, red), suggestive of a neurosecretory function. **(D)** Positive control tissue (brain) for Syp antibody (green). Numerous punctate dots indicate Syp+ synapses along nerve processes and neuronal cell bodies. **(E)** Punctate Syp+ dots along cutaneous nerves (arrector pili muscle nerve shown) indicate sites of synaptic vesicle accumulation. NC, NeuroChrom pan-neuronal antibody; scale is indicated in each panel.

It was also observed that FNB contains calcitonin gene-related peptide (CGRP). CGRP is a neuropeptide that has been previously reported in cutaneous nerve fibres (Peters *et al.*, 2001; Kestell *et al.*, 2015). Interestingly, CGRP appeared to be restricted to CNFs (Figure 3.7A) and was also completely absent from the infundibular nerve supply (Figure 3.7B). As a positive control tissue, mouse dorsal root ganglia were incubated with anti-CGRP antibody, which revealed a sub-population of CGRP+ neurons, as previously reported (Figure 3.7C) (Kestell *et al.*, 2015). Operating on the premise that the function of these CGRP+ neurons could be specifically manipulated pharmacologically; dorsal root ganglia were co-stained for CGRP and transient receptor potential cation channel subfamily V member 1 (TRPV1). As previously shown, CGRP appeared to be restricted to neurons expressing relatively higher levels of TRPV1 (Figure 3.7D) (Kestell *et al.*, 2015).

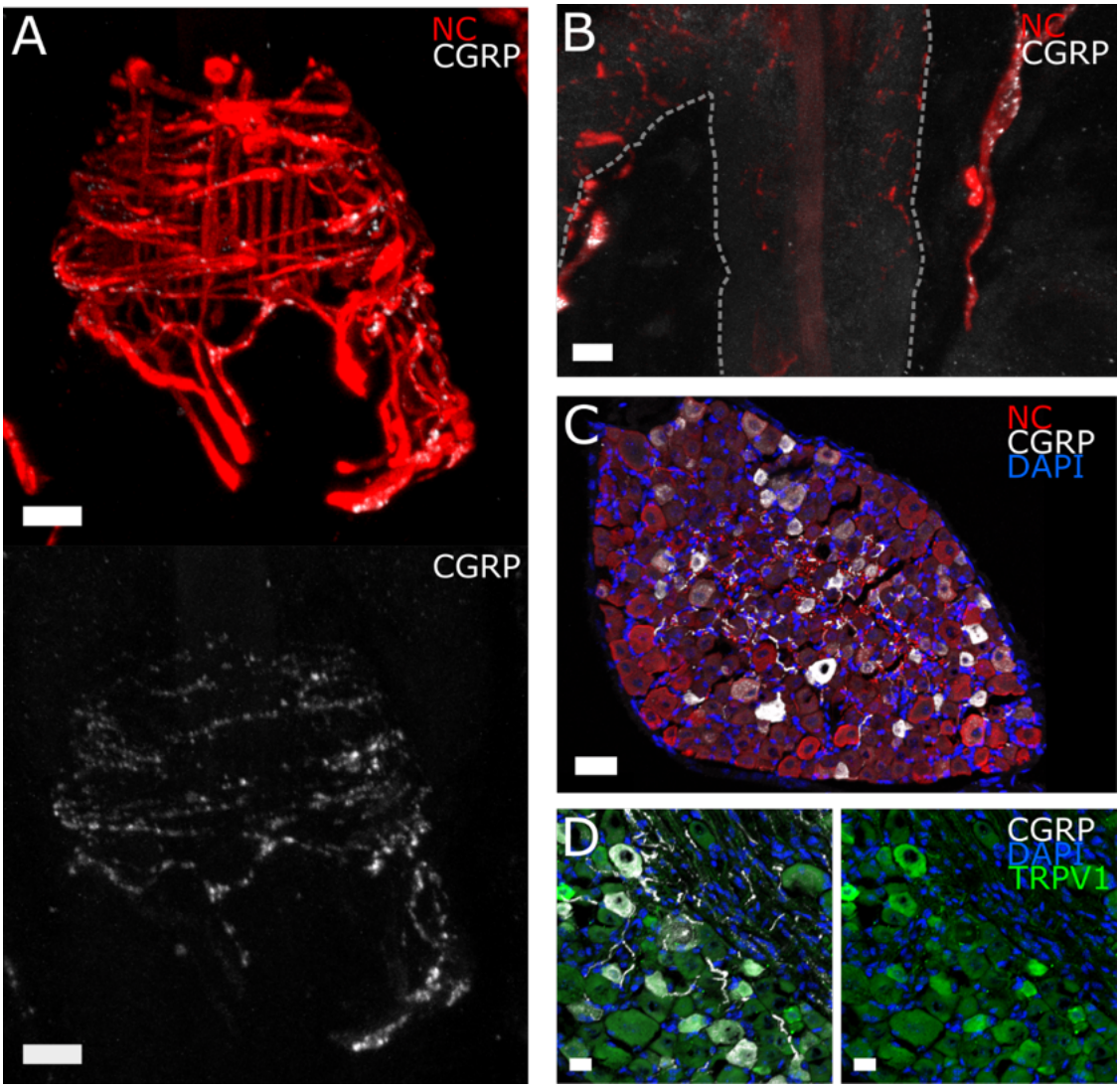

Figure 3.7. Nerves of follicular nerve network B contain calcitonin gene-related peptide.

(A) Z-projection of murine follicular nerve network B (FNB). The circular nerve fibres (CNFs) are observed to contain the neuropeptide calcitonin gene-related peptide (CGRP, white). Scale = 10 µm. (B) Nerve fibres supplying the infundibulum (outlined) do not contain CGRP, but dermal nerve fibres are CGRP+. Scale = 10 µm. (C) Presence of CGRP within a sub-population of sensory neuronal cell bodies in mouse dorsal root ganglia. Scale = 50 µm. (D) CGRP+ neurons express relatively higher levels of TRPV1 (transient receptor potential cation channel subfamily V member 1). Left and right panels show the same field of view, with and without CGRP-staining overlaid. Scale = 20 µm.

3.2.4 Transmission electron microscopy of murine follicular nerve network B

To confirm the observations regarding lack of SG innervation, FNB was more closely examined via TEM. It was hypothesised that previously undetected neuronal-sebocyte interactions might be observable as electron-dense synaptic structures. Alternatively, if nerves do not directly contact the SG epithelium, it was speculated that nerves may

nevertheless form unilateral synapses, with presynaptic specialisation only (Goyal & Chaudhury, 2013). An additional aim was to confirm the observations of synaptophysin and CGRP expression in FNB, by looking for the presence of large dense-core vesicles (LDCVs) in nerves. SGs from dorsal, auricular and whisker pad skin of mice were examined.

In dorsal skin, four separate SGs were examined in multiple serial sections through a depth of approximately 30 μm. The distance between 14 separate CNFs and the SG epithelium was quantified, which ranged from 0.5 μm to 1 μm. However, no direct contact between nerves and sebocytes was observed (Figure 3.8A). While LDCVs could be observed, there was no obvious accumulation of vesicles that would indicate the presence of unilateral synapses (Figure 3.8A). In whisker pad skin, eight SGs were imaged through a depth of 100 μm, and 11 nerve fibres were assessed for the distance to the SG epithelium, which ranged from 0.5 μm to 4 μm. Again, LDCVs could be observed, but no innervation of the SG epithelium was seen (Figure 3.9A). The same structure of nerve fibres could be observed in the mouse ear (Figure 3.10A). As previously observed via immunofluorescence, FNB nerve fibres are more closely associated with the follicular epithelium (Figure 3.8A, 3.10A).

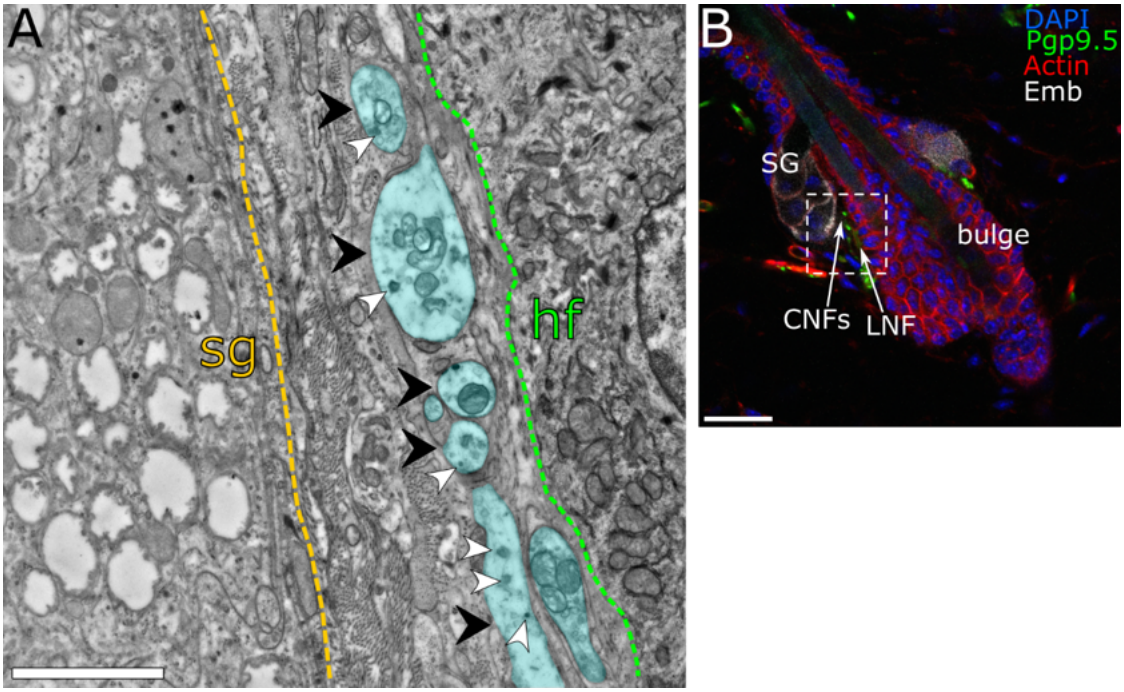

Figure 3.8. Follicular nerve network B and sebaceous glands in dorsal skin.

(A) Transmission electron micrograph showing longitudinal nerve fibres (LNFs) and circular nerve fibres (CNFs) in cross section between the sebaceous (SG) and follicular (HF) epithelia in dorsal skin. Nerves (blue, black arrows) are unmyelinated and contain large dense core vesicles (white arrows). Relatively, nerves are more closely associated with the follicular epithelium. Scale = 2 µm. **(B)** Immunofluorescence of a telogen HF in mouse dorsal skin. Approximate plane of the TEM section is indicated by the dashed line. PGP9.5, nerve fibre marker (green); Emb, embigin (white). Scale = 20 µm.

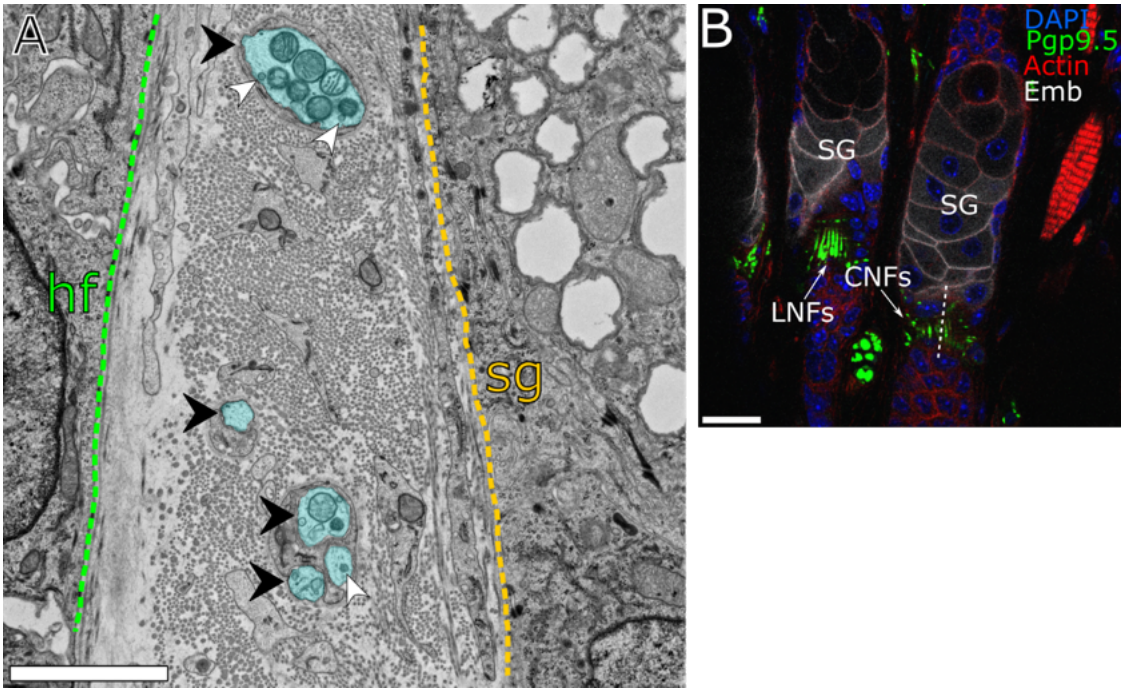

Figure 3.9. Follicular nerve network B and sebaceous glands in the mouse whisker pad.

(A) Transmission electron micrograph demonstrating circular nerve fibres (CNFs) in the mesenchymal space between a non-vibrissae whisker follicle (HF) and associated sebaceous gland (SG). Nerves indicated by black arrows and blue colouration. White arrows indicate observed large dense core vesicles. Scale = 2

µm. **(B)** Immunofluorescence of a non-vibrissae pilosebaceous unit in mouse whisker pad skin. Approximate plane of the TEM section is indicated by the dashed line. Pgp9.5, nerve fibre marker (green); Emb, embigin (white). Scale = 20 µm.

Interestingly, LDCVs were not restricted to CNFs, as the pattern of CGRP expression might indicate (Figure 3.7A). In dorsal skin, over four different TEM sections, the diameter of 13 putative LDCVs was measured. On average, the diameter was approximately 120 nm (1 S.D. 38 nm), which aligns with the reported size of LDCVs in rodent skin from published data (Ruocco *et al.*, 2001).

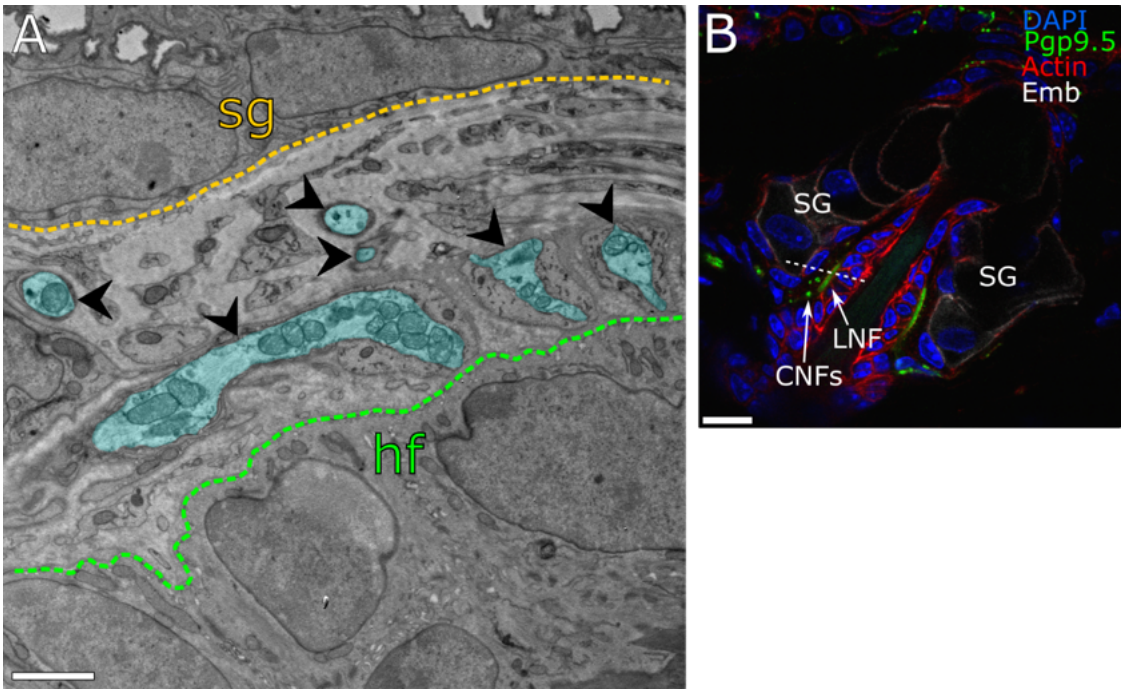

Figure 3.10. Follicular nerve network B and sebaceous glands in the murine auricular skin.

(A) Transmission electron micrograph of longitudinal nerve fibres (LNFs) and circular nerve fibres (CNFs) in the mesenchymal space between an auricular follicle (HF) and associated sebaceous gland (SG). Nerves indicated by black arrows and blue colouration. Scale = 2 µm. Follicular keratinocytes are directly contacted by LNFs. **(B)** Immunofluorescence of an auricular pilosebaceous unit. Approximate plane of the TEM section is indicated by the dashed line. Pgp9.5, nerve fibre marker (green); Emb, embigin (white). Scale = 10 µm.

3.3 Discussion

The data presented here are aligned with preceding works that have concluded that the SG epithelium is not directly innervated (Hurley *et al.*, 1953; Hellmann, 1955; Montagna & Ellis, 1957a). While nerves can be seen to approach and come into close proximity with human SGs (Figure 3.1; Figure 3.2; Figure 3.3), there is no clear order to the arrangement of nerve fibres, and no direct contact between nerve fibres or the SG epithelium appears to occur. The size of human SGs makes it difficult to examine neuroanatomy in totality. The effort is further confounded by the discrete and winding nature of nerve fibres in three-dimensional space. Together, these factors may make the detection of any direct innervation of human SGs impracticable.

Therefore, the approach was shifted towards more definitively mapping nerve endings in relation to SGs in mouse skin. By identifying anatomical relationships between SGs and nerves in mouse, the approach of any future research that seeks to re-examine innervation of the human SG may narrow its search along similar anatomical lines. As reported previously (Botchkarev *et al.*, 1997), the murine PSU exhibits two distinct networks of nerve fibres (Figure 3.4) of which, FNB is most closely located with respect to the SG. However, no direct innervation of the murine SG was observed either (Figure 3.4; Figure 3.5). Nonetheless, nerves of FNB contain synaptophysin and CGRP, which is suggestive of a neurosecretory function (Figure 3.6; Figure 3.7). However, it is not clear whether SGs might be competent to respond to diffusely secreted substances from these nerves.

Importantly, it should be noted that the number of nerve fibres comprising follicular neuronal networks, as well as the presence of peptidergic and non-peptidergic neurotransmitters, has been reported to exhibit profound HC dependence (Botchkarev *et al.*, 1997, 1999; Peters *et al.*, 2001). As the focus here for immunofluorescence and TEM analysis was in telogen mouse skin, the possibility for development of SG innervation

during anagen cannot be excluded. Moving forward, the described regions of dense pilosebaceous innervation should be correlated with the SG epithelium throughout the hair growth cycle.

It was observed, however, that the proximal portion of the LRIG1+ JZ of the mouse PSU is directly contacted by nerve endings. Importantly, *Lrig1* expression is considered a marker for intrafollicular progenitor cells that generate both the SG and infundibulum (Page *et al.*, 2013). Therefore, there is the possibility that neuronal control of SGs occurs through regulation of SG progenitors. Furthermore, innervation of LRIG1+ cells indicates the possibility for neuronal control of infundibular homeostasis, which could have translational relevance with regards to comedo formation in acne (Saurat, 2015).

Finally, the observed differential pattern of innervation in mice between the HF and SG aligns with known expression of neurotrophins, which are molecules that dictate neuronal outgrowth and maintenance. For example, keratinocytes of the outer bulge have been shown, through single-cell RNA sequencing (scRNAseq) analysis, to specifically express several neurotrophins (Joost *et al.*, 2016). Moreover, isolation and sequencing of mRNAs from *Gli1*-expressing cells in the bulge of the PSU shows that these cells express many genes related to neurogenesis and synaptic maintenance, including neurturin and brain-derived neurotrophic factor (Joost *et al.*, 2016; Cheng *et al.*, 2018). If a specific marker for a putative, innervated, intrafollicular SG progenitor could be identified in mice, this would allow for informative lineage tracing in the context of denervation or following treatment with neuromodulatory substances.

Chapter 4: Investigating the functional requirement of sebaceous glands for input from the peripheral nervous system

4.1 Introduction

4.1.1 Cutaneous denervation and associated phenotypes relevant to sebaceous homeostasis

Clinical observations of dysfunctional sebum production in cases of neuronal deficit point towards neuronal control of SG function (Burton *et al.*, 1971a; Summerly *et al.*, 1971; Thomas *et al.*, 1985). More recently, botulinum toxin has been observed to reduce sebum production in humans (Jankovic & Diamond, 2006; Shah, 2008; Li *et al.*, 2013b; Min *et al.*, 2015), strengthening the case for regulation of SGs by the nervous system.

In mice, surgical cutaneous denervation is a valuable and effective experimental technique for investigating the role of nerve fibres in skin homeostasis, function and disease. By this method, the nerve supply to skin can be entirely removed, including all sensory and autonomic branches (Maurer *et al.*, 1998; Brownell *et al.*, 2012; Peterson *et al.*, 2016).

While there are currently no reports of SG phenotypes following experimental denervation, certain findings have interesting implications, drawing on what is known about SG homeostasis. For example, expression of *Lgr6* in the PSU and epidermis has been shown to depend on intact innervation (Liao & Nguyen, 2014). As mentioned previously, *Lgr6*-expressing cells may represent a SG-resident sebocyte progenitor cell type (Gong *et al.*, 2012; Page *et al.*, 2013; Liao & Nguyen, 2014; Kretzschmar *et al.*, 2016). Schwann cells are closely associated with *Lgr6*-expressing cells in the mouse HF and epidermis, and denervation of mouse dorsal skin leads to a loss of both Schwann cells and *Lgr6* expression in both compartments (Liao & Nguyen, 2014). Additionally, LGR6+ cells throughout the PSU are enriched for genes related to axonal outgrowth and synapse maintenance, which suggests these cells may interact with the peripheral nervous system (Füllgrabe *et al.*, 2015).

Another finding of potential interest is that in mouse skin, SHH is produced by a sub-population of follicular nerves, which is required for maintenance of *Gli1* expression in keratinocytes of the upper bulge (UB). Following denervation, *Gli1* expression is lost. Lineage tracing demonstrates that these cells normally contribute to the cycling portion of the HF, but can also regenerate the epidermis and contribute to the SG following wounding (Brownell *et al.*, 2012). RNA sequencing of isolated GLI1+ cells from mouse skin has revealed that these cells express several genes related to neurogenesis, suggestive of direct innervation (Cheng *et al.*, 2018). Moreover, given the long range signalling capabilities of Shh (Goetz *et al.*, 2002), it is conceivable that nerve-derived SHH also acts on *Gli1*-expressing cells that have been reported within the SG (Niemann *et al.*, 2003).

4.1.2 Experimental aims

From the work described above, it can be hypothesised that denervation may result in SG atrophy due to loss of potential progenitor cells and/or nerve-derived trophic factors. However, the observed lack of SG innervation (Chapter 3) brings into question whether the nervous system is truly of any relevance with regards to SG function.

In order to definitively establish whether SGs are at all dependent on the peripheral nervous system, an established technique for unilateral surgical cutaneous denervation (SCD) of mouse dorsal skin was used (Peterson *et al.*, 2016). The chief aim of the following experiments was to establish whether there is any SG phenotype following denervation.

The key experimental aims were as follows:

- Establish whether, and under what conditions, the SG is affected by cutaneous denervation.

- Assess any resulting SG phenotype by quantification of SG size.
- Identify the mechanism resulting in any change in SG size by investigating lipid production, cell number, and proliferation within the PSU.

4.2 Results

4.2.1 Surgical denervation of mouse skin has no effect on SG volume during telogen, but results in smaller SGs in anagen skin

To definitively establish whether murine SGs are functionally reliant on input from the peripheral nervous system, mice underwent SCD, which results in unilateral loss of all sensory and autonomic nerve endings (Peterson *et al.*, 2016). Adult male mice aged 10-11 weeks underwent SCD and were then maintained for either 14-17 days or 90 days post-denervation (PD). The range of 14-17 days was arrived at via happenstance, due to issues regarding when the mice were able to be euthanised. The intention was to have an early timepoint corresponding to roughly two weeks. Subsequently, thick sections of skin from each flank were stained for imaging of sebaceous lipid and nuclei. A time point of 5 days post-denervation was later included to examine loss of NFs at an earlier period (as this was the time point of depilation and induction used in subsequent experiments; Sections 4.2.4 and 5.2.1).

Successful denervation was readily demonstrable via loss of immunostaining for PGP9.5+ NFs (Figure 4.1). Qualitatively, the loss of NFs following denervation appears to occur progressively, first being lost from the superficial layers of skin before affecting the dermis and deeper strata (Figure 4.1). For example, at 5 days PD, a profound reduction in PGP9.5 immunoreactivity is already evident in the IFE and infundibulum, while some PGP9.5+ staining persists in FNB at 5 days, 14-17 days, and even up to 90 days PD

(Figure 4.1). Importantly, this residual PGP9.5 staining in FNB was consistently present, suggesting that this immunoreactivity is not due to reinnervation of skin, and no return of PGP9.5 staining in the IFE or other compartments was observed (Figure 4.1). In assessing whether skin was functionally denervated to progress with SG analyses, the loss of IFE and infundibular NFs was taken as a positive indicator.

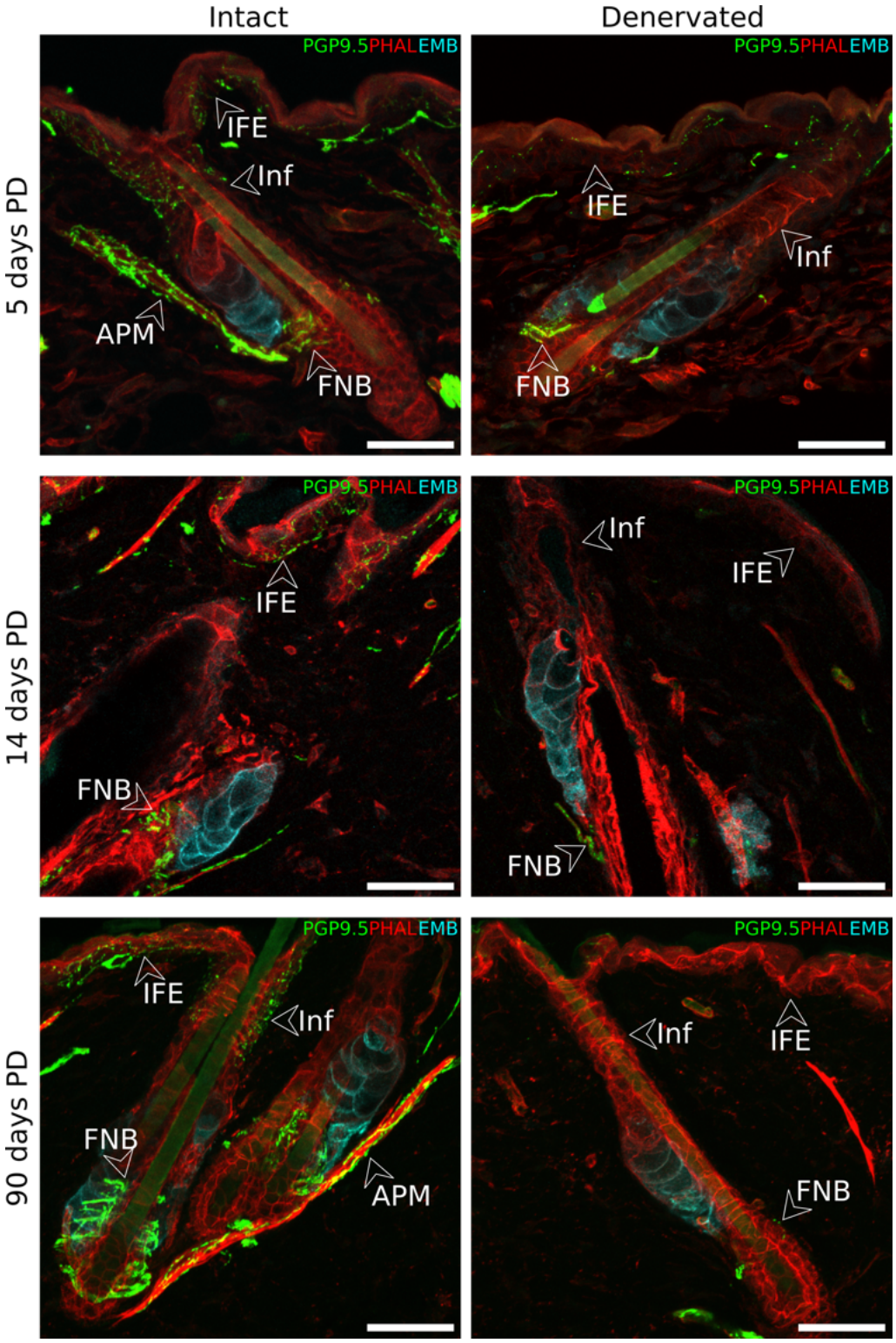

Figure 4.1. Surgical cutaneous denervation results in progressive loss of PGP9.5 immunoreactive nerve fibres in mouse skin.

Immediate loss of nerve fibres (NFs, green) from the interfollicular epidermis (IFE) and infundibulum (Inf) is evident at 5 days post-denervation (PD), and proceeds to be completely lost by 14 days PD. Some PGP9.5+ NFs persist within follicular nerve network B (FNB), even at 90 days PD. APM = arrector pili muscle; Green = Nerves, labelled with anti-PGP9.5 antibody; Red = Actin, labelled with phalloidin; Cyan = SGs, labelled with anti-embigin antibody; Scale = 50 μm.

Mice maintained to 14-17 days PD exhibited a 25% reduction in SG volume in the denervated flank that was statistically significant (average of 130000μm^3 vs 100000μm^3; Figure 4.2A, B). Unexpectedly, mice at 90 days PD showed a much smaller, non-significant difference between the intact and denervated flanks (both approximately 70000μm^3 on average) (Figure 4.2B). Importantly, the mean volume of intact SGs in mice at 14-17 days PD was roughly two-fold greater than that of SGs at 90 days PD. Furthermore, denervated SGs at 14-17 days PD, while smaller than their intact counterparts, were still significantly larger than denervated SGs at 90 days PD (Figure 4.2B). Together, these findings suggested that denervation results in smaller SG size, but that this effect may be conditional. It was later hypothesised that the effect of denervation could be dependent on HC stage (described below).

These trends for SG volume were correlated with similar changes in total number of nuclei per SG (Figure 4.2C). Sebocyte nuclei were most numerous (approximately 150 nuclei/SG) in intact SGs at 14-17 days PD and, while denervated SGs at 14-17 days PD exhibited a reduction in total nuclei, this remained substantially elevated compared to both intact and denervated skin at 90 days PD (approximately 100 nuclei/SG versus 60 nuclei/SG; Figure 4.2C). By normalising cell numbers/SG for total SG volume, it was revealed that both intact and denervated SGs at 14-17 days PD contained more cells per unit volume than at 90 days PD (Figure 4.2D). There did not appear to be any significant difference in cells per unit volume between intact and denervated skin at either time point (Figure 4.2D).

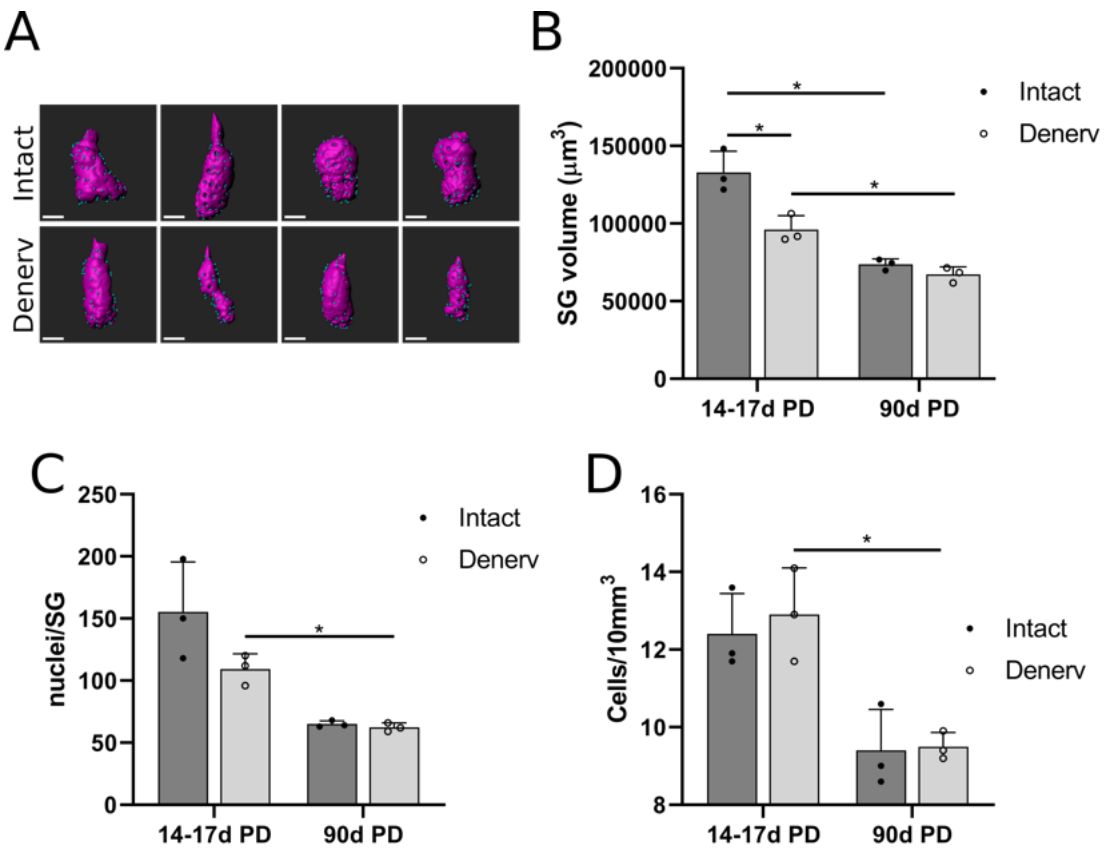

Figure 4.2. Cutaneous denervation results in reduced SG volume at 2 weeks PD, but not at 3 months PD.

(A) Representative 3D-renders of SGs from intact (top) and denervated (bottom) flanks of mice 14-17 days PD, based on LipidTOX stain of SG lipids**.** Scale bars = 30 µm. **(B)** Comparison of SG volumes between intact and denervated (denerv) flanks at time points of 14-17 days PD and 90 days PD. Denervated SGs at 14-17 days PD are significantly smaller than their intact counterparts, while the difference at 90 days PD is limited and not statistically significant. Importantly, the volume of intact SGs between the two time points show a significant difference. Comparison of denervated glands also shows a significant, albeit smaller difference in volume. **(C)** Number of nuclei per SG between intact and denervated flanks. **(D)** Volume-normalised cell numbers per SG. The number of sebocytes in a given volume appears to be increased in both intact and denervated flanks at 14-17 days PD compared to 90 days. All bars represent means of n=3 animals (10-40 SGs), +1 SD; * = $P<0.05$. Individual animal means are shown as data points.

As the effect of denervation appeared to be conditional, the mice were examined for differences that could account for the varied effect of denervation on SG size. It was observed that the back skins of the mice comprising each time point could also be segregated by HC stage (Figure 4.3A). Based on the colour of the dorsal skin, at 14-17 days PD, most of the dorsal skin appeared to be undergoing active hair growth, while no hair growth appeared to be occurring in mice at 90 days PD. Given the age of the mice at time of SCD (10-11 weeks) and the length of the experiment, mice maintained to 14-17d

PD were likely still within the period of anagen that begins at week 12 (Figure 1.2) (Müller-Röver *et al.*, 2001), while mice at later time point had likely completed this anagen stage and subsequently entered telogen. Closer inspection of hair follicles via fluorescent microscopy revealed that each time point corresponded to mid-anagen (approximately anagen VI, based on hair shaft length) and telogen HC stages, respectively (Figure 4.3B). Subsequently, it was hypothesised that the observed SG phenotype following denervation is HC-dependent, rather than dependent on time point PD.

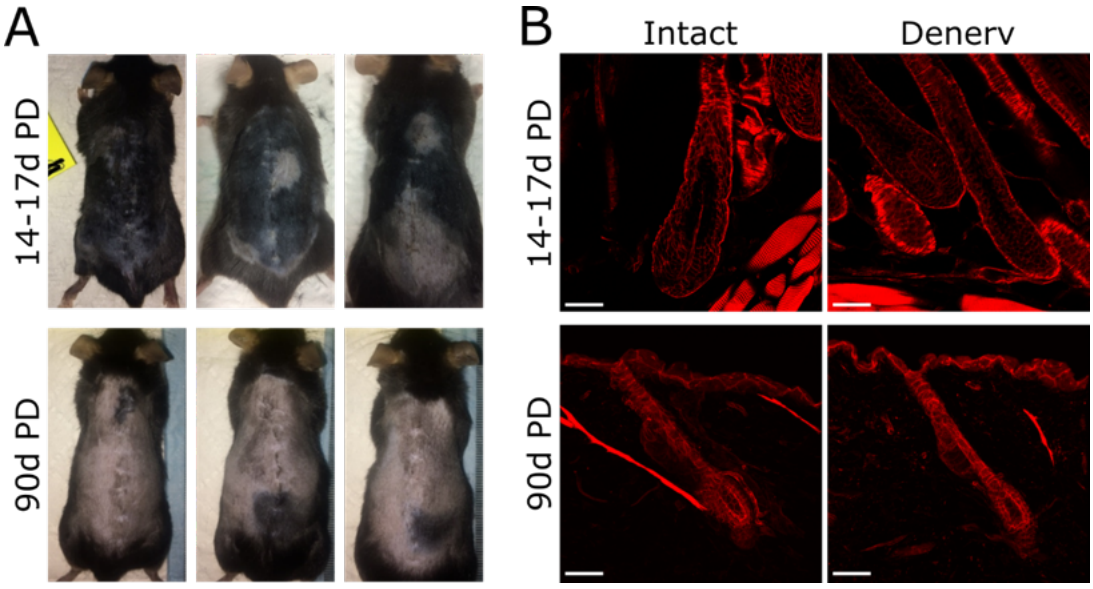

Figure 4.3. Different hair cycle stages between mice at 14-17d PD versus 90d PD.

(A) Images of whole back skins of adult male C57BL/6J mice that have undergone surgical cutaneous denervation. At 14-17d PD, the back skins are primarily in anagen, while at 90d PD, there is little active hair growth. Hair growth in the left (denervated) flanks of mice at 14-17d PD does not appear to be adversely affected. **(B)** Fluorescent confocal images of HFs at each time point, showing actin stained with phalloidin (red). Top row images are single confocal slices. Images on the bottom row are projections through a volume of 20 µm. Scale bars = 50 µm.

4.2.2 Denervation has a minimal effect on SGs in young mice undergoing synchronous hair cycling

To control for both time and HC following denervation, SCD was performed in synchronous and spontaneously hair-cycling mice (Figure 1.2) (Müller-Röver *et al.*,

2001). Male mice underwent SCD during telogen at p21 and were maintained for two-weeks to p35, which is known to correspond approximately to the mid-anagen stage of the HC (Müller-Röver *et al.*, 2001). Grossly, hair growth appeared to be unaffected in the denervated flank (Figure 4.4A-B). Surprisingly, we observed no significant difference in SG volume between the intact and denervated flanks (Figure 4.4C). Moreover, the average size of SGs in the intact flank of p35 male mice is much smaller than those reported above for adult mice that are also in anagen (approximately 60000µm versus 140000µm; Figure 4.2B). These findings are indicative of both a developmental increase in SG size with age, and of a delayed onset of SG-dependence on HC stage and innervation.

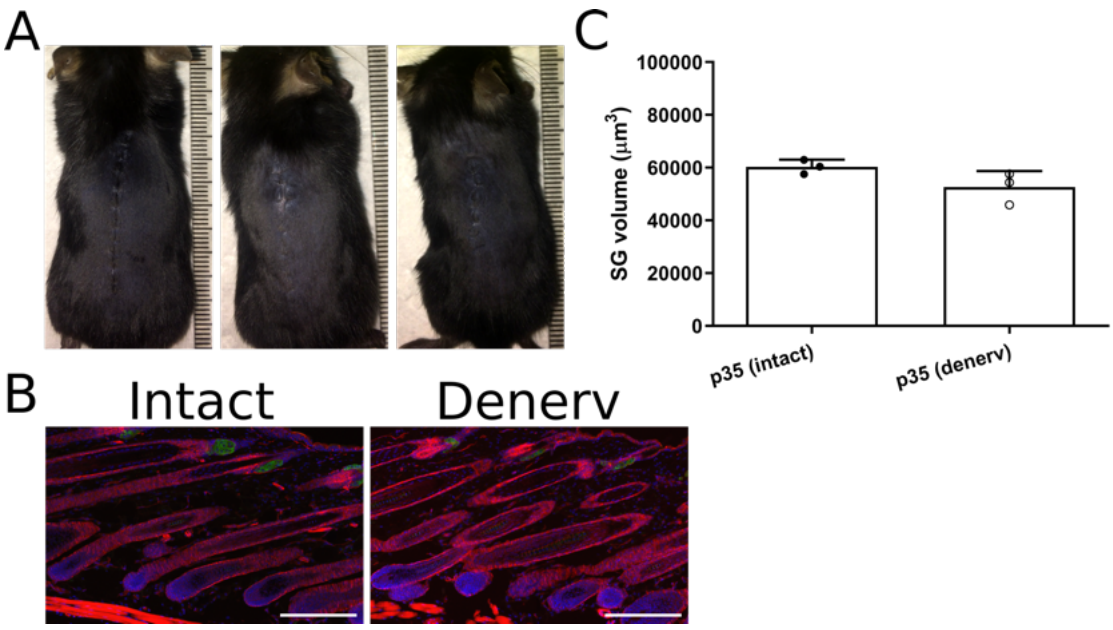

Figure 4.4. Denervation does not affect SG volume in spontaneous, synchronously-hair cycling mice, observed at p35.

(A) Images of whole dorsal skins of male C57BL/6J mice aged post-natal day 35 (p35), which corresponds to mid-anagen (anagen VI). Hair growth is apparent, with no obvious deficit comparing the left to right flank. **(B)** Confocal fluorescent images of anagen hair follicles in both the intact and denervated flanks at p35. Images are projections through a volume of approximately 20 µm. Blue = DAPI; green = adipophilin-stained SGs; red = phalloidin; Scale = 200 µm. **(C)** Comparison of SG volumes between intact and denervated skin at p35. A modest reduction in SG volume is evident, but not significant. Bars represent means of n=3 animals (10-40 SGs), +1 SD. Individual animal means are shown as data points.

4.2.3 Denervation results in attenuated SG enlargement throughout depilation-induced anagen

Working on the premise that dependence on HC stage and innervation may only be present in adult mice, SCD was again performed in adult mice, with HC stage controlled by means of waxing depilation-induced hair growth (Botchkarev *et al.*, 1997; Paus *et al.*, 1997). As it was also intended to look at the behaviour of LRIG1+ cells via GIFM, these depilatory experiments were performed on *Lrig1-CreERT2:Rosa-mTmG* transgenic mice, which were originally developed from the C57BL/6J strain (Powell *et al.*, 2012). The fate mapping data from these experiments is described and discussed in Chapter 5.

Adult mice (male and female) aged 7-8 weeks underwent SCD. This age corresponds to a period of 'refractory telogen', which exists throughout roughly 6-10 weeks of age, and where resting HFs are recalcitrant to anagen-induction via adjacent regions of anagen skin (Figure 1.2) (Geyfman *et al.*, 2015). At 5-days PD, hair growth was induced bilaterally via depilatory waxing. Mice were then euthanized at 3, 6, and 9-days following waxing which, based on previous work, correspond approximately to early, mid- and late anagen, respectively (Maurer *et al.*, 1998). Non-depilated control mice were maintained along with the 9 days post-depilation group (both for a total time of 14 days PD).

Importantly, induction of hair growth did not appear to be adversely affected in the denervated flank (Figure 4.5A), in line with previously published data (Maurer *et al.*, 1998). The progression of anagen at each time point was evident by the development and progressive darkening of a grey/black colouration of the skin, produced by the formation of pigmented hair shafts (Figure 4.5A-B). At 9 days post-depilation, the growth of hair shafts beyond the IFE indicated the growing hairs had reached anagen VI (late anagen, Figure 4.5B) (Müller-Röver *et al.*, 2001).

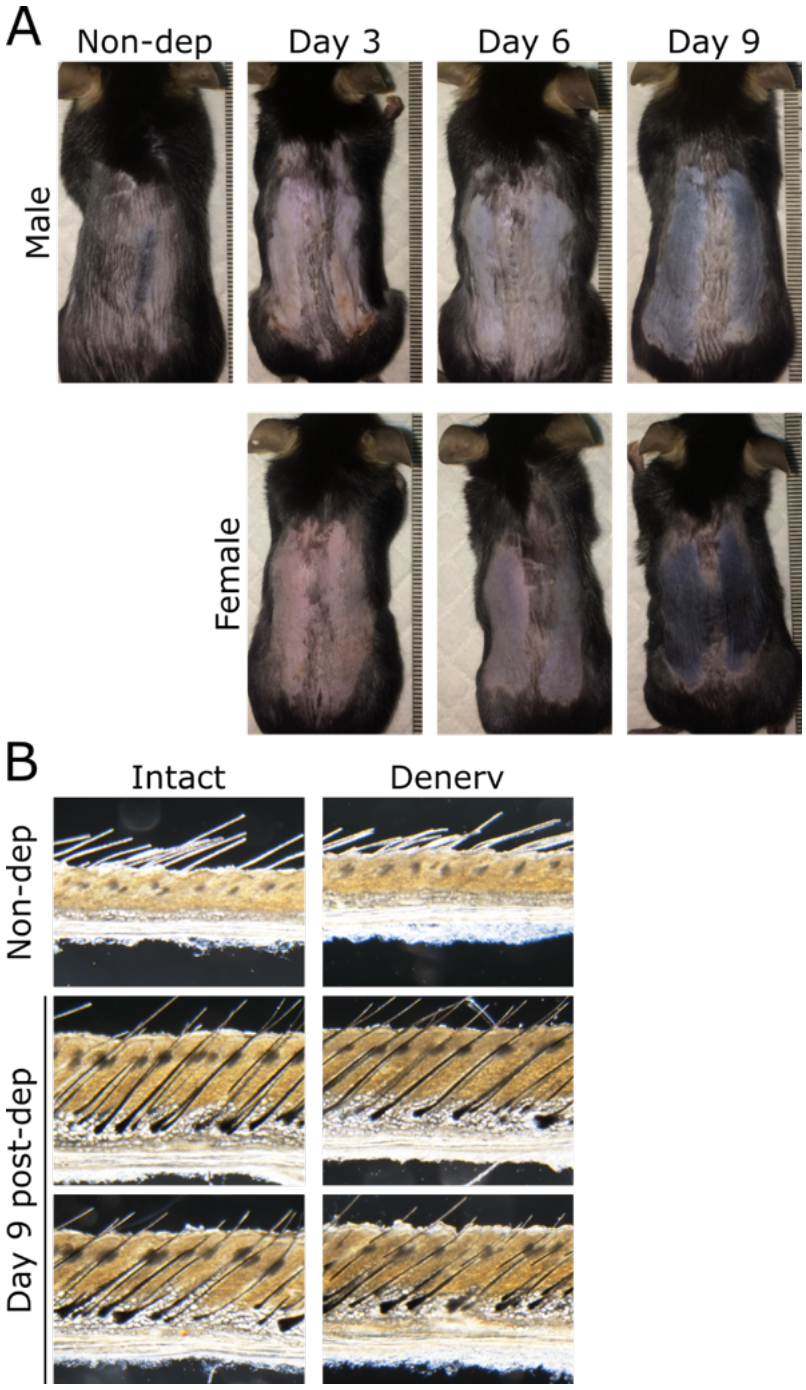

Figure 4.5. Induction of hair growth via depilatory waxing.

(A) Representative images of back skins of both adult male and female *Lrig1-CreERT2:Rosa-mTmG* mice. Hair growth was induced bilaterally in unilaterally denervated mice by waxing depilation during the 'refractory telogen' phase of the mouse hair cycle. Hair growth and progression of anagen is indicated by the development of grey/black colouration. **(B)** Stereo-microscope brightfield images of thick sections of non-depilated and 9 days post-depilated male mouse skin at 14 days PD. The elongation and pigmentation of hair shafts and thickening of both the dermal adipose and panniculus carnosus is indicative of anagen in depilated skin, both denervated and intact. The growth of new hair shafts beyond the skin surface is indicative of anagen VI.

SGs in both intact and denervated skin showed a trend of increasing volume as depilation-induced anagen progressed (Figure 4.6A). Consistently, SGs in the denervated flank were smaller in size compared to intact SGs at the same time point (Figure 4.6A), and the difference between intact and denervated SG volume was statistically significant at 9 days post-depilation (Figure 4.6A). However, the most profound difference was observed at 3 days post-depilation, where SGs were on average 67% the intact volume at the same time point (Figure 4.6B). Importantly, the size of intact and denervated SGs in non-depilated skin was comparable to those observed at 90 days post-denervation previously (Figure 4.2B), supporting the assertion that the observed phenotype is HC-dependent, rather than dependent on time post-denervation.

Overall, these results support the hypothesis that SGs change in size co-ordinately with HC stage, and that cutaneous innervation is required for proper SG enlargement during hair growth. However, innervation appears to be largely dispensable for basal maintenance of SGs while HFs are in the resting state.

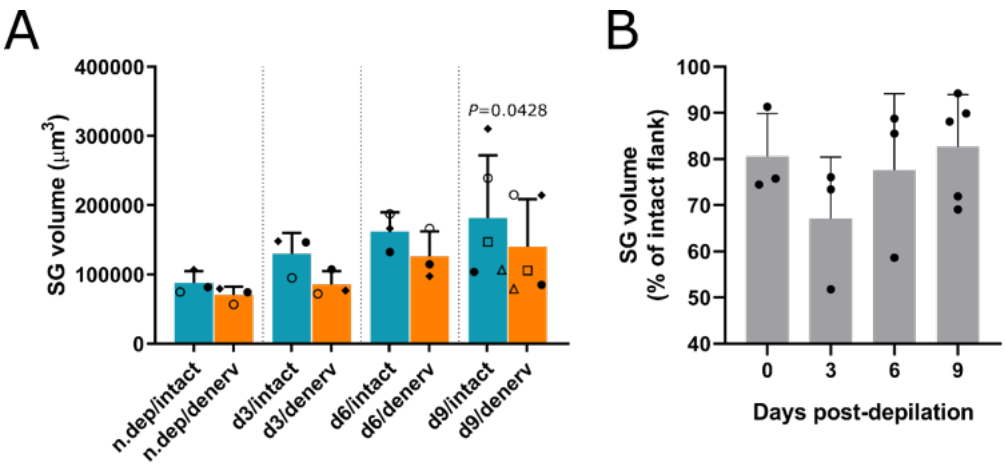

Figure 4.6. Cutaneous denervation attenuates enlargement of SGs throughout depilation-induced anagen progression.

(A) Comparison of SG volumes between intact and denervated dorsal skin in depilated and non-depilated (n.dep) skin. Dotted lines separate each time point post-depilation. SG volume progressively increases throughout depilation-induced anagen. SG volume in denervated skin also shows a progressive increase, but consistently remains smaller than that exhibited by intact skin. At 9 days post-depilation, the difference in intact and denervated SG volume is statistically significant. **(B)** Mean SG volumes in the denervated flank of each animal, expressed as a percentage of the mean SG volume in the corresponding intact flank. All time points post-depilation show a reduction in SG volume compared to the intact flank. The effect is greatest at 3 days post-depilation. All bars represent means of n=3 (for d9, n=5) animals (10-40 SGs), +1

SD; Individual animal means are shown as data points. In (A), matching data point symbols within each time point represent the intact and denervated means of the same animal.

4.2.4 SGs in male and female mice exhibit differential responses to depilation and dependence on cutaneous innervation

As a denervated SG phenotype was not evident in younger male mice (Figure 4.4C) but could be observed in adults (Figure 4.2B, Figure 4.6), it was speculated that the effect of denervation may have different results depending on the presence of systemic factors, such as hormones. Development of sexual maturity is highly variable but is usually completed by the age of 7 weeks in mice (Bronson, Dagg, & Snell, 1966) and, in humans, it is known that SGs undergo considerable secondary development during adolescence (Cotterill *et al.*, 1972). SG function also varies between the sexes (Cotterill *et al.*, 1972; Shuster & Thody, 1974). Therefore, it was further hypothesised that a difference in SG phenotype following denervation might be observed between male and female mice. The data for SG volume in denervated, depilated mice (Figure 4.6) was subsequently resolved on the basis of gender.

The presence of comparatively smaller SGs in denervated skin was conserved between male and female mice at all time points post-depilation (Figure 4.7A-D). Interestingly however, the enlargement of SGs following depilation was more prominent in male mice (Figure 4.7E), and at 9 days post-depilation, both intact and denervated male SGs were significantly larger than intact female SGs at the same time point (Figure 4.7D). These results indicate that SG-cycling may be gender dependent. However, the effect of denervation to relatively reduce SG volume appears to be consistent between male and female adult mice.

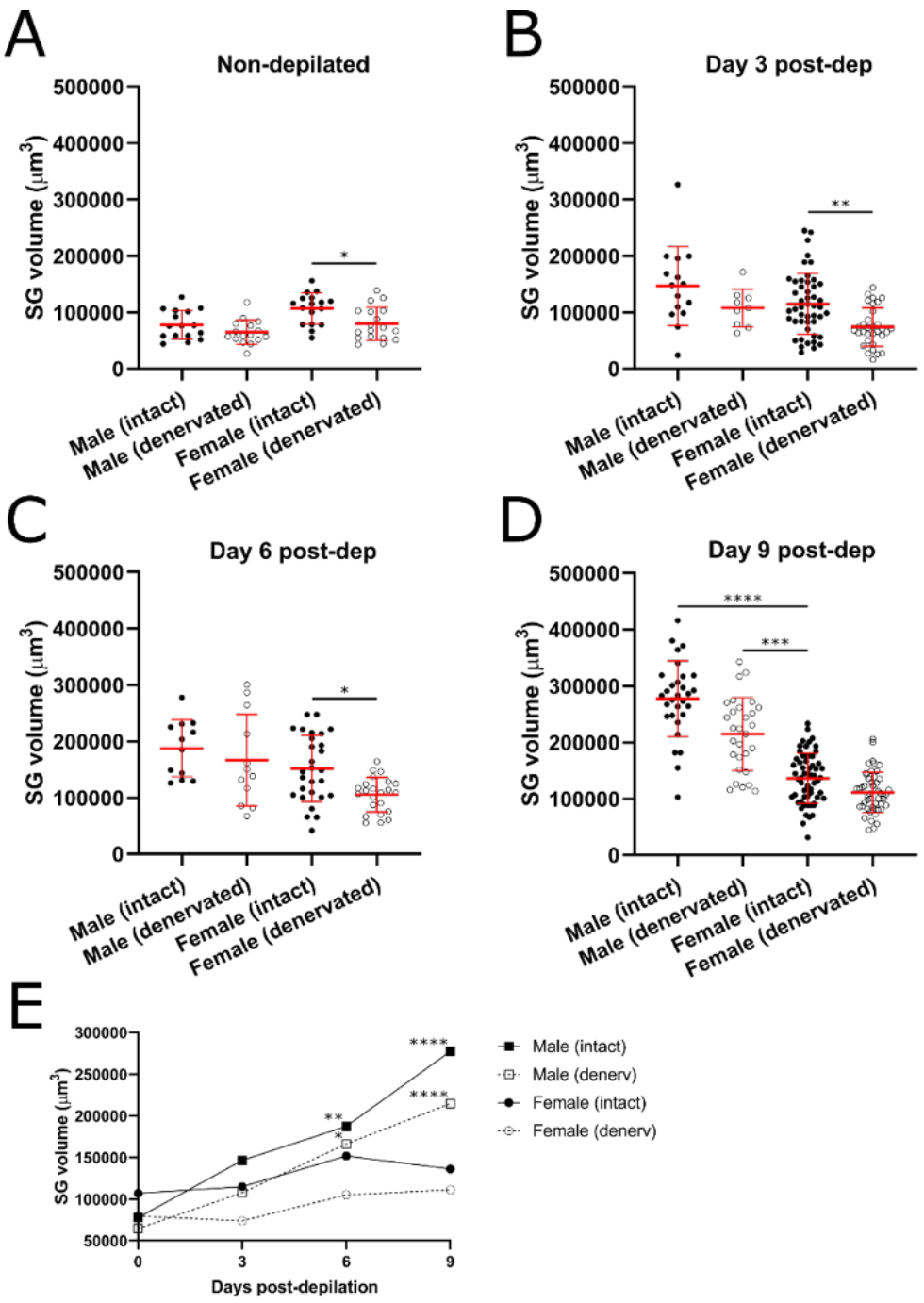

Figure 4.7. Male-female comparison of the effects of denervation on SGs throughout depilation-induced anagen.

(A) Intact and denervated SG volumes in non-depilated male and female mice. Means calculated from n = 16 SGs (male, intact and male, denervated) from 2 mice, n = 17 (female, intact) and n = 18 (female, denervated) from 1 mouse. **(B)** Intact and denervated SG volumes in male and female mice 3 days post-depilation. Means calculated from n = 15 (male, intact) and n = 9 (male, denervated) from 1 mouse, and n = 48 (female, intact) and n = 32 (female, denervated) from 2 mice. **(C)** Intact and denervated SG volumes in male and female mice 6 days post-depilation. Means calculated from n = 12 (male, intact) and n = 12 (male, denervated) from 1 mouse, and n = 28 (female, intact) and n = 23 (female, denervated) from 2 mice. **(D)** Intact and denervated SG volumes in male and female mice 9 days post-depilation. Male SGs, whether intact or denervated, are significantly larger than intact female SGs. Means calculated from n = 30 (male, intact) and n = 29 (male, denervated) from 2 mice, and n = 59 (female, intact) and n = 50 (female, denervated) from 3 mice. **(E)** Plot of male vs female (intact and denervated) SG volume over time post-depilation. Significance given in relation to each mean compared to the mean value for corresponding non-

depilated SGs at the origin. Means (A-D) shown +/- 1 SD; * = $P<0.05$; ** = $P<0.01$; *** = $P<0.001$; **** = $P<0.0001$.

4.2.5 Lipid intensity per SG is increased in female SGs following denervation

The effect of denervation and depilation on sebum composition was examined and inferred from changes in LipidTOX staining intensity per SG (Figure 4.8A). LipidTOX compounds are used as fluorescent dyes for neutral lipids (Grandl & Schmitz, 2009). Therefore, changes in area-normalised fluorescence intensity can be indicative of alterations in the concentration of neutral sebaceous lipid species.

Initially, the mean lipid intensity for intact and denervated SGs were pooled, irrespective of gender or time point post-depilation. In two separate experiments using different variants of LipidTOX, a significant but modest increase in lipid intensity was observed in denervated SGs (Figure 4.8B). On examination of the different time points post-depilation, it was apparent that sebaceous lipid intensity increases abruptly at 3 days post-depilation, then appears to show the beginnings of a gentle recovery to pre-depilation levels (Figure 4.8C).

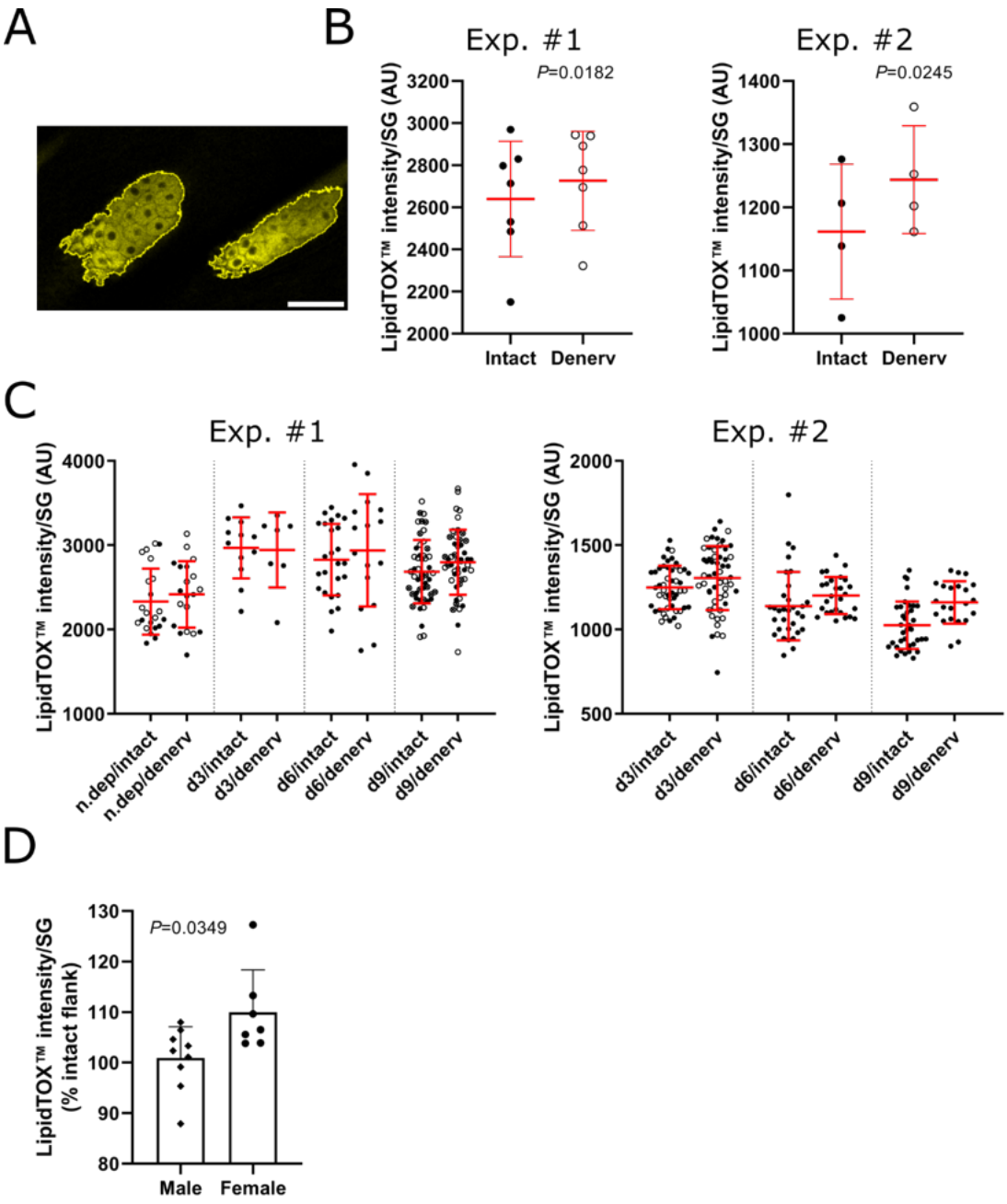

Figure 4.8. Depilation increases SG lipid intensity, and denervation is associated with increased lipid intensity per SG in female mice.

(A) Image depicting methodology for lipid intensity analysis. Demarcated are male, intact SGs at 6 days post-depilation, stained with LipidTOX**.** Scale bar = 50 µm. **(B)** Two separate experiments using different LipidTOX dyes to analyse lipid intensity. In denervated skin, SGs show a significant increase in LipidTOX fluorescence intensity. Data points represent mean SG lipid intensity per mouse. Mice were pooled irrespective of time point or gender. For Exp. #1, n = 7 (~10-40 SGs for each flank). For Exp. #2, n = 4 (~10-40 SGs for each flank). **(C)** Individual SG volumes from (B) resolved on the basis of time point post-depilation. Depilation causes a rapid increase in lipid intensity which appears to slowly recover to normal. Matching data point symbols within each time point indicate SGs from the same mouse (intact and denervated). **(D)** Comparison of lipid intensity per SG in denervated skin between males and females, irrespective of time point post-depilation. On average, female mice show approximately a 10 % increase in SG lipid intensity, which is statistically significant. Data points represent mean lipid intensity per SG in the denervated flank of each animal, expressed as a percentage of the mean SG volume in the corresponding intact flank. All means are given +/-1 SD.

Again, the lipid intensity in denervated SGs was, on average, slightly greater than that observed in the intact flank (Figure 4.8C). Generally, the difference between intact and denervated SG lipid intensity did not appear to be dependent on time point post-depilation (Figure 4.8C).

The data were then normalised against the lipid intensities for the corresponding intact flanks and grouped according to gender. It was observed that, on average, lipid intensity in denervated male SGs did not deviate from the corresponding controls, whereas denervated female SGs exhibited, on average, an almost 10% increase in normalised SG lipid intensity (Figure 4.8D). Overall, these results show that there is increased SG lipid intensity following depilation-induced anagen, and that, in female mice, denervation results in further increased sebaceous lipid intensity.

4.2.6 Investigating proliferation in the pilosebaceous unit following denervation

In order to explain the mechanism resulting in reduced SG size in denervated skin, the proliferative index was examined in PSUs using an antibody against the proliferative marker protein, Ki67. The number of Ki67+ cells was determined for SGs and in the JZ/upper bulge (JZ/UB) in denervated and intact skin, both non-depilated and depilated. Where possible, the proliferative index was also calculated for the infundibulum (Figure 4.9A). At this juncture, preliminary data was acquired for n = 1 mouse per condition. All the mice examined were male, except for 6 days post-depilation. This is because the imaging was conducted on a three-channel epi-fluorescent microscope which could not image in the far-red. Therefore, in order to perform the Ki67 analysis, a non-induced *Lrig1-CreERT2:Rosa-mTmG* had to be used, and there were no available non-induced male mice for the required time point.

Depilation resulted in a trend towards increased proliferative index in SGs at 3 days post-depilation, which had returned to baseline levels by 6 days post-depilation (Figure 4.9B). The percentage of proliferative cells per SG and relationship between the different time points post-depilation was comparable between intact and denervated skin (Figure 4.9B). In the infundibulum, the degree of proliferation was also elevated immediately following depilation and had returned to non-depilated levels by 9 days post-depilation. In denervated skin however, there appeared to be a more gradual proliferative response to depilation, with the proliferative index at each time point being higher than the previous time point and peaking at 9 days post-depilation (Figure 4.9B). In the JZ/UB, depletion resulted in increased proliferation, but had returned to baseline levels by 9 days post-depilation. Interestingly, in denervated skin, the proliferative response to depilation in the JZ/UB appears to be exacerbated, but the relative degree of proliferation between the time points post-depilation was comparable (Figure 4.9B).

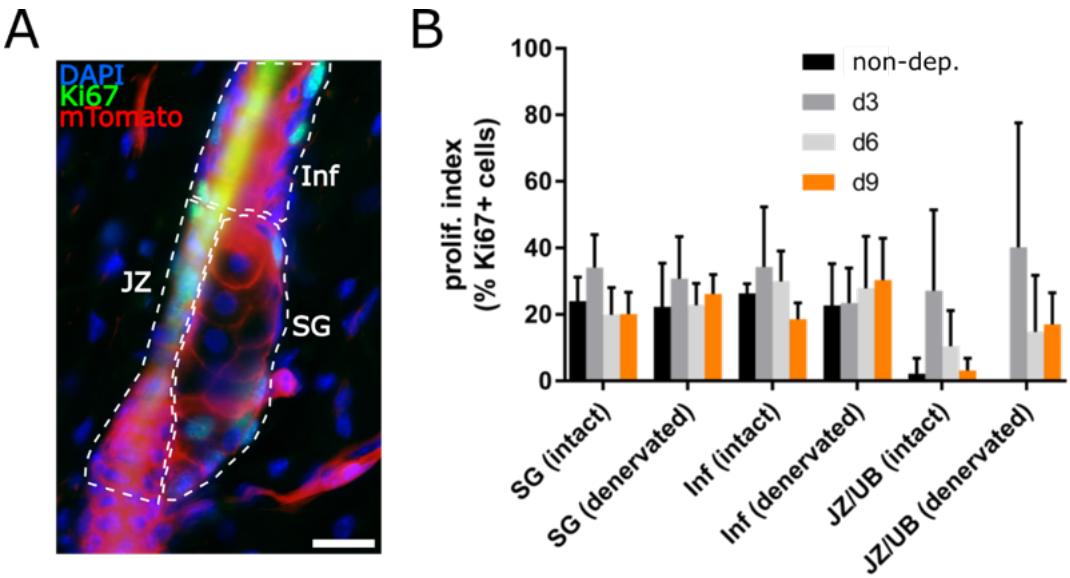

Figure 4.9. Preliminary assessment of proliferation in denervated skin following depilatory waxing.

(A) Image depicting method used for compartmentalisation of PSU and quantification of Ki67+ nuclei. The total number of nuclei and number of Ki67+ cells is determined for the SG, junctional zone/upper bulge (JZ/UB) and infundibulum (Inf). A non-depilated, denervated PSU is shown. Scale = 20 µm. **(B)** Percentage of Ki67+ cells (proliferative index) per compartment in non-depilated skin or over depilation-induced anagen, intact or denervated. Proliferation in the JZ/UB may be more perturbed following denervation than in other compartments. Bars represent means of 5-20 SGs or 3-10 Inf/JZ/UB measured in 1 mouse per time point. All examined mice are male (except 6 days post-depilation). Means given +1 SD.

These preliminary data would suggest that depilation-induced anagen is associated with a general proliferative response in all the examined compartments. However, the phenotype of reduced SG size in denervated skin does not appear to be due to any clear deficit in the number of proliferative sebocytes (Figure4.9B). Conversely, given the apparent alterations in proliferative index in these compartments, a denervated phenotype may be evident in both the infundibulum and JZ (Figure 4.9B). Given that sebocytes may be derived from cellular inputs from the JZ, aberrant proliferation here could possibly contribute to the denervated SG phenotype.

4.3 Discussion

4.3.1 Intact cutaneous innervation is required for sebaceous gland homeostasis during hair growth

The described cutaneous denervation experiments have shown that the SG requires input from the peripheral nervous system. Dependence of SGs on the peripheral nervous system appears to have a HC-dependent component. Basal maintenance of SGs is relatively unaffected by denervation, whereas during hair growth, a significant attenuation of SG enlargement can be seen in denervated skin (Figure 4.2; Figure 4.6). The implied co-ordination between hair growth, SG enlargement and HC-dependent plasticity in pilosebaceous innervation (Botchkarev *et al.*, 1997) are very suggestive of a synergistic mechanism between these components. Presumably, the driving force behind these changes is the HF, as induction of hair growth induces SG enlargement and remodelling of the follicular nerve supply. The effect of denervation has a very limited effect on hair growth and HF cycling (Paus *et al.*, 1997), suggesting that the nervous system does not

contribute a driving force to dynamic turnover of the follicular appendage. It is therefore quite interesting that the nervous system seemingly *is* required for dynamic turnover of the SG, suggesting that follicular nerve networks might serve as a means of communication between the HF and the SG.

It remains to be seen what nerve-derived factors might facilitate such communication between the HF and SG. It is further unknown whether denervation would have any other long-term effects on SGs. While from the given data, it can be concluded that the SG does not seem to require the peripheral nervous system in the short term, other than in the context of hair growth, it cannot yet be ruled out that there exists a subtle basal dependence that would become manifest in the long-term. Indeed, the slight but non-significant trend towards smaller SGs in resting, denervated skin (Figure 4.2; Figure 4.4; Figure 4.6) would suggest that this is the case.

A modest but significant effect of denervation on the lipid content of SGs was also observed (Figure 4.8). Interestingly, the ability of denervation to affect sebaceous lipid content appeared to be restricted to female mice (Figure 4.8). This would suggest that the nervous system may be able to modulate sebum production and composition through control of lipid synthesis, rather than solely through control of SG size. Nerve-derived substances, such as ACh, have been shown *in vitro* to modulate sebum production (Li *et al.*, 2013b). The importance of sebum composition to skin physiology and health has been described in Chapter 1 (Section 1.2) and this result suggests that neuromodulation could be a viable way of tuning sebum composition.

4.3.2 The sebaceous gland exhibits cyclical fluctuation in homeostasis that is co-ordinated with the hair cycle

The presence of a 'SG cycle' has long been postulated (Chase, Montagna, & Malone, 1953). The observations of increased SG size during hair growth, as shown (Figure 4.2; Figure 4.6), is supported by recent research which has demonstrated an increase in SG cross-sectional area during anagen when compared to telogen (Reichenbach *et al.*, 2018). Earlier research has reported that the SG does not change over the course of the HC (Chase *et al.*, 1953; Hamilton, 1974; Hamilton *et al.*, 1974), but this may reflect that this research examined young mice undergoing synchronous hair cycling which, according to the data presented here (Figure 4.2; Figure 4.4), do not exhibit a profound dependence of SGs on HC stage.

One hypothesis explaining the apparent lack of HC-dependent enlargement of SGs in younger mice is due to reproductive immaturity (Bronson *et al.*, 1966). Humans SGs undergo a dramatic change in size and function with the onset of puberty, which is associated with increased systemic androgen levels (Pochi, Strauss, & Downing, 1977). It would be interesting to see whether the HC-dependence of SGs is manifest in adult mice that have undergone orchidectomy or been treated with anti-androgens. Indeed, it is already known that hair growth is itself dependent on levels of systemic hormones. The differential effects of systemic factors on the PSU may explain the gender-specific effects of hair cycling on SGs (Figure 4.7; Figure 4.8) (Plikus & Chuong, 2008).

Chapter 5: Identifying the cell and molecular basis of neuroregulation of sebaceous gland function

5.1 Introduction

5.1.1 Placing neuroregulation within models of sebaceous gland homeostasis

As outlined in the introduction, homeostasis of the SG can be divided into four distinct processes: specification of sebaceous progenitor cells, proliferation of committed pre-sebocytes, differentiation, and finally, holocrine secretion (cell death).

Conceivably, input of the peripheral nervous system into any of these processes would affect SG homeostasis, but each would be associated with distinct translational perspectives. For example, if nerves only regulate SG homeostasis through direct communication with committed sebocytes, then pharmacological neuromodulation could be a useful way of specifically targeting sebum production in skin. Alternatively, if nerves regulate SGs by modulating the behaviour of intrafollicular progenitors, then neuromodulation might have effects beyond the sebaceous compartment, and could potentially be used to affect infundibular homeostasis as well, especially in the context of acne and comedo formation (Saurat, 2015; Clayton *et al.*, 2019).

Given that the mouse SG itself is not innervated (Figure 3.4) it can be reasonably hypothesised that neuroregulation of SGs may be mediated through LRIG1+ intrafollicular progenitors for the SG (Page *et al.*, 2013). Various mouse models exist which allow genetic inducible fate mapping (GIFM) of such *Lrig1*-expressing cells (Powell *et al.*, 2012; Page *et al.*, 2013), allowing for examination of their contribution to the SG in a denervated background.

5.1.2 Nerve-derived substances and receptors implicated in regulation of sebaceous gland biology

A small body of previous work already implicates several nerve derived substances in the regulation of sebaceous gland function, which will now be outlined and discussed below.

Neurons that synthesise ACh can be detected using colorimetric staining techniques that rely on the activity of cholinesterase, an important enzyme in ACh metabolism (Saxod, 1978). Cholinesterase-positive nerve fibres have been observed within the CTS of human SGs (Montagna & Ellis, 1957a), and cholinergic receptors have also been detected in human SGs. For example, the muscarinic receptor m2AChR is reportedly detectable in suprabasal sebocytes via immunofluorescence, while the nicotinic receptors nAChRα7, nAChRα10 and nAChRβ4 are expressed throughout the basal, suprabasal and ductal cells of the SG (Kurzen *et al.*, 2004). Of particular note is nAChRα7, of which both mRNA and protein is produced in human primary sebocytes (Kurzen *et al.*, 2004; Li *et al.*, 2013b). Mouse SGs are also immunoreactive for nAChRα7 (Fan *et al.*, 2011).

Treatment of primary human facial sebocytes with ACh dose-dependently increases lipid production (1-10 nM ACh), and this effect can be partially abrogated using the nAChRα7 antagonist, alpha-bungarotoxin (Li *et al.*, 2013b). These observations suggest that sebocytes can be directly stimulated by nerve-derived ACh, however, stimulation by non-neuronal sources of ACh in the skin remains a possibility, as keratinocytes have been shown to produce ACh (Wessler *et al.*, 2003; Kurzen *et al.*, 2007; Wessler & Kirkpatrick, 2008). In further support of a direct action of ACh on SGs, treatment of immortalised human meibocytes with the broad-spectrum cholinergic agonist carbachol causes an increase in proliferation and an influx of intracellular calcium (Kam & Sullivan, 2011). Furthermore, concentrations of pilocarpine akin to those associated with use of anti-glaucoma eye drops are able to inhibit epidermal growth factor (EGF)- and bovine

pituitary extract-mediated proliferation of immortalised human meibocytes (Zhang *et al.*, 2017).

Substance P is the primary member of the tachykinin family of neuropeptides. In skin, the neuropeptide substance P modulates nociception, inflammation, and vasodilation (Polak & Bloom, 1981; Paus, Theoharides, & Arck, 2006; Sahbaie *et al.*, 2009; Wei *et al.*, 2012). Nerve fibres that produce this prototypic stress- and neurogenic inflammation-associated neuropeptide have been shown to pass within the CTS of rat SGs (Ruocco *et al.*, 2001). Substance P immunoreactive nerve fibres have also been observed in the connective tissue surrounding human SGs, but only in glands that are associated with acne lesions (Toyoda *et al.*, 2002a), as stated previously.

Treatment of mouse skin with 0.1μM Substance P *ex vivo* increases the cross-sectional area of SGs and individual sebocytes, as well as the number of vacuoles in differentiating sebocytes *in situ*, indicating heightened lipid production (Toyoda & Morohashi, 2001). Primary human sebocytes, treated with 1μM Substance P, exhibit a pro-inflammatory phenotype, indicated by increased production of interleukins IL-1 and IL-6, as well as increased expression of tumour necrosis factor-α (TNFα) and PPARγ (Lee *et al.*, 2008). These effects of Substance P can be partially reduced by co-application with the corticosteroid dexamethasone, which has well-described anti-inflammatory effects (Newton, 2000; Lee *et al.*, 2008). The evident pro-lipogenic and pro-inflammatory action of Substance P on sebocytes would implicate Substance P as a potential aetiologic factor within the proposed inflammatory model of acne pathogenesis (Tanghetti, 2013; Zouboulis *et al.*, 2014). Alternatively, Substance P may not play any role in initial acne lesion formation, but may contribute to the inflammatory component of late-stage acne lesions (Toyoda *et al.*, 2002a).

5.1.3 Experimental aims

Given that a HC-dependent SG phenotype was observed following denervation, the cell biological and molecular basis for neuro-regulation of SG homeostasis was further investigated. As the mouse SG itself does not appear to be directly innervated (Chapter 3, Figure 3.4; Figure 3.5), it was hypothesised that the anagen-dependent upregulation of SG size by nerve fibres might be a result of direct innervation and regulation of SG progenitors in the HF (Jensen *et al.*, 2009b). Therefore, a lineage tracing approach was taken to identify whether there may be a deficit in the contribution of intrafollicular SG progenitors following denervation.

In parallel, and by leveraging the existing body of literature indicating potential neuroregulatory factors, mouse PSUs were probed for expression of several key candidate genes implicated in neuroregulation of SG biology, including neurotransmitter and neuropeptide receptors, transporters, enzymes, and downstream signalling mediators. It was hypothesised that such elements may be expressed in the JZ. Alternatively, despite the observed lack of innervation, nerve-derived substances might act at a distance on sebocytes.

The key experimental aims were as follows:

- Determine whether the contribution of *Lrig1*-expressing cells to the SG and infundibulum is perturbed following denervation (by fate mapping labelled cells in *Lrig1-Cre* reporter mice).
- If a LRIG1+ cell phenotype is evident following denervation, determine the molecular basis for neuroregulation of these cells.
- Probe murine PSUs for expression of the substance P receptor (*Tacr1*), metabotropic glutamate receptor 5 (*Grm5*), glutamate aspartate transporter

(*Slc1a3*), nicotinic ACh receptor alpha 7 (*Chrna7*), AMY1 CGRP receptor (*Calcr*), CGRP receptor (*Calclr*), and the SHH-effector Gli1 (*Gli1*).

The *in situ* hybridisation experiment probing for *Calclr*, described in section 5.2.3 (Figure 5.7) was carried out by Dr Wei Shang (Skin Research Institute of Singapore) at the request of the author.

5.2 Results

5.2.1 Denervation results in reduced contribution of Lrig1-positive cells to the sebaceous gland

Given that the SG epithelium does not appear to be innervated, while LNFs terminate in close proximity to LRIG1+ cells in the JZ (Figure 3.5), it was hypothesized that the observed HC-dependent enlargement of SGs during anagen is mediated through neuronal interaction with intrafollicular SG progenitors. To investigate this, GFP+ cells were quantified in the SG, JZ and infundibulum via genetic-inducible fate mapping (GIFM) in *Lrig1-CreER2:Rosa-mTmG* transgenic mice (Figure 2.1; Figure 2.3) (Powell *et al.*, 2012).

CreER2-mediated recombination, induced by application of 4-OHT, results in GFP labelling of *Lrig1*-expressing cells and their subsequent progeny. Adult male and female mice, aged 7-8 weeks, were denervated, then at 5 days PD, depilated via waxing whilst simultaneously induced recombination using 4-OHT. Topical application of 4-OHT was used in order to avoid potential side-effects caused by systemic administration of an oestrogenic compound. Mice were then sacrificed after a further 3, 6- or 9-days post-depilation.

In a separate experiment, expression of *Lrig1* in the JZ was examined in adult male mice at 30 days PD. Importantly, immunoreactivity for LRIG1 was not significantly downregulated in denervated skin (Figure 5.1B), allowing for direct comparison of lineage tracing data between the denervated and intact flanks. Following induction by 4-OHT, the amount of GFP per SG was quantified, and normalised for SG size.

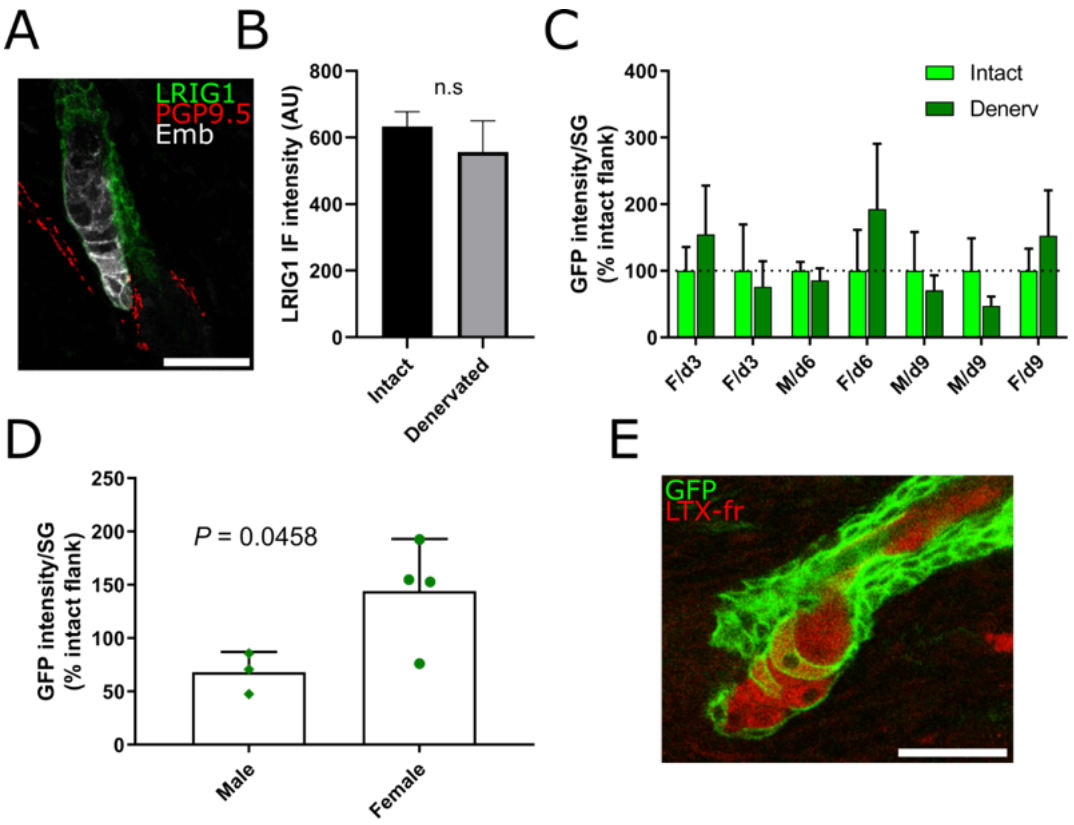

Figure 5.1. Differential effect of denervation on the degree of SG GFP-labelling between male and female *Lrig1-Cre:Rosa-mTmG* mice.

(A) Immunofluorescence demonstrating LRIG1 immunoreactivity and nerves in a telogen PSU. *Lrig1* expression is enriched in the junctional zone and is a potential marker for intrafollicular progenitors for the SG (Page et al., 2013). Scale bar = 50 µm. **(B)** Quantification of LRIG1 immunofluorescence intensity (given in arbitrary units; AU) in adult male mice at 30 days PD. There may be a small reduction in LRIG1 expression in the JZ following denervation, but this is not statistically significant (n = 3 mice, 5-10 JZs each, per condition). **(C)** Area normalised GFP intensity per SG following denervation, expressed as a percentage of the mean GFP intensity for each intact flank. Average percentages for n = 7 mice (10-40 SGs each) shown separately. SG GFP labelling shows no clear trend over time point following depilation, or indeed, following denervation. **(D)** Significant difference between GFP labelling of SGs following denervation between male and female mice. The data in (C) was resolved according to gender. Males exhibit a decrease in SG labelling, whereas in females, labelling is increased in denervated SGs, on average. **(E)** Example image of a GFP labelled PSU, counterstained with HCS LipidTOX DeepRed Neutral Lipid Stain (intact, 3 days post-depilation, female). Scale bar = 50 µm.

It was observed that in denervated skin, the effects on GFP-labelling of SGs were varied and differed considerably between mice (Figure 5.1C). As it had been previously discovered that the effects of denervation on SG size and function may be different between male and female mice (Figure 4.7), the results of lineage tracing were split according to gender. Interestingly, in male mice, denervation resulted in reduced GFP labelling of SGs compared to intact skin, whereas the opposite effect was observed for female mice (Figure 5.1D). On average, GFP-labelling of denervated male SGs was approximately 70% of that observed for the corresponding intact value for each mouse (Figure 5.1D). In female mice, denervated SG labelling was increased to approximately 140% on average (Figure 5.1D). One of the female mice represented an outlier and showed a percentage labelling that was similar to male mice (Figure 5.1D). All four of the female mice used in this experiment were littermates, and were denervated/depilated at the same age, differing only in the timepoint of 4-OHT application. The mice also had similar body weights (ranging from 16.5g - 17.1g). It is possible that this discrepancy is due to this mouse perhaps being in a different stage of the oestrous cycle, given that group-housed females can develop irregular oestrous cycles, according to the 'Lee-Boot effect' (van Der Lee & Boot, 1955; Norris & Carr, 2013; Yeadon, 2014).

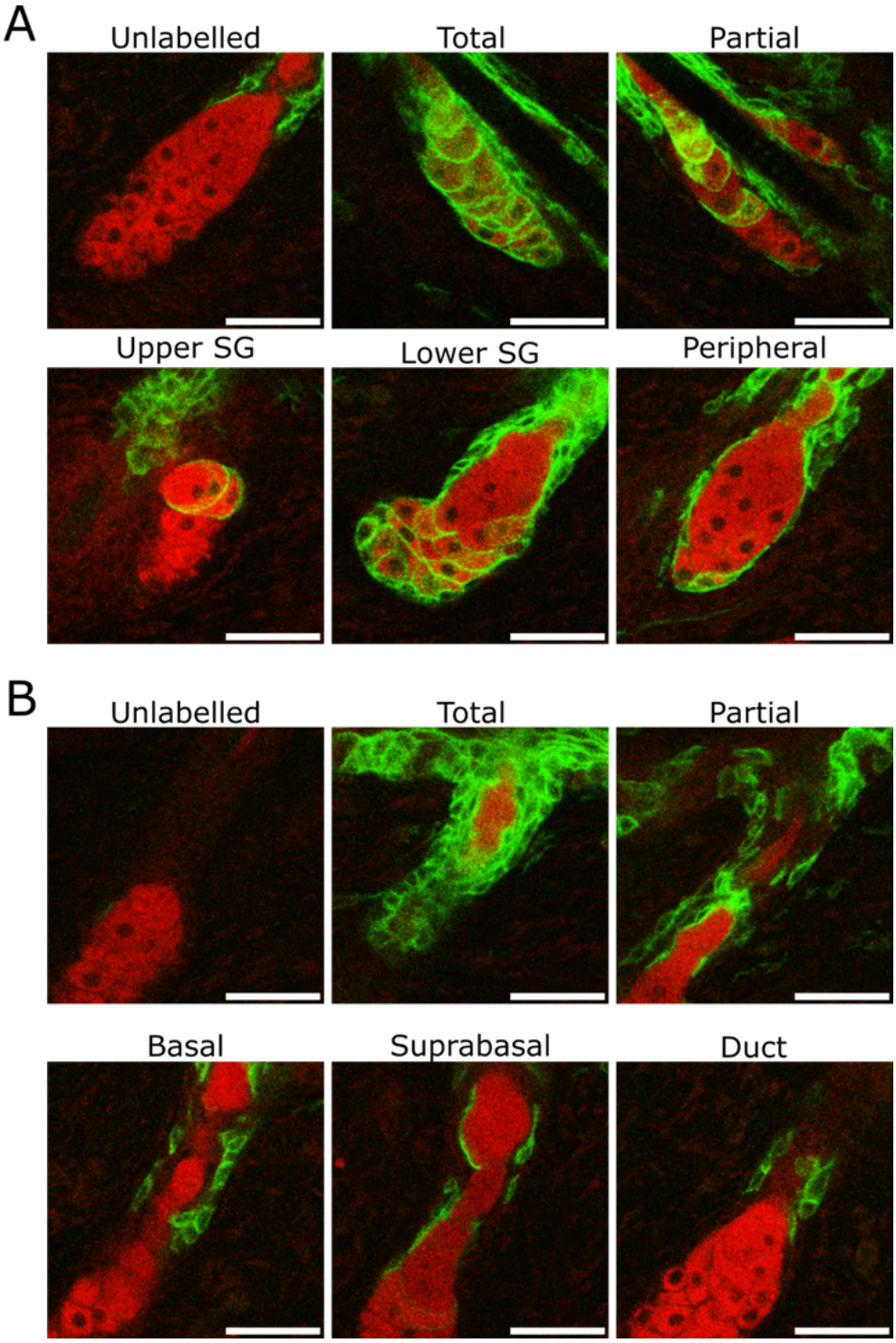

Figure 5.2. Categorisation of different patterns of SG and infundibular GFP-labelling following induction in *Lrig1-Cre:Rosa-mTmG* mice.

(A) Types of labelling of SGs. Unlabelled, no GFP+ sebocytes; Total, labelling of entire SG; Partial, any sub-total labelling of SGs that does not fit into any of the other categories; Upper SG, restriction of labelling to the upper half of the SG; Lower SG, restriction of labelling to the lower half of the SG; Peripheral, only peripheral sebocytes on the edge of the SG are labelled. **(B)** Types of labelling of the infundibulum. Unlabelled, no GFP+ keratinocytes; Total, the entire infundibulum from the SG to IFE is labelled; Partial, mixed labelling that does not fit into the other categories; Basal, restriction of GFP to basal keratinocytes; Suprabasal, only keratinocytes superior to the basal layer are labelled; Duct, a small population of keratinocytes around the SG duct are labelled. All scale bars = 30 μm; GFP (green); LipidTOX DeepRed Neutral Lipid Stain (red).

The patterns of SG labelling in female mice were further quantified and categorised (Figure 5.2A), based on previously published work (Oulès *et al.*, 2019). As LRIG1+ cells are also thought to contribute to the infundibulum (Page *et al.*, 2013), labelling of infundibula between denervated and intact skin was also examined and categorised along similar lines as for the SG (Figure 5.2B). Patterns of SG-labelling were divided into unlabelled, totally labelled, partially labelled, and restriction of labelling to either the upper SG, lower SG, or peripheral sebocytes (Figure 5.2A). For infundibula, labelling was categorised into unlabelled, totally labelled, partially labelled, and restriction of labelling to the basal compartment, suprabasal compartment, or SG duct (Figure 5.2B).

In line with the observed results for quantification of GFP intensity per SG (Figure 5.1C-D), denervation was associated with an increased proportion of labelled SGs at all time points (Figure 5.3). Similarly, there was an increase in the percentage of labelled infundibula in denervated mice at 6- and 9-days post-depilation (Figure 5.3). At 3 days post-depilation, there is a relatively larger proportion of SGs exhibiting peripheral restriction of labelling (Figure 5.3), which may reflect the model of SG homeostasis, where intrafollicular cellular contributions to the SG must first move into the peripheral layer before differentiating (Niemann & Horsley, 2012).

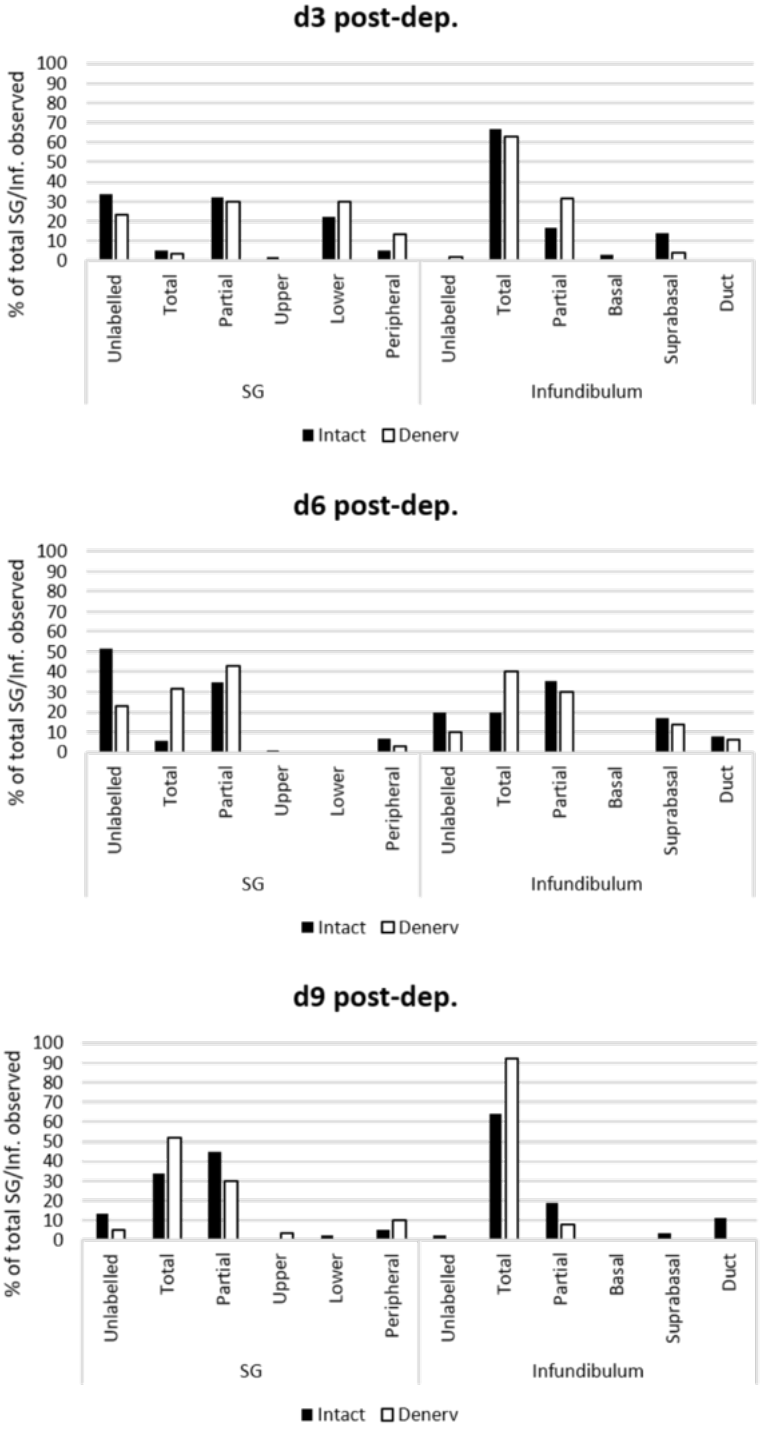

Figure 5.3. Preliminary quantification of patterns of GFP-labelling in denervated, depilated female mice.

SGs and infundibula were categorised according to patterns of GFP-labelling following induction in female *Lrig1-Cre:Rosa-mTmG* mice. Observed quantities were expressed as a percentage of the total number of SGs or infundibula examined. For each time point, n=1 female mouse that had previously demonstrated increased overall GFP intensity per SG. At each time point, the overall number of unlabelled SGs in denervated skin is decreased. Similarly, at day 6 and day 9 post-depilation, the number of unlabelled infundibula is also reduced. The relatively larger proportion of SGs exhibiting 'peripheral' or 'lower' labelling at 3 days post-dep compared to other time points, may reflect the model that cellular input to the SG from the follicular compartment must first move into the peripheral layer of the SG before differentiating.

5.2.2 Isthmus *Gli1* expression is lost after denervation, and *Gli1*-expressing cells in the UB also express *Lrig1*

In parallel to lineage tracing of LRIG1+ cells, mouse skin was probed for expression of candidate neurotransmitter receptors and other factors implicated in neuroregulation of pilosebaceous biology. This work was undertaken in order to try an identify what nerve-derived substances could be responsible for regulation of SG biology which, when missing in denervated skin, results in the observed SG phenotypes. Previous research has indicated that within the UB region, there resides a population of innervated cells that express *Gli1*, which is an important downstream mediator of SHH signalling (Brownell *et al.*, 2012; Cheng *et al.*, 2018).

Denervation has already been shown to result in specific loss of *Gli1* expression in the UB (Brownell *et al.*, 2012). As the previously described lineage tracing data would suggest, following denervation, the behaviour of innervated intrafollicular cells may become abnormal (Figure 5.1; Figure 5.3). It was hypothesised that loss of nerve derived SHH may be responsible for this effect. It was further hypothesised that there may be a subpopulation of GLI1+/LRIG1+ cells in the JZ/UB, which are directly innervated, and which contribute to the SG during hair growth.

As previously reported, *Gli1* mRNA is present in the isthmus of murine PSUs (Figure 5.4A), and loss of *Gli1* mRNA in the isthmus can be observed following denervation (Figure 5.4B). Using a duplex RNAscope method, it was found that in normal mouse telogen skin, *Gli1* expression overlaps with the *Lrig1*-expressing domain (Figure 5.5). Both the size of the GLI1+ and LRIG1+ compartments appears to expand with the onset of depilation induced anagen (Figure 5.5B). As previously shown (Figure 5.1B) expression of *Lrig1* in the isthmus following denervation appears to be unchanged (Figure

5.5 B-D). Similarly, the observed persistence of *Gli1* in denervated skin at 8-days PD (Figure 5.5B) is aligned with that previously shown, where *Gli1*-mediated X-gal staining is reduced, but still present, in denervated skin at 1-week PD, but is lost almost entirely in skin at 2-weeks PD (Brownell *et al.*, 2012).

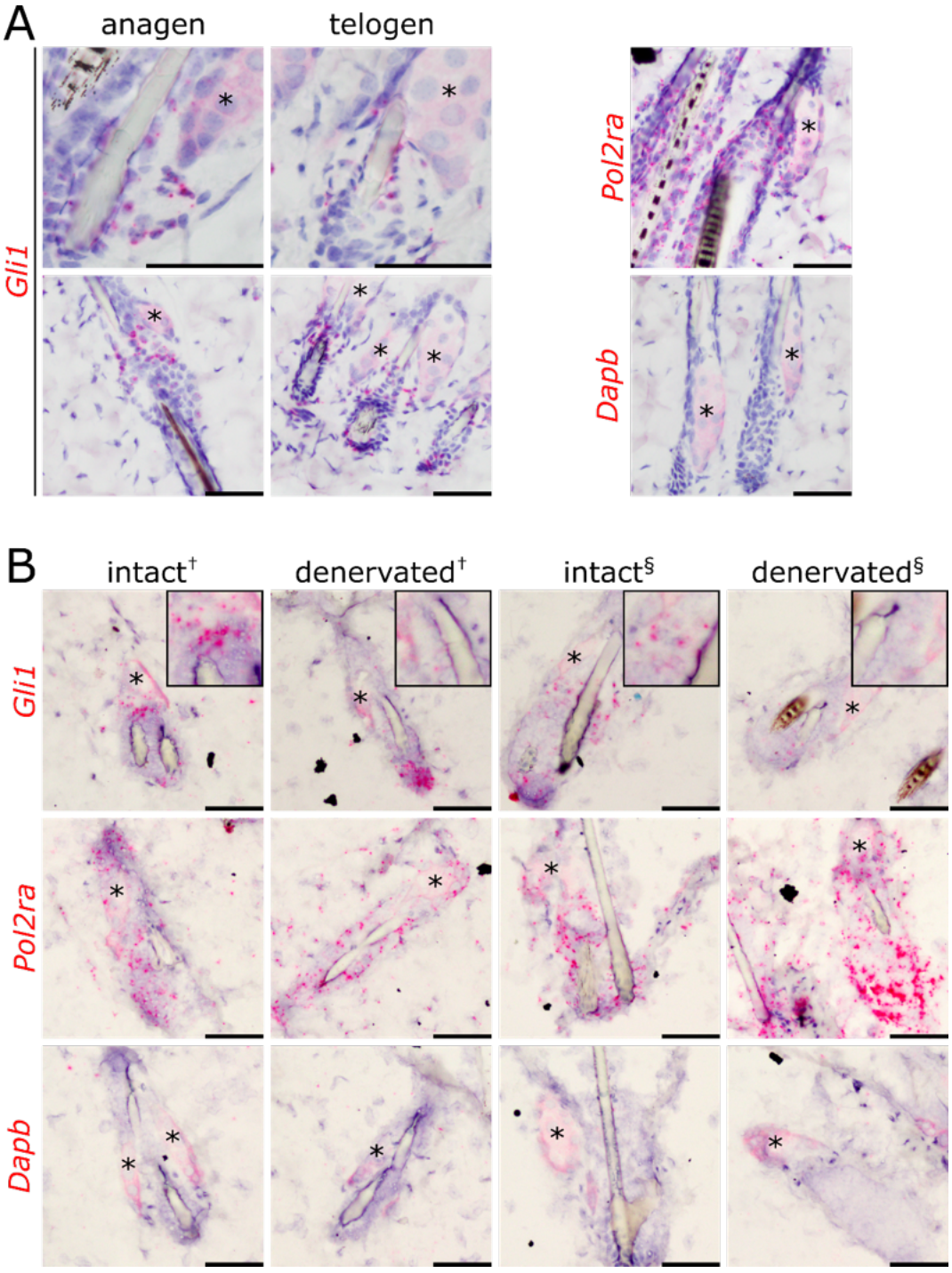

Figure 5.4. Expression of mRNA for the sonic hedgehog effector *Gli1* is lost in the UB of the PSU following denervation.

(A) Comparison of *Gli1* mRNA expression in the PSU between telogen and spontaneous anagen within the same adult male mouse (90 days PD). *Gli1* mRNA is present in the follicular epithelium at the level of the lower JZ/UB. Qualitatively, the pattern and degree of expression does not vary between telogen or anagen. *Gli1* mRNA is also observed in mesenchymal cells between the sebaceous and follicular epithelia. Images are representative from n=1 mouse. Top two images were taken with a 40X lens; bottom two images were taken with a 20X lens. **(B)** Loss of *Gli1* expression following denervation is in line with previously published data (Brownell et al., 2012). Images for intact and denervated skin from two separate hybridisation experiments. *Gli1* mRNA is exclusively lost in the JZ/UB following denervation (90 days PD). Insets are 2X optical zooms centred on the JZ/UB. Paired columns represent n=2 mice. Scale bars = 50 µm. Positive control probe, *Pol2ra*; negative control probe, *Dapb*. Symbols (†,§) indicate two separate hybridisation experiments. *indicates SGs in each image.

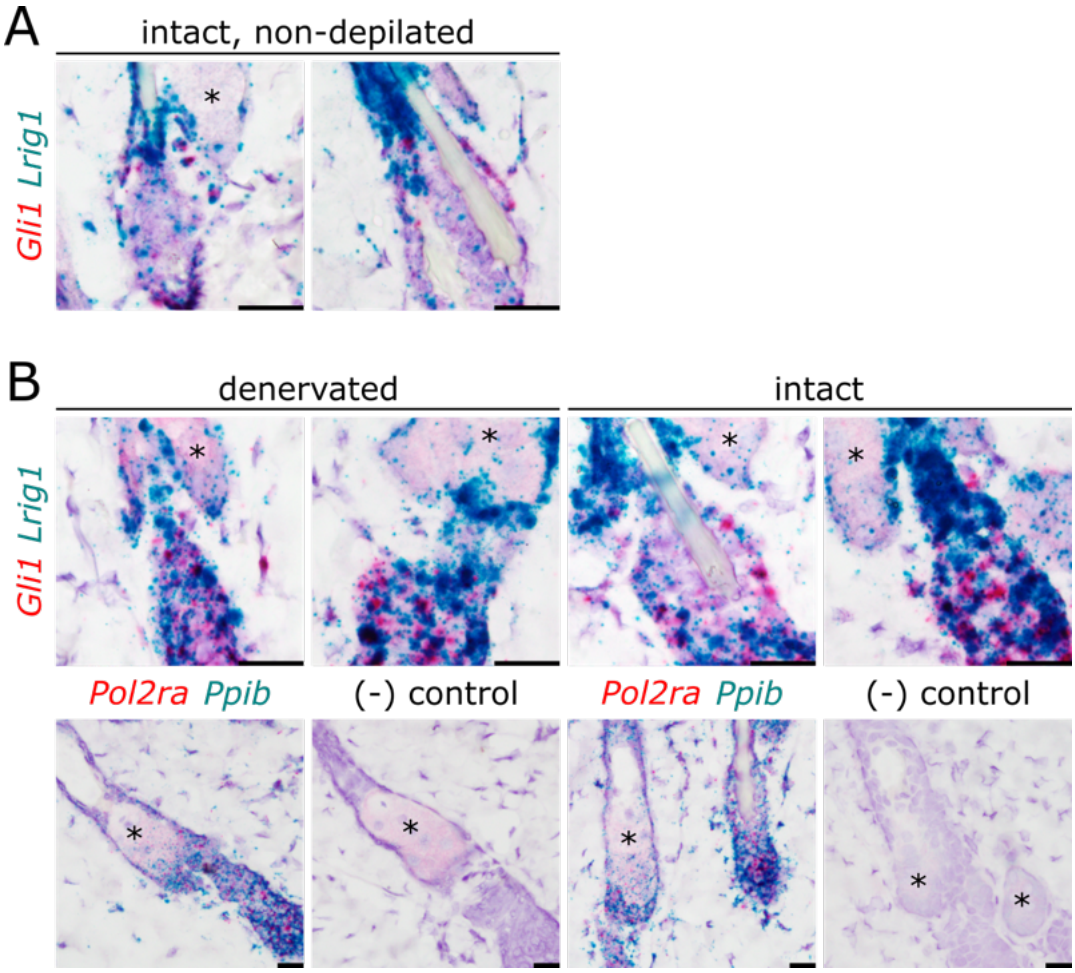

Figure 5.5. *Lrig1* mRNA expression overlaps with *Gli1* mRNA expression in the JZ/UB, and *Gli1* expression is progressively lost following denervation in depilated mice.

(A) Representative images demonstrating *Gli1* (red) and *Lrig1* (green) mRNA localisation in non-depilated PSUs (adult, male). *Lrig1* and *gli1* expression domains in the follicular epithelium show significant overlap. **(B)** *Gli1* mRNA expression and co-expression with *lrig1* is maintained in mice at 3 days following waxing depilation (total of 8 days PD). Onset of depilation induced anagen is associated with expansion of both the *lrig1* and *gli1*-expressing compartments. Images are representative from n=1 mouse each for non-depilated skin and 3 days post-depilation. Positive control probes, *Pol2ra* and *Ppib*; negative control probes are proprietary (ACDbio). *indicates SGs in each image; scale bars = 20 μm.

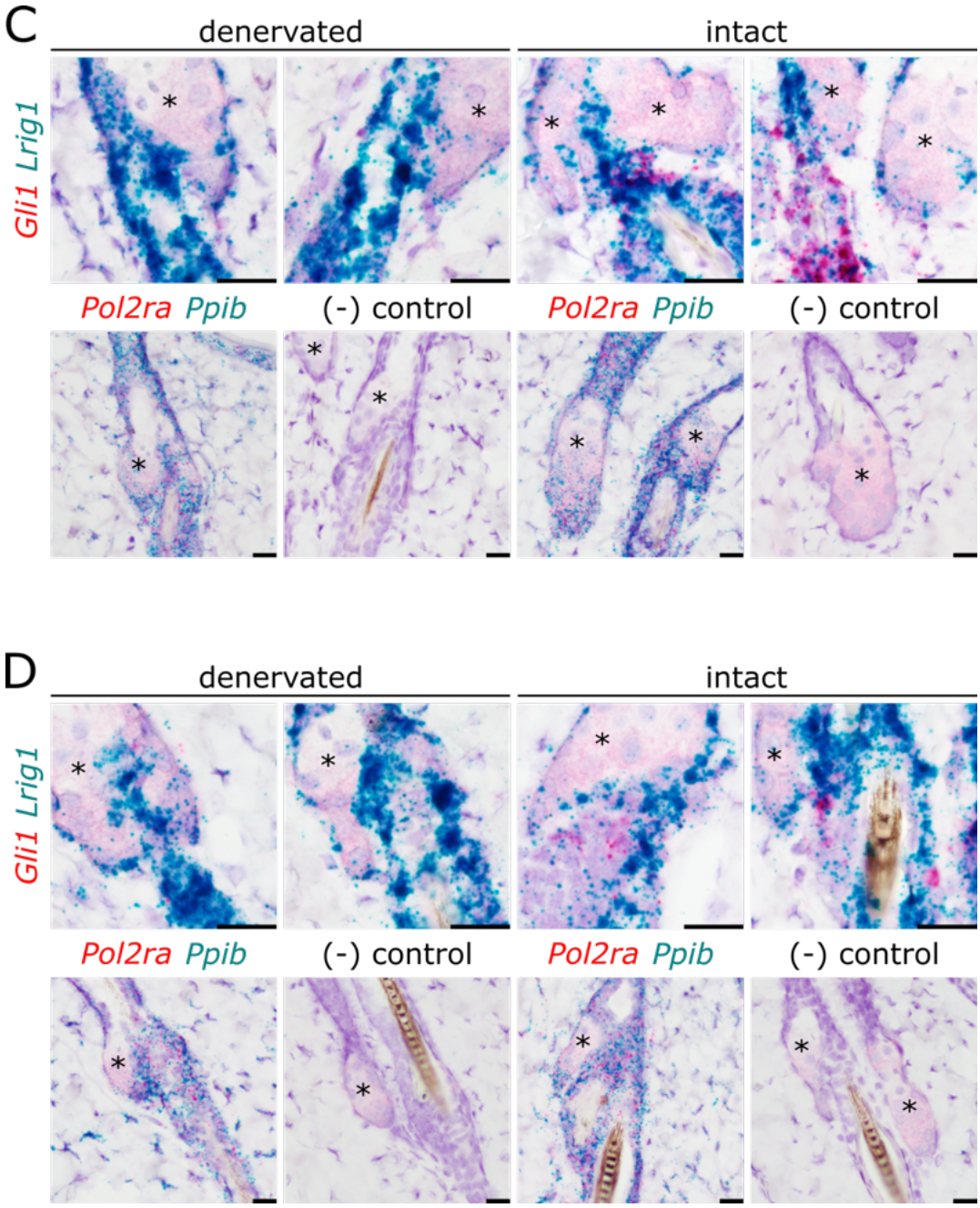

Figure 5.5 continued. *Lrig1* mRNA expression overlaps with *Gli1* mRNA expression in the JZ/UB, and *Gli1* expression is progressively lost following denervation in depilated mice.

(A) *Gli1* mRNA expression is completely lost in the JZ/UB following denervation at 6 days post depilation (total of 11 days PD), while the presence of *Lrig1* mRNA remains robust. **(B)** At 9 days post-depilation (14 days following SCD), *Gli1* mRNA expression in the JZ/UB remains absent. Qualitatively, in non-denervated skin, *Gli1* expression is reduced at this time point post-depilation, compared to earlier stages of depilation-induced anagen (Figure 4B-C). Images are representative from n=1 mouse for each time point. Positive control probes, *Pol2ra* and *Ppib*; negative control probes are proprietary (ACDbio); *indicates SGs in each image; scale bars = 20 μm.

As the expression of Lrig1 does not appear to change substantially following denervation (Figure 5.1B, Figure 5.5B-D), it seems probable that these GLI1+ cells are not lost, but

may lose expression of *Gli1* in the absence of SHH secreted by cutaneous nerves (Brownell et al. 2012). It could be speculated that this nerve-derived SHH is required to recruit LRIG1+/GLI1+ cells to the SG during hair growth.

5.2.3 The CGRP receptor, but not the AMY_1 or substance P receptors, are expressed in the murine junctional zone and infundibulum

The neuropeptide CGRP mediates its effects primarily through two GPCRs, the CGRP receptor (referred to as CTR in human), and the amylin subtype 1 receptor ($AMY_{1)}$. Both forms are coupled to the heterotrimeric G protein Gs, and thus stimulate adenylate cyclase signalling (Hay & Walker, 2017). Each receptor is a heterodimer, consisting of receptor activity modifying protein 1 (*Ramp1*) and, in the case of the CGRP receptor, calcitonin receptor-like receptor (*Calclr*), or calcitonin receptor (*Calcr*) for the AMY_1 receptor complex (Hay & Walker, 2017). As the presence of CGRP in cutaneous nerve endings was observed (Figure 3.7) (Peters *et al.*, 2001), primarily in the CNFs that comprise part of the follicular nerve network at the level of the SG, mouse skin was probed for both *Calcrl* and *Calcr* mRNA, in order to deduce whether SGs or any other part of the pilosebaceous unit, might be sensitive to nerve-derived CGRP.

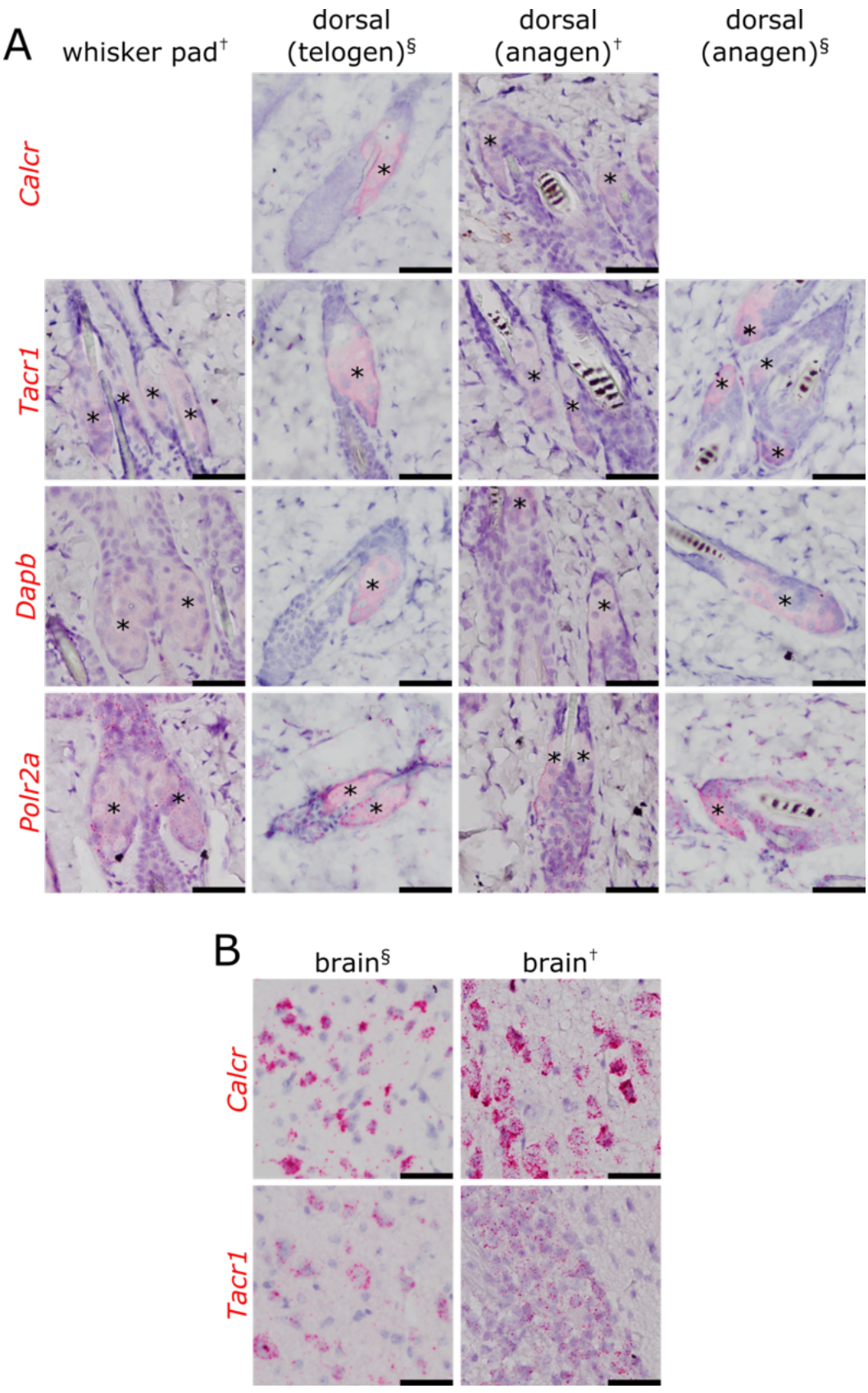

Figure 5.6. Neither the substance P receptor (*Tacr*1) or CGRP receptor AMY1 (*Calcr*) are expressed in murine PSUs.

(A) Probing for *Tacr1* and *Calcr* mRNA in mouse skin. **(B)** Positive signal using probes for *Tacr1* and *Calcr* in mouse brain. Scale bars = 50 μm. Positive control probe, *Pol2ra*; negative control probe, *Dapb*. Symbols (§,†) indicate two separate hybridisation experiments. Each column represents tissue from different mice. *indicates SGs in each image.

Despite evident signal for *Calcr* mRNA in positive control tissue, *Calcr* mRNA was not detectable in mouse dorsal skin, either telogen or anagen, nor in whisker pad skin (Figure 5.6). However, *Calcrl* was detectable in both positive control tissue and in skin (Figure 5.7). *Calcrl* mRNA appeared to be present throughout the IFE, infundibulum and junctional zone, and was especially enriched in the APM (Figure 5.7). Occasionally, *Calcrl* mRNA could be observed in peripheral sebocytes, whereas the presence in infundibular and JZ keratinocytes was more consistently seen (Figure 5.7). The presence of CGRP within follicular nerve endings and expression of *Calcrl* mRNA in the PSU would indicate the existence of a CGRP signalling axis in mouse skin.

It was also investigated whether tachykinin receptor 1 (*Tacr1*), the primary substance P receptor, was expressed in SGs or in the rest of the PSU. Despite robust positive control signal in mouse brain, *Tacr1* mRNA was not demonstrable in mouse skin, including the SGs and HFs (Figure 5.6). This result is in line with the inability to demonstrate substance P immunoreactivity in follicular nerve networks as also previously reported (Peters *et al.*, 2001).

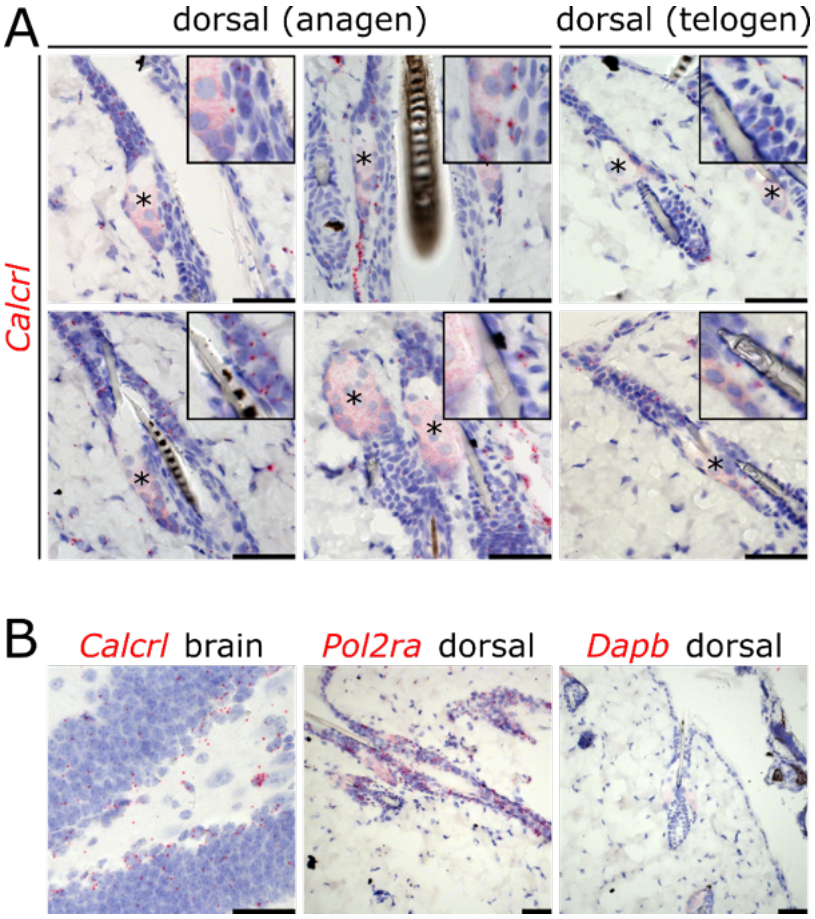

Figure 5.7. Reactivity for *Calcrl* mRNA in the JZ indicates expression of the CGRP receptor.

(A) Probing for *Calcrl* mRNA in adult male mouse skin during anagen and telogen. *Calcrl* mRNA was repeatedly observed in the JZ and infundibulum during hair growth and resting state. Peripheral sebocytes may also express a limited amount of *Calcrl* expression. Insets are 2X optical zooms centred on sites of positive signal. **(B)** Positive signal for *Calcrl* in mouse brain and positive and negative control probes used in the same tissue as for (A). Scale bars = 50 µm. Images are representative from n=1 mouse. Positive control probe, *Pol2ra*; negative control probe, *Dapb*. *indicates SGs in each image. Hybridisation and imaging were carried out by Dr Wei Shang (Skin Research Institute of Singapore) at the request of the author.

5.2.4 Mouse skin contains non-neuronal sources of ACh, but nicotinic ACh receptor α7 does not appear to be expressed in mouse SGs *in vivo*

The nicotinic ACh receptor α7 (*CHRNA7*) is expressed in human primary and immortalised sebocytes, and has been implicated in the regulation of sebaceous lipid synthesis (Li *et al.*, 2013b). Additionally, neuronal and non-neuronal sources of ACh have been reported in human skin (Kurzen *et al.*, 2007; Wessler & Kirkpatrick, 2008).

To explore the possibility of using mouse skin as a valid model system for further dissection of ACh signalling, it was investigated whether murine SGs *in vivo* also express *Chrna7*. Alpha-bungarotoxin (α-BTX) is a selective, high-affinity antagonist for CHRNA7 (Mulcahy, Paulo, & Hawrot, 2018), and fluorophore-conjugated forms of α-BTX can be used to visualise the presence of CHRNA7 protein directly (Akaaboune *et al.*, 2002). To probe for *Chrna7* expression in mouse skin, a GFP-conjugated form of alpha-bungarotoxin (α-BTX-GFP) was used. Whisker pad skin can be used as positive control tissue in this context, as neuromuscular junctions present along skeletal muscle fibres in the whisker pad are enriched for *Chrna7* expression, and are readily demonstrable through incubation with α-BTX-GFP (Figure 5.8) (Akaaboune *et al.*, 2002). However, no staining in either whisker pad or dorsal skin was observed that would indicate expression of *Chrna7* in SGs, or throughout the PSU (Figure 5.8).

Mouse skin was also probed for *Chrna7* mRNA via RNAscope *in situ* hybridisation. No reactivity for *Chrna7* mRNA was demonstrable in whisker pad skin or in dorsal skin, in either telogen or anagen phases of the hair cycle (Figure 5.9). However, a positive control signal for *Chrna7* in whisker pad skeletal muscle or mouse brain was not ascertained, despite all tissues readily demonstrating reactivity for positive control mRNAs (Figure 5.9). These data would suggest that the particular *Chrna7* probe used was non-functional, given the ease with which *Chrna7* expression is demonstrable in skeletal muscle using α-BTX-GFP (Figure 5.8). The lack of α-BTX-GFP labelling would suggest that that chrna7 is not expressed in mouse skin (Figure 5.8).

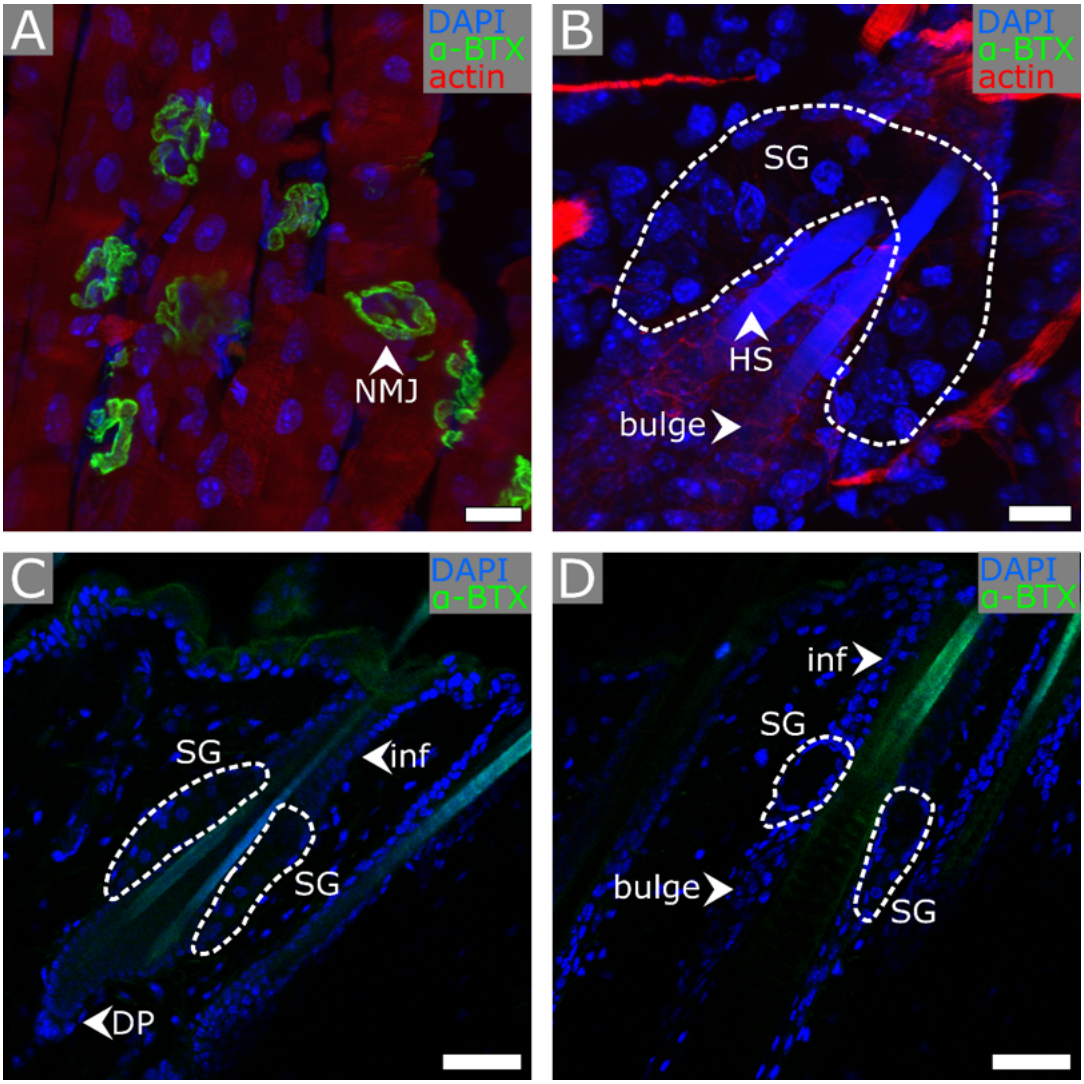

Figure 5.8. Incubation of mouse skin with GFP-conjugated α-Bungarotoxin (α-BTX) does not result in labelling of the PSU.

(A) Nicotinic ACh receptor α7 (*Chrna7*), which is enriched in neuromuscular junctions (NMJs) is readily labelled in mouse skeletal muscle, using α-BTX. **(B)** Projection view of SGs, JZ and bulge of a PSU in mouse whisker pad skin (adult, male). **(C)** Transverse section of a telogen PSU in adult male dorsal skin. Inf = infundibulum; DP = dermal papilla; **(D)** Transverse section of an anagen PSU in adult, male dorsal skin. No detectable GFP fluorescence from α-BTX is distinguishable from autofluorescence (B-D). Each image represents tissue from different mice. Scale (A-B) = 15 μm. Scale (C-D) = 50 μm.

In parallel, the prevailing hypothesis that sources of ACh in skin are non-neuronal in origin was further investigated (Kurzen & Schallreuter, 2004; Kurzen *et al.*, 2004; Li *et al.*, 2013b). RNAscope *in situ* hybridisation was performed for choline acetyltransferase (*Chat*) to identify potential sources of ACh in mouse skin. Interestingly, *Chat* expression was observed specifically in bulge follicular keratinocytes, in both anagen and telogen skin, and in non-vibrissae whisker pad PSUs (figure 5.10). While the nature of the

putative ACh receptor(s) in mouse sebocytes or sebaceous progenitors remains unclear, the possibility of keratinocyte derived ACh regulating SG function remains a possibility (Kurzen & Schallreuter, 2004; Kurzen *et al.*, 2004).

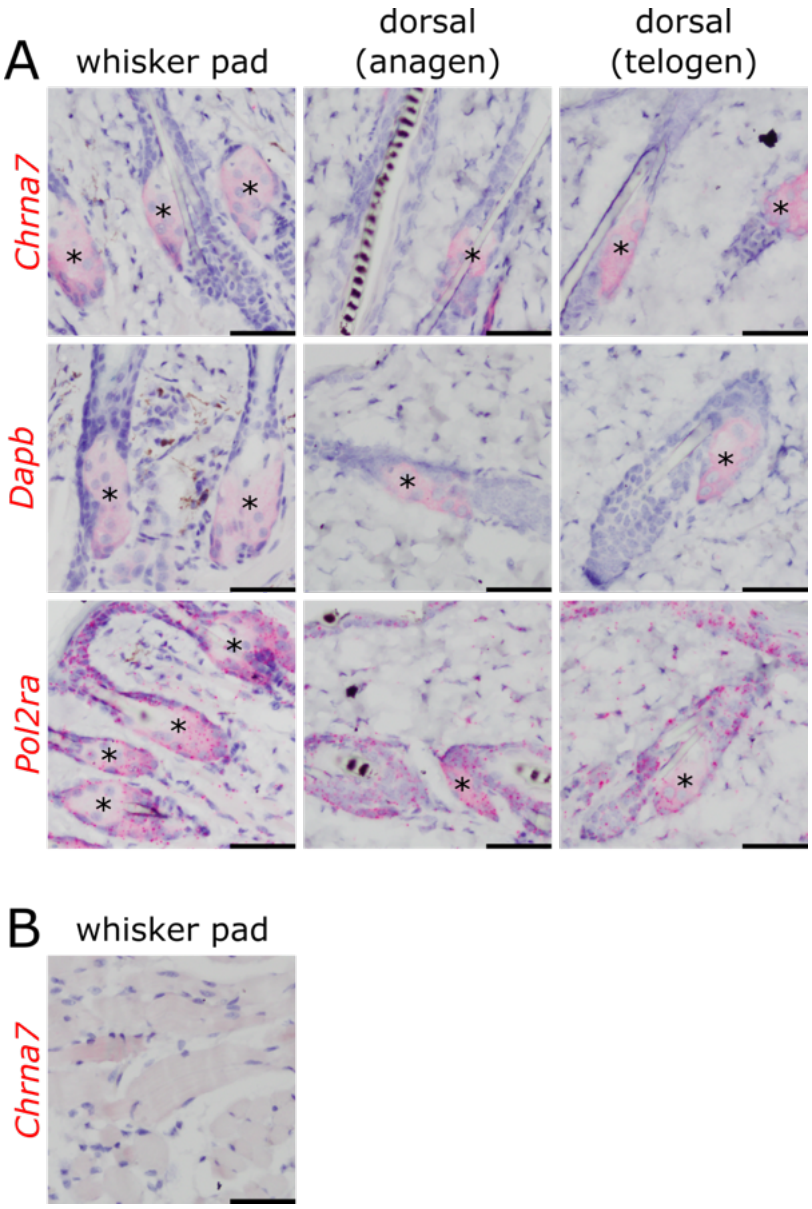

Figure 5.9. *Chrna7* mRNA is not detectable in adult mouse skin.

(A) Probing for *Chrna7* mRNA in adult male mouse skin during anagen and telogen, and in whisker pad tissue. Reactivity for *Chrna7* was not observed. Positive control probe, *Pol2ra*; negative control probe, *Dapb*. Each column represents tissue from different mice. **(B)** Expected positive signal for *Chrna7* in skeletal muscle of the mouse whisker pad is absent, suggesting that the probe may be non-functional. Scale bars = 50 μm. *indicates SGs in each image.

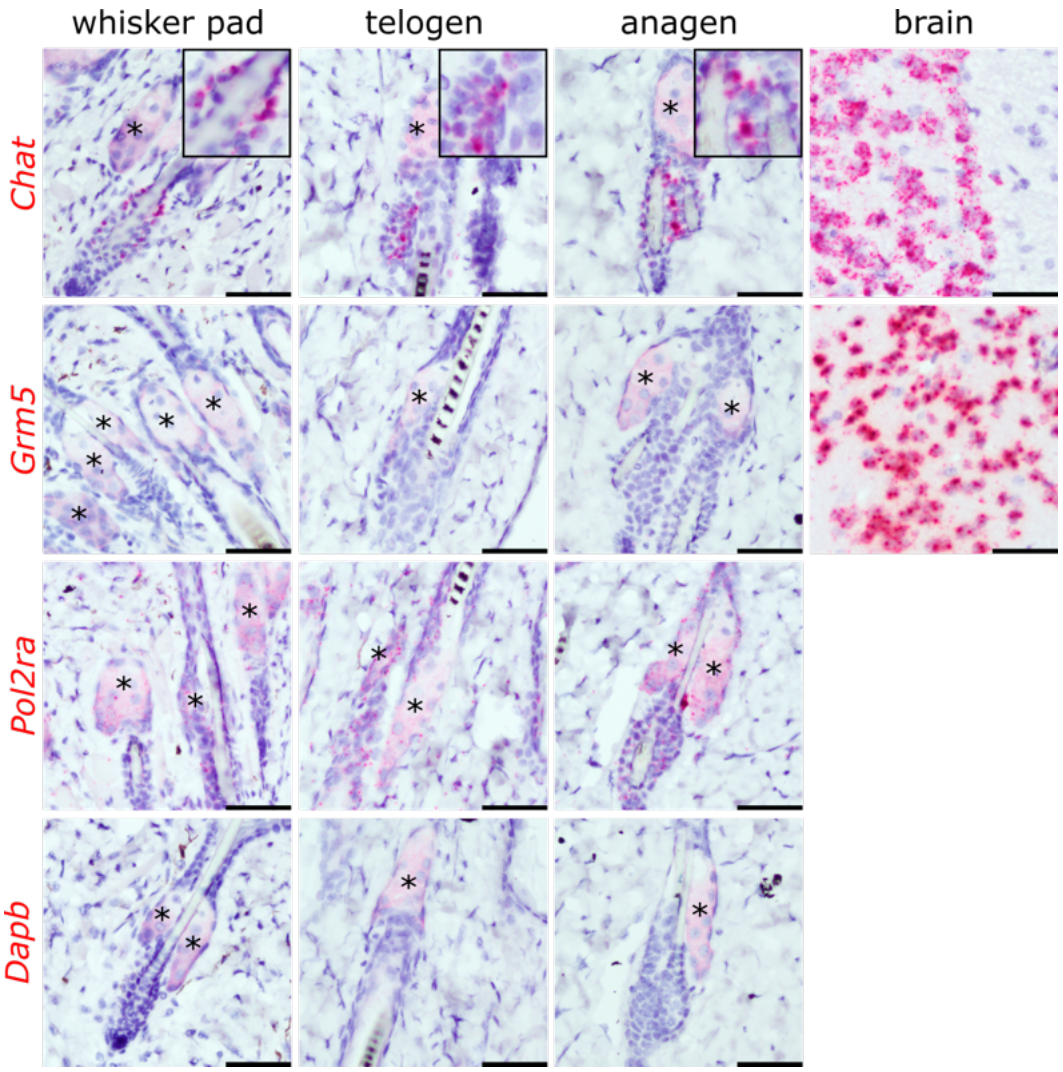

Figure 5.10. Choline acetyltransferase (*Chat*) mRNA is expressed in bulge keratinocytes, but metabotropic glutamate receptor 5 (*Grm5*) is not detectable in mouse skin.

Chat mRNA was evident in the bulge of whisker pad, telogen and anagen HFs and, interestingly, appeared to be enriched in follicular keratinocytes between that reside between the bulge and club hair. Conversely, *Grm5* was not detected in any of the examined mouse skin. Robust positive signal for *Chat* and *Grm5* was observed in positive control tissue (mouse brain). Images for anagen and telogen are representative from n=1 adult male mouse which had skin of mixed HC-stages. Each column represents sections taken from the same block of tissue and hybridised with the indicated probes. Positive control probe, *Pol2ra*; negative control probe, *Dapb*; *indicates SGs in each image; scale bars = 50 µm.

5.2.5 Peripheral sebocytes express the glutamate transporter *Slc1a3*, but not the metabotropic glutamate receptor *Grm5*

It has recently been reported that SG enlargement during anagen is at least partly dependent on the activity of the glutamate aspartate transporter *Slc1a3* (Solute carrier family 1, member 3) (Reichenbach *et al.*, 2018). In the central nervous system, this protein

plays an important role in regulating the concentration of extra-neuronal glutamate, which is a vital and universal excitatory neurotransmitter in the brain (Petroff, 2002). Moreover, pharmacological stimulation of the metabolic glutamate receptor Grm5 could rescue the phenotype of *Slc1a3* null mice in which anagen-dependent SG enlargement was lost (Reichenbach *et al.*, 2018). Given the clear relevance of both of these genes to the hypothesis of neuroregulation of SGs, their expression and localisation in mouse skin was clarified here using RNAscope *in situ* hybridisation.

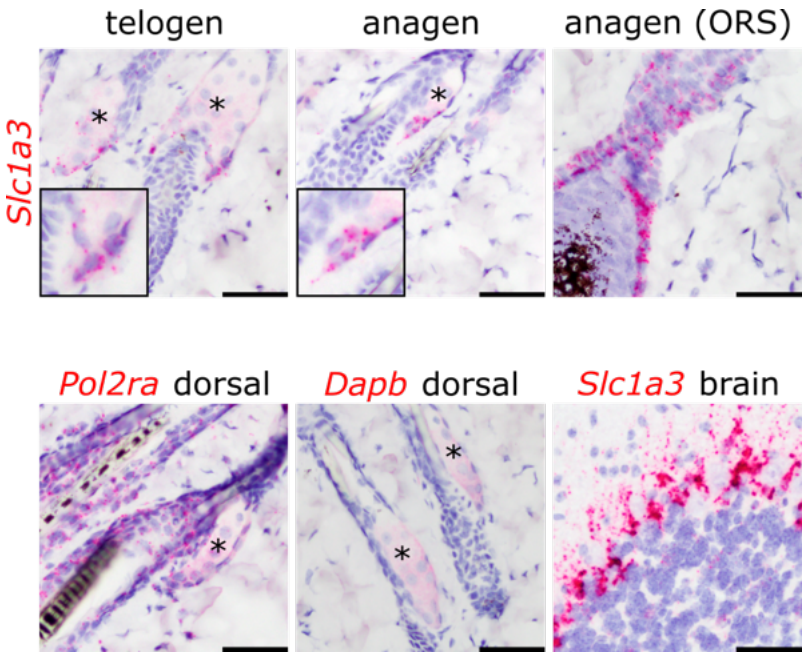

Figure 5.11. The glutamate transporter *Slc1a3* is expressed in peripheral sebocytes of mouse SGs.

Slc1a3 mRNA was observed to be expressed in peripheral sebocytes, primarily within the 'tip' of the SG (lower SG). During anagen, expression of *Slc1a3* mRNA also developed in the outer root sheath (ORS) of hair follicles. Clear positive signal for *Slc1a3* was also demonstrable in mouse brain (cerebellar Purkinje neurons shown). Insets are 2X optical zooms centred on sites of positive signal. Images are representative from n=1 adult male mouse. Positive control probe, *Pol2ra*; negative control probe, *Dapb*; *indicates SGs in each image; scale bars = 50 μm.

Slc1a3 mRNA, as expected, was readily detectable throughout the mouse brain (cerebellar Purkinje cells shown) (Figure 5.11). *Slc1a3* mRNA was present in murine SGs and demonstrated a clear selective expression in peripheral sebocytes towards the lower tip of the SG (Figure 5.11). The same expression pattern was present in SGs comparing

telogen to anagen skin. Diffuse *Slc1a3* mRNA was also observed in infundibular keratinocytes and throughout the IFE. During anagen, the HF ORS showed dramatic upregulation in *Slc1a3* mRNA (Figure 5.11).

In contrast, *Grm5* mRNA, while evidently present in mouse brain, could not be observed in mouse skin, either dorsal skin in anagen or telogen, or in non-vibrissae whisker pad PSUs (Figure 5.10). This observation is contradictory to that previously reported for GRM5 immunoreactivity in mouse skin (Reichenbach *et al.*, 2018).

5.3 Discussion

5.3.1 Neurons are required for proper contribution of intrafollicular progenitor cells to the SG

The observed pattern of follicular innervation (Chapter 3) would suggest that any SG phenotype resulting from denervation would likely result from changes in the behaviour of intrafollicular cells which may serve as stem cells for the SG. *Lrig1* is considered a marker of SG progenitors, and is primarily expressed in the JZ (Page *et al.*, 2013), so it was hypothesised that denervation might affect SG homeostasis by modulation of the behaviour of *Lrig1*-expressing cells. Hypothetically, it may be possible, in spite of lack of direct neuronal contacts, for nerves to directly signal to the SG epithelium using long-distance neurotransmitters, or indirectly through interstitial cells, such as fibroblasts, immune cells, or Schwann cells. A further, alternative possibility is that the signal associated with denervation is communicated indirectly to basal cells in the SG through lateral, cell-cell communication from the innervated population.

However, it was observed that denervation results in altered contributions of LRIG11+ cells to the SG (Figure 5.1C-D). Interestingly, the effect of denervation appeared to be gender specific, with male mice exhibiting reduced GFP labelling following induction, and female mice showing increased labelling (Figure 5.1D). It is known that sex steroids can differentially effect the behaviour of stem cells (Ray *et al.*, 2008), and the presence of an outlier female mouse may be due to variations in the stage of oestrous cycle in which the lineage tracing might have been conducted. The evident gender-dependent phenotype would suggest a modulatory function of sex steroids in regulation of LRIG1+ cells, and hormonal fluctuations through the oestrous cycle may well have an effect (Norris & Carr, 2013).

Furthermore, as described in the introduction, during development, *Lrig1* and *Sox9* are initially expressed together in a group of follicular cells immediately prior to the formation of the SG (Niemann & Horsley, 2012). Importantly, *Sox9* is known for its crucial role in the development of primary male sex characteristics (Jakob & Lovell-Badge, 2011). It can be reasonably hypothesised therefore that there are intrinsic sex-dependent differences in the biology of LRIG1+ stem cells.

An additional caveat of this study is that induction of lineage tracing is achieved through administration of 4-OHT, which is an oestrogenic compound. While differential effects of oestrogens of hair cycling have been reported (Plikus & Chuong, 2008), no obvious difference in depilation-induced hair growth was observed between male and female mice that had also been induced with 4-OHT (Figure 4.5). Furthermore, the reported inhibitory effects of oestrogens on SG function are thought to be mediated via systemic inhibition of androgens, rather than by direct action on SGs (Clayton *et al.*, 2019). Murine SGs do reportedly express oestrogen receptors however (Azzi, El-Alfy, & Labrie, 2006) so potentially confounding effects of 4-OHT treatment cannot be ruled out.

5.3.2 Nerve-derived sonic hedgehog as a niche factor for hair cycle-activated intrafollicular progenitors

GLI1 is a crucial effector of SHH signalling (Villavicencio, Walterhouse, & Iannaccone, 2000). There is substantial evidence indicating that GLI1+ cells in the isthmus of the mouse PSU are a population of directly innervated cells (Cheng *et al.*, 2018). As shown here (Figure 5.4; Figure 5.5) and reported previously, *Gli1* expression is lost following denervation (Brownell *et al.*, 2012). RNA sequencing of GLI1+ cells in the PSU reveals a network of genes related to neuronal outgrowth and synaptic maintenance (Joost *et al.*, 2016; Cheng *et al.*, 2018). Furthermore, genetic manipulation of the extracellular matrix components produced by these cells results in aberrant patterns of follicular innervation (Cheng *et al.*, 2018).

Here, it has been demonstrated that GLI1+ cells also appear to express *Lrig1* mRNA, and that denervation results in aberrant behaviour of LRIG1+ cells, as indicated by GIFM (Figure 5.1; Figure 5.3). Furthermore, there is a body of previous work showing the importance of SHH signalling to normal SG homeostasis (Gat *et al.*, 1998; Niemann *et al.*, 2002; Lo Celso *et al.*, 2008; Kakanj *et al.*, 2013). Taken together, the data presented here along with previous findings suggest the following hypothesis: nerve-derived SHH acts to regulate GLI1+/LRIG1+ cells, directing them to contribute to the SG in a HC-dependent fashion.

Nerve-derived SHH is known to regulate the behaviour of *Gli1*-expressing mesenchymal stem cells in other systems, such as in the mouse incisor (Zhao *et al.*, 2014). To investigate further, existing *Gli1* reporter mice (Brownell *et al.*, 2012; Zhao *et al.*, 2014) could be used to fate map *Gli1*-expressing cells during hair growth and in a denervated context. *Gli1*-reporter mice could also be crossed with *Lrig1*-reporters to permit simultaneous

observation of GLI1-/LRIG1+, GLI1+/LRIG1+, and GLI1+/LRIG1- populations. A further step might involve isolation of double GLI1+/LRIG1+ cells via flow cytometry, and subsequent gene expression analyses to identify unique markers. These markers could then allow generation of novel transgenic animals to better probe the function of GLI1+/LRIG1+ cells.

5.3.3 The CGRP receptor, but not the *Tacr1* substance P receptor, is expressed in the mouse PSU

The presence of CGRP immunoreactivity in follicular nerve fibres (Figure 3.7), and expression of *Calcrl* mRNA in the junctional zone (Figure 5.7) would strongly indicate the presence of a CGRP-CTR axis in skin that could potentially regulate SG function by modulating intrafollicular sebaceous progenitors.

However, in combination with other forms of receptor activity modifying proteins (RAMPs) other than RAMP1, CALCRL forms other, non-exclusive CGRP receptors. For example, a RAMP2-CALCRL heterocomplex forms the adrenomedullin receptor AM_1. Together, RAMP3-CALCRL form a dual CGRP/adrenomedullin receptor referred to as AM_2 (Hay & Walker, 2017). Therefore, without probing for the various forms of RAMPs, it cannot be conclusively stated that it is the definitive CGRP receptor that is present in the mouse JZ or infundibulum. However, given the presence of CGRP in follicular nerves (Figure 3.7), it is reasonable to assume that *Calcrl* expression indicates the presence of the CGRP receptor, as the affinity of AM_2 for CGRP is reportedly limited (Hay & Walker, 2017). While adrenomedullin is reportedly highly expressed in human skin, there is very limited evidence indicating any role of the peptide in regulating skin appendage growth or function (Müller *et al.*, 2003).

The observed lack of *Tacr1* expression in the mouse PSU is peculiar (Figure 5.6), given the preceding literature suggesting that substance P have a role in regulating human SG function and acne pathogenesis (Toyoda & Morohashi, 2001, 2003; Toyoda *et al.*, 2002a). It may be possible that modulation of SGs by substance P is unique to humans, and perhaps further restricted to the pathological state of acne. The expression of alternative substance P receptors in both mouse and human skin is a possibility that should next be explored (Schank & Heilig, 2017).

5.3.4 Potential role of neuronal and non-neuronal ACh in regulating sebaceous gland function

As *Chrna7* mRNA was not demonstrable in whisker pad skin (Figure 5.9 B), where GFP-conjugated alpha-bungarotoxin labels Chrna7 Figure 5.8 A), it can be concluded that this particular probe for *Chrna7* mRNA is non-functional. However, the results of GFP-bungarotoxin labelling would suggest that *Chrna7* is not expressed in mouse skin (Figure 5.8 C-D). The data here is in contrast to a previous immunohistochemical-based report of the presence of nAChRα7 in mouse SGs (Fan *et al.*, 2011). It is possible that ACh-mediated stimulation of lipid production is unique to human sebocytes (Li *et al.*, 2013b), or that mouse SGs rely on other ACh receptors.

Interestingly, it was observed that *Chat* mRNA was specifically expressed and localised in bulge keratinocytes (Figure 5.10). This finding is supported by scRNAseq data that has also reported the presence of *Chat* mRNA in K15+ bulge cells from murine HFs (Joost *et al.*, 2016). This would strongly suggest that these cells synthesise and secrete ACh. However, it is not clear which cells would be recipient to this secreted ACh. Future work may aim to screen for expression of different ACh receptors, either via use of antibodies or *in situ* hybridisation. Alternatively, the presence of different ACh receptors could be

pharmacologically dissected by treating sebocytes with a range of cholinergic agonists or antagonists.

In the nervous system, post-synaptic neurons recipient of ACh express acetylcholinesterase (AChE), which breaks down ACh (Silman & Sussman, 2017). Interestingly, scRNAseq data has also shown that an AChE-related protein, butyrylcholinesterase (BChE), is exclusively present in the mouse SG at levels comparable to other SG-specific markers, such as PPARγ and Elovl3 (Joost *et al.*, 2016). These findings would suggest that sebocytes are active metabolisers of ACh and related compounds. However, as stated, it is not clear whether the mouse SG expresses ACh receptors. It is possible that a signalling mechanism exists between the HF and SG that uses ACh as a mediator, but which does not rely on ACh receptors. For example, metabolites of ACh, such as trimethylglycine (betaine), are known to exert several cell biological effects, such as regulation of osmolarity and cell volume (Kempson, Zhou, & Danbolt, 2014) which in turn can impact differentiation (Guo *et al.*, 2017). Betaine has also been shown to promote PPARγ-mediated lipogenesis in skeletal muscle cells (Wu *et al.*, 2018). These findings raise the question of whether betaine or other ACh metabolites could similarly regulate sebocyte function.

In any case, it remains unclear whether neuronal ACh is of any relevance to regulation of SGs. A key experiment moving forward would be to investigate whether treatment of mouse skin with cholinergic antagonists can phenocopy the effect of cutaneous denervation.

5.3.5 Potential role of glutamate in regulating sebaceous gland function

Slc1a3 mRNA is present specifically within peripheral sebocytes (Figure 5.11), supporting previous evidence indicating a functional requirement of Slc1a3 in SG homeostasis (Reichenbach *et al.*, 2018). This would indicate that SGs are perhaps dependent on nerve-derived glutamate signalling, however, it remains to be seen whether *Slc1a3* expression is critical to SG function in the context of facilitating glutamate as a neurotransmitter, albeit one that must act at long-range, given the observed patterns of innervation (Chapter 3). Crucially, *Slc1a3* was identified as being required for hair cycle-dependent enlargement of SG area (Reichenbach *et al.*, 2018). Therefore, glutamate is a prime candidate molecule for neuroregulation of HC-dependent SG homeostasis.

The role of *Slc1a3* in SG function could be further dissected in the context of cutaneous denervation, and tested pharmacologically using inhibitors for excitatory amino acid transporters, such as DL-threo-beta-benzyloxyaspartate, or inhibitors specific for *Slc1a3* (Jensen *et al.*, 2009a). In contrast to previous findings, mRNA for *Grm5* was not found to be present in SGs or throughout the wider PSU (Figure 5.10). While the used RNAscope probe should be specific for *Grm5*, it is possible that the antibody used exhibits cross-reactivity with Grm3 (Reichenbach *et al.*, 2018), and that the reported immunoreactivity does not actually represent *Grm5* expression. It might also be the case that turnover of Grm5 protein is low and only transient transcription is required to maintain expression (Vogel & Marcotte, 2013), thus explaining the observed lack of signal for *Grm5* mRNA. However, the ability of the allosteric GRM5 antagonist 3-((2-Methyl-4-thiazolyl)ethynyl)pyridine (MTEP) to inhibit SG enlargement during anagen would indicate both the presence and functional role of GRM5 protein in SG homeostasis (Reichenbach *et al.*, 2018).

Chapter 6: General discussion

6.1 Murine sebaceous glands require intact cutaneous innervation in a hair cycle dependent context

The data presented here clearly indicate that intact cutaneous innervation is required for normal SG homeostasis (Figure 4.2; Figure 4.6). Importantly, it is shown that while the peripheral nervous system is largely dispensable for basal SG maintenance, it is required for upregulation of SG size during active hair growth (anagen) (Figure 4.2; Figure 4.6). By examining SG neuroanatomy, it is concluded that the SG is not directly innervated (Figure 3.4), but the possibility of neurotransmitters acting via long range mechanisms on sebocytes cannot be yet be excluded.

It is worth noting that direct innervation of at least one type of SG does occur *in vivo*. Meibomian glands exhibit an extensive network of nerve fibres within their surrounding connective tissue, and these nerves produce several key neurotransmitters and neuropeptides, including calcitonin gene-related peptide, vasoactive intestinal peptide, SP and ACh (Montagna & Parakkal, 1974c; Seifert & Spitznas, 1996; Cox & Nichols, 2014). At the ultrastructural level, unmyelinated axons can be seen to pass within 1 μm of the cell membranes of basal meibocytes (Seifert & Spitznas, 1996).

However, in the context of dorsal murine SGs, it is demonstrated here that a subpopulation of LRIG1+ cells in the JZ/UB is directly innervated (Figure 3.5), and it is further shown that denervation results in aberrant behavior of LRIG1+ cells with regards to their contributions to the SG. These cells may be the same population as the previously reported, GLI1+ cells in the isthmus, which lose *Gli1* expression following denervation (Figure 5.5) (Brownell *et al.*, 2012).

It was recently demonstrated that all of the basal cells in the murine SG act as equipotent progenitors generating the gland, and that cells outside of the SG do not normally contribute to the SG (Andersen *et al.*, 2019). This would support the observations made

here of a lack of effect of denervation on SGs under homeostatic conditions (Figure 4.2; Figure 4.4). However, as yet, it has not been definitively demonstrated whether or not non-SG-resident progenitors can contribute to the SG during non-homeostatic conditions, such as hair growth. The data presented here would suggest that LRIG1+ cells outside of the SG can contribute to the SG during depilation-induced anagen (Figure 4.6; Figure 5.1; Figure 5.3). However, as the method for GIFM used here did not explicitly focus on clonal lineage tracing, we cannot exclude the small possibility that the altered GFP labelling in denervated *Lrig1-Cre:Rosa-mTmG* mice is due to some effect mediated by LRIG1+ cells that may exist within the SG.

An alternative possibility that has not been explored is that nerves are somehow required for hair-cycle dependent remodelling of the SG stroma, which would facilitate enlargement of SGs through expansion of SG-resident progenitors by promoting symmetric renewal, in accordance with recent data (Andersen *et al.*, 2019). It has been recently shown that SG enlargement does not necessarily require increased proliferation of basal sebocytes. Indeed, the oncogenic KrasG12D mutation mediates enlargement of SGs by promoting symmetric renewal in basal sebocytes, thus increasing the number of basal cells (Andersen *et al.*, 2019). KrasG12D causes a shift in sebocyte behaviour that is similar to that found during morphogenesis, when expansion of the number of basal progenitor cells is required. The shift in behaviour between morphogenesis and homeostasis is associated with a changes in genes related to the extracellular matrix (Andersen *et al.*, 2019), as the homeostatic period is associated with decreased levels of fibronectin and increased levels of collagen and elasticity (Andersen *et al.*, 2019). It may be possible that hair cycle-dependent remodelling of the mesenchyme facilitates SG expansion during hair growth, but that denervation somehow prevents or ameliorates this remodelling, thus preventing SG enlargement.

It is further unknown whether human SGs also exhibit a similar dependence on hair cycle stage. Generally, SGs associated with actively growing terminal hairs like those of the scalp and beard are large, while those associated with non-growing vellus hairs are smaller (Montagna & Parakkal, 1974c). However, clear exceptions to this trend can be found in Meibomian glands (Butovich, 2017), and in sebaceous follicles, which are chiefly associated with acne (Kligman & Shelley, 1958).

Finally, the apparent differential effects of denervation on SGs and LRIG1+ cells between male and female mice might explain the variability in sebum production observed in studies where the gender composition of patient populations was not resolved (Burton *et al.*, 1971a; Summerly *et al.*, 1971). Intriguingly, as denervation in female mice appears to selectively increase LRIG1+ cell contributions to both the SG and infundibulum (Figure 5.1; Figure 5.3), neuromodulation may represent a unique therapeutic strategy for manipulation of sebum production and treatment of acne in women.

6.2 Other unexplored aspects of sebaceous gland neuroregulation

6.2.1 Adrenaline

Adrenaline (epinephrine) is a major neurotransmitter of the sympathetic nervous system and a hormonal product of the adrenal glands. Propranolol-mediated blockade of adrenergic β-receptors over 8-10 weeks does not affect either sebum excretion rate or acne grade in patients with acne vulgaris (Cunliffe & Cotterill, 1970). This is consistent with earlier observations that intradermal injections of adrenaline also do not alter the rate of sebum secretion in humans (Miescher & Schonberg, 1944; Ikai, 1958; Kligman & Shelley, 1958). Furthermore, mapping of adrenergic receptor expression in skin via use

of radio-labelled ligands reveals that SGs do not express either β1 or β2-adrenergic receptors (Steinkraus *et al.*, 1996).

Differentiation of human Meibomian gland cells has also been shown to be positively regulated by brimonidine, an α2-adrenoreceptor agonist (Han *et al.*, 2018). Furthermore, in mice, lack of Meibomian gland innervation by dopamine beta hydroxylase-expressing neurons is associated with blepharoptosis (drooping eyelids) and corneal ulceration, which are symptoms of Meibomian gland dysfunction (Eldredge *et al.*, 2008). Therefore, it cannot yet be ruled out that adrenergic innervation and catecholamines play a role in SG physiology, at least through α-adrenoceptors (Ambadkar & Vyas, 1980).

Interestingly, the β2-adrenocreceptor has been demonstrated to be selectively upregulated in the isthmus of murine HFs during early anagen (Botchkarev *et al.*, 1999). Given that SGs exhibit an anagen-dependent upregulation in size (Figure 4.2; Figure 4.6) (Reichenbach *et al.*, 2018), it could be reasonably hypothesised that the abrupt and transient expression of β2-adrenocreceptor reflects a similarly brief involvement of adrenergic signalling in recruitment of sebaceous progenitors to the SG. This model might also explain why attempts to modulate sebum secretion in humans with adrenergic compounds have not been successful (Miescher & Schonberg, 1944; Ikai, 1958; Kligman & Shelley, 1958; Cunliffe & Cotterill, 1970), given that the percentage of HFs undergoing the telogen-to-anagen transition in human skin at any particular time is small (Van Scott *et al.*, 1957; Kligman, 1959; Saitoh, Uzuka, & Sakamoto, 1970).

6.2.2 Neurotrophins

Neurotrophins are a class of secreted proteins that guide axonal outgrowth and provide trophic support to neurons (Skaper, 2012). Immunoreactivity for neurotrophin-3 (NT3)

(Adly *et al.*, 2005), nerve growth factor (NGF) (Toyoda & Morohashi, 2003; Adly *et al.*, 2006b), glial-derived neurotrophic factor (GDNF) (Adly *et al.*, 2006a), and pigment epithelium-derived factor (PEDF) (Li *et al.*, 2013a) have all been reported in human SGs. The presence of neurotrophins does not appear to be restricted to any particular zone of the SG, except for GDNF, which is confined to peripheral sebocytes (Adly *et al.*, 2006a). Furthermore, NGF protein can be detected in the peripheral sebocytes of acne-associated SGs, but not in the glands of healthy skin (Toyoda, Nakamura, & Morohashi, 2002b; Toyoda & Morohashi, 2003).

Interestingly, NGF expression can be induced in peripheral sebocytes by incubation of human skin with IL-6 (Toyoda & Morohashi, 2003). Sebaceous production of neurotrophins supports the hypothesis that the SG epithelium can attract a supply of nerve fibres to the gland, possibly under the pro-inflammatory conditions associated with acne. Interestingly, human SGs also exhibit immunoreactivity for several neurotrophin receptors including TrkA, TrkC, GFRα1/2 and p75NTR (Adly *et al.*, 2005, 2006b, 2006a; Adly, Assaf, & Hussein, 2009), suggesting that neurotrophins can exert a direct effect on sebocytes.

Yet, what role neurotrophins may play in the control of sebocyte function remains unclear. A striking historical report demonstrated that subcutaneous injection of murine NGF (0.2 mg/ml) in mice produces a three-fold enlargement of SGs near the injection site after two weeks (Reams, 1967). Furthermore, mice that are null for the protein Egr3 (early growth response 3), a downstream effector of NGF signalling, develop symptoms of MG dysfunction and exhibit a loss of MG innervation (Eldredge *et al.*, 2008). A distinction must be made here between several different potential modes of action of neurotrophins on SGs. The reported expression of both neurotrophins and neurotrophin receptors would suggest the existence of a paracrine, or possibly autocrine, mechanism of neurotrophin regulation of sebocytes (Toyoda & Morohashi, 2003; Adly *et al.*, 2005,

2006b, 2006a, 2009). Alternatively, neurotrophins may indirectly control SG function by modulating the recruitment of nerve fibres to either the SG, or perhaps sebaceous progenitor cells within the follicular epithelium.

Interestingly, HF morphogenesis and cycling in mice have been found to be dependent on neurotrophins (Botchkarev *et al.*, 2004; Peters *et al.*, 2006; Zhou *et al.*, 2006), though cutaneous denervation does not affect hair growth or hair cycle progression (Maurer *et al.*, 1998; Brownell *et al.*, 2012). This would suggest that neurotrophins primarily act as paracrine and/or autocrine hormones within the PSU, rather than solely promoting innervation, though it remains to be seen whether this is true for the SG specifically.

6.2.3 Endocannabinoids

Endocannabinoids (ECs) are a group of neuromodulatory, poly-unsaturated fatty acids that are synthesised throughout the mammalian nervous system, but also in many other tissues, including cutaneous epithelia (Maccarrone *et al.*, 2015). In the nervous system, ECs, such as anandamide (AEA) or 2-arachidonoylglycerol (2-AG), are synthesised and released from the post-synapse in response to depolarisation of the post-synaptic membrane. These ECs then bind and activate G-protein-coupled receptors within the pre-synaptic membrane. Activation of these cannabinoid receptors (CB1 or CB2) has several effects including modulation of neuronal excitability and altering gene expression. Cannabinoids can also bind and activate transient receptor potential (TRP) receptors (Caterina, 2014).

Plant-derived cannabinoid compounds are referred to as phytocannabinoids (*phyto* - *plant*), and these include the psychoactive tetrahydrocannabinol (THC) from the *Cannabis* plant (Di Marzo & Piscitelli, 2015). Collectively, ECs, their associated

receptors, and the enzymes involved in ECs synthesis throughout the central and peripheral nervous systems are referred to as the endocannabinoid system (ECS). In the central nervous system, ECs serve a number of important functions, such as the regulation of satiety, sleep, mood, and sensation of pain (Fride, 2005). In cutaneous nerves of humans and rodents, the ECS appears to modulate both nociception and temperature sensation (Cravatt *et al.*, 2001; Potenzieri, Brink, & Simone, 2009; Guindon *et al.*, 2011, 2013; Caterina, 2014). Only recently has a non-neuronal ECS been described in human skin, which also appears to regulate several key aspects of sebocyte biology (Maccarrone *et al.*, 2015; Oláh *et al.*, 2016; Zákány *et al.*, 2018).

SZ95 sebocytes produce the ECs AEA and 2-AG, and also express several receptors capable of binding cannabinoid compounds, including CB2 (Dobrosi *et al.*, 2008), TRPV1, TRPV2, and TRPV4 (Oláh *et al.*, 2014). Both AEA and 2-AG promote lipogenesis in SZ95 cells, and up-regulate PPARγ and COX2 (cyclooxygenase-2) expression through activation of MAPK (Mitogen-activated protein kinase) signalling (Dobrosi *et al.*, 2008). Recently, it was shown that inhibition of endocannabinoid uptake by SZ95 sebocytes suppressed lipopolysaccharide-induced production of inflammatory cytokines (Zákány *et al.*, 2018). Overall, the function of the ECS in sebocytes appears to be to promote both lipogenesis and a shift towards a pro-inflammatory phenotype.

In contrast to ECs, several phytocannabinoids have been shown to negatively regulate lipid and interleukin production in SZ95 cells (Oláh *et al.*, 2014, 2016). For example, cannabidiol (CBD) dose-dependently reverses AEA-induced lipogenesis in SZ95 cells and organ cultured human SGs. CBD also reduces lipid synthesis and production of inflammatory mediators elicited by incubation with arachidonic acid, linoleic acid, and testosterone (Oláh *et al.*, 2014). Importantly, these effects of CBD are mediated by a CB1/CB2-independent mechanism, through activation of TRPV4 vanniloid receptors (Oláh *et al.*, 2014).

Given that some of the observations summarized above were made in organ-cultured normal human skin, it is likely that the ECS also regulates human SG function *in vivo*. Yet, this remains to be formally demonstrated. Nevertheless, it has been reported that human SGs are immunoreactive for both cannabinoid receptors, CB1 and CB2 (Ständer *et al.*, 2005; Dobrosi *et al.*, 2008). Furthermore, mouse and human SGs are immunoreactive for CB2, as well as several enzymes involved in endocannabinoid synthesis (Ma *et al.*, 2011; Zheng *et al.*, 2012; Zákány *et al.*, 2018).

Based on the SZ95 data described, it could be hypothesised that sebocyte-produced ECs work in an autocrine fashion to modulate both lipid synthesis and the production of inflammatory mediators. Whether such a system operates independently of the ECS that is present in cutaneous nerves is not known.

6.2.4 ACh in other glandular organs and appendages

As discussed previously, ACh stimulates lipid production in human sebocytes *in vitro* through the nicotinic ACh receptor *Chrna7* (Li *et al.*, 2013b). However, in this thesis, the nicotinic ACh receptor *Chrna7* could not be detected in murine SGs (Figure 5.8; Figure 5.9), which brings into question whether the observed SG phenotype following denervation could be due to loss of nerve derived ACh.

Better understood examples of ACh-modulated skin appendages are the eccrine/apocrine gland (otherwise known as sweat glands). Sweat glands are ductal skin appendages which resemble a coiled, tubular structure (Montagna & Parakkal, 1974b). In human skin, eccrine glands, which are more numerous, serve a thermoregulatory role by secreting liquid (sweat) on to the surface of the skin, which has a cooling effect as it evaporates (Segal, 2009). Conversely, the primary function of apocrine glands, which are

predominantly confined to the axilla, is to secrete odorous substances (Segal, 2009). Sweat glands are richly innervated by cholinesterase-positive nerve fibres (Montagna & Parakkal, 1974b), and sweat gland secretion is chiefly regulated via cholinergic sympathetic neurons and muscarinic ACh receptors (Richerson, 2009; Segal, 2009; Hu *et al.*, 2018).

Another example can be found in Meibomian glands, which are also surrounded by an extensive network of nerve fibres that can be labelled using the cholinesterase technique (Montagna & Ellis, 1957b; Montagna & Parakkal, 1974c) or by expression of various neuropeptides (Cox & Nichols, 2014). As mentioned previously, Meibomian glands are a specialised form of SG in the eyelid (Montagna & Parakkal, 1974c), and development of Meibomian glands is dependent on meibocyte secretion of neurotrophins and innervation (Eldredge *et al.*, 2008). Immortalised human meibocytes express muscarinic ACh receptors (Kam & Sullivan, 2011) and, in further support of a functional role of ACh in Meibomian gland function, treatment of immortalised human meibocytes with the broad-spectrum cholinergic agonist carbachol results in increased proliferation and activation of adenylate cyclase signalling (Kam & Sullivan, 2011). Furthermore, the M3 cholinergic agonist pilocarpine exerts an anti-apoptotic and anti-proliferative effect on immortalised meibocytes (Zhang *et al.*, 2017).

Parallels can be drawn here with what is known about the role of ACh in salivary glands. Similar to Meibomian glands, development of salivary glands is dependent on autonomic innervation (Knox *et al.*, 2010; Nedvetsky *et al.*, 2014). In this context, cholinergic nerve fibres are required to prevent premature differentiation of K5+ progenitors as the salivary gland forms (Knox *et al.*, 2010). Interestingly, *K5* expression also marks label-retaining cells in the periphery of Meibomian glands (Parfitt *et al.*, 2016), suggesting that perhaps nerves are similarly required to modulate K5+ cell behaviour in Meibomian glands. In adult salivary glands, ACh promotes pluripotency in SOX2+ cells (Emmerson *et al.*,

2018), which act as progenitor cells for salivary acini (Emmerson *et al.*, 2017). Denervation results in depletion of SOX2+ cells and impaired acinar regeneration, which can be rescued by treatment with carbachol (Emmerson *et al.*, 2018).

It would be worthwhile using the work described above as a framework for future research investigating ACh and SG biology. As a first step, the expression of cholinergic receptors in sebocytes or sebocyte progenitors should be comprehensively investigated either pharmacologically or via gene expression analyses. In parallel, the presence of cholinergic nerves should be examined with respect to markers of progenitor cell populations in the PSU. Once candidate receptors have been identified, introduction of relevant agonists in a denervated background will provide evidence of a functional role of ACh in SG biology.

6.3 Translational relevance of neuroregulation of sebaceous glands

The efficacy of anti-acne therapies is usually determined through observation of reduced sebum production or SG involution (Jalian *et al.*, 2015; Pan, Wang, & Tu, 2017; Trivedi *et al.*, 2018), but these may not be a desirable outcomes for maintenance of overall skin health, if sebum indeed serves important physiological roles (Smith & Thiboutot, 2008; Ehrmann & Schneider, 2016; Dahlhoff *et al.*, 2016a; Kobayashi *et al.*, 2019). Loss of sebum production might also be related to pathogenesis of other dermatoses such as psoriasis and atopic dermatitis (van Smeden *et al.*, 2014; Shi *et al.*, 2015; Szántó *et al.*, 2019). Furthermore, it seems that certain components of sebum, as well as sebocyte-derived cytokines and inflammatory mediators, could exacerbate acne (Zouboulis *et al.*, 2014; Choi *et al.*, 2019) or perhaps contribute to comedo formation itself (Motoyoshi, 1983; Kim, Lee, & Lee, 2019).

Therefore, in the context of acne, future research needs to identify signals and factors that can modulate sebum composition and sebocyte behaviour, rather than abrogate sebum production entirely (Zákány *et al.*, 2018; Törőcsik *et al.*, 2018). In this context, it may be possible, by manipulating the differentiation of progenitors for the infundibulum and SG (Jensen *et al.*, 2009b; Page *et al.*, 2013; Barnes *et al.*, 2017; Fontao *et al.*, 2017), to prevent comedo formation in acne without negatively affecting sebum secretion, or indeed, specifically restore or modulate sebum production. Moreover, innervation of sebaceous progenitors would indicate the nervous system as a potentially important player in SG carcinoma (Quist *et al.*, 2016).

By demonstrating that SGs are dependent on intact cutaneous innervation, this thesis has indicated directions of further research that will attempt to identify nerve-derived substances with the potential to impact sebocyte function and determine the effects of various neuromediators on sebum production, composition, and the production of inflammatory mediators.

6.4 Working hypotheses and future work

Drawing on the findings of this thesis, the primary working hypothesis moving forward can be formulated as follows:

The nervous system regulates the behavior of LRIG1+/GLI1+ intrafollicular sebaceous progenitor cells and directs them to contribute to the SG under non-homeostatic conditions, resulting in modulation of SG size (Figure 6).

Following from this working hypothesis, the next logical experiment would be to fate map the progeny of GLI1+ cells in PSUs following denervation and over HC progression. With regards to candidate neuromediators that could control this process, nerve-derived sonic hedgehog is a prime candidate. It may also be interesting to observe whether *Shh*

mRNA expression in the mouse dorsal root ganglia also fluctuates over hair cycle. Skin taken from cancer patients using Smoothened (*Smo*) inhibitors as part of chemotherapy could also be examined for a SG phenotype. Sebocytes or SGs could be also treated ex vivo with compounds that manipulate SHH signalling.

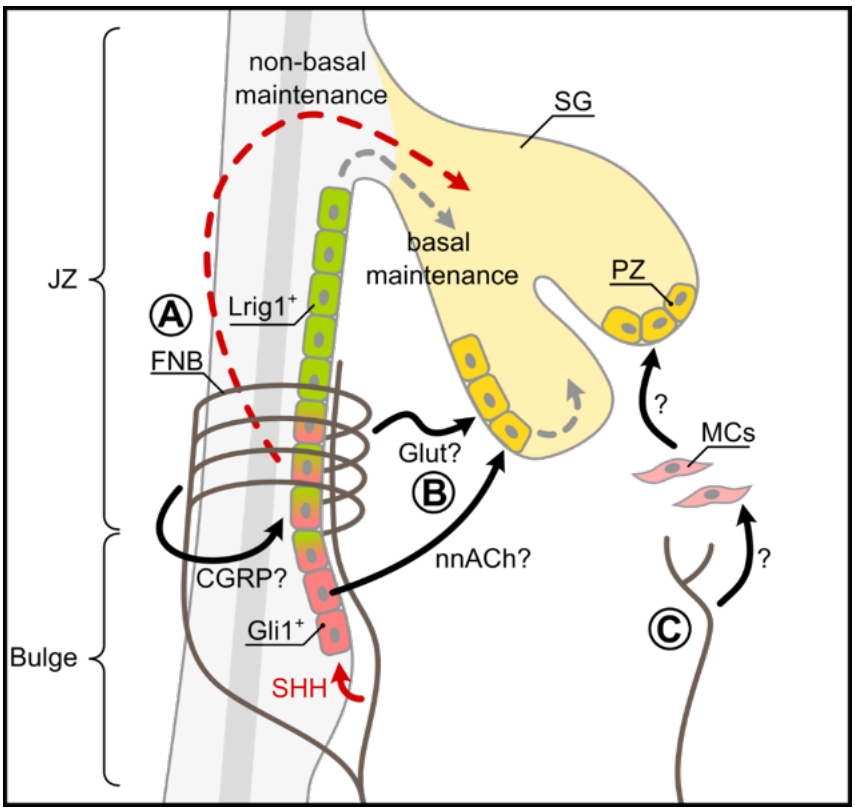

Figure 6. Regulation of sebaceous glands by cutaneous nerves: working hypotheses.

(A) Neuronal regulation of SG stem cells (SCs) in the hair follicle (HF) epithelium. The junctional zone (JZ)/upper bulge contains cells that express both leucine-rich repeats and immunoglobulin-like domains protein 1 (*Lrig1*) and *Gli1*. These cells may be directly innervated by longitudinal nerve fibres comprising follicular nerve network B (FNB). Under homeostatic conditions, the SG is maintained by contribution of Lrig1+ cells in the JZ and by asymmetric division of peripheral sebocytes. Under non-homeostatic conditions, such as during hair growth, the innervated LRIG1+/GLI1+ population is recruited to the SG to facilitate an increase in SG size. Candidate nerve derived substances that may modulate the behaviour of these cells include, calcitonin-gene related peptide (CGRP) and sonic hedgehog (SHH). **(B)** Non-neuronal ACh (nnACh) or nerve derived glutamate may act directly on peripheral sebocytes, modulating their function. **(C)** Nerves may regulate SGs indirectly by communicating with intermediary mesenchymal cells (MCs), such as fibroblasts or Schwann cells. Figure was created by the author and Dr Ivo de Vos.

CGRP and glutamate represent two other interesting candidate neuromediators worth investigating further. As CGRP neurons are TRPV1+ (Figure 3.7C-D), release of neuronal CGRP *in vivo* might be elicited via application of capsaicin, which is an agonist

for TRPV1 receptors (Julius *et al.*, 1999). A similar approach has been used to deduce the importance of neuronal CGRP in the pancreas (Jaworek, Konturek, & Szlachcic, 1997). Capsaicin could then be used in both an intact and denervated context, to investigate the role of CGRP in regulating SGs and the upper PSU. Performing this experiment in the context of denervated skin would allow the dissection of neuronal TRPV1 activation from activation of TRPV1 that is, at least in the case of human skin, expressed in sebocytes (Tóth *et al.*, 2009).

Given the similarity in evidence for requirement of both innervation and *Slc1a3* for SG homeostasis during hair growth (Reichenbach *et al.*, 2018), the existence of a glutamatergic mechanism controlling SG function is compelling. Future work should seek to establish whether follicular nerve fibres synthesise and secrete glutamate as a neurotransmitter and seek to identify the expression and localisation of glutamate receptors in the PSU.

Chapter 7: References

ABBAS, O. & MAHALINGAM, M. (2009) Cutaneous sebaceous neoplasms as markers of Muir-Torre syndrome: a diagnostic algorithm. *Journal of Cutaneous Pathology* **36**, 613–619.

ADLY, M.A., ASSAF, H.A., HUSSEIN, M.R. & PAUS, R. (2006a) Analysis of the expression pattern of glial cell line-derived neurotrophic factor, neurturin, their cognate receptors GFRalpha-1 and GFRalpha-2, and a common signal transduction element c-Ret in the human scalp skin. *Journal of Cutaneous Pathology* **33**, 799–808.

ADLY, M.A., ASSAF, H.A. & HUSSEIN, M.R.A. (2009) Expression pattern of p75 neurotrophin receptor protein in human scalp skin and hair follicles: Hair cycle-dependent expression. *Journal of the American Academy of Dermatology* **60**, 99–109.

ADLY, M.A., ASSAF, H.A., NADA, E.A., SOLIMAN, M. & HUSSEIN, M. (2005) Human scalp skin and hair follicles express neurotrophin-3 and its high-affinity receptor tyrosine kinase C, and show hair cycle-dependent alterations in expression. *British Journal of Dermatology* **153**, 514–520.

ADLY, M.A., ASSAF, H.A., NADA, E.A., SOLIMAN, M. & HUSSEIN, M. (2006b) Expression of nerve growth factor and its high-affinity receptor, tyrosine kinase A proteins, in the human scalp skin. *Journal of Cutaneous Pathology* **33**, 559–568.

AHNERT-HILGER, G., MÜNSTER-WANDOWSKI, A. & HÖLTJE, M. (2013) Synaptic Vesicle Proteins: Targets and Routes for Botulinum Neurotoxins. In *Botulinum Neurotoxins* (eds A. RUMMEL & T. BINZ), pp. 159–177. Springer, Berlin, Heidelberg.

AKAABOUNE, M., GRADY, R.M., TURNEY, S., SANES, J.R. & LICHTMAN, J.W. (2002) Neurotransmitter Receptor Dynamics Studied In Vivo by Reversible Photo-Unbinding of Fluorescent Ligands. *Neuron* **34**, 865–876.

AKAMATSU, H., ZOUBOULIS, C.C. & ORFANOS, C.E. (1992) Control of human sebocyte proliferation in vitro by testosterone and 5-alpha-dihydrotestosterone is dependent on the localization of the sebaceous glands. *Journal of Investigative Dermatology* **99**, 509–511.

AKAZA, N., AKAMATSU, H., NUMATA, S., MATSUSUE, M., MASHIMA, Y., MIYAWAKI, M., YAMADA, S., YAGAMI, A., NAKATA, S. & MATSUNAGA, K. (2014) Fatty acid compositions of triglycerides and free fatty acids in sebum depend on amount of triglycerides, and do not differ in presence or absence of acne vulgaris. *Journal of Dermatology* **41**, 1069–1076.

AKIMOTO, N., SATO, T., SAKIGUCHI, T., KITAMURA, K., KOHNO, Y. & ITO, A. (2002) Cell Proliferation and Lipid Formation in Hamster Sebaceous Gland Cells. *Dermatology* **204**, 118–123.

ALLEN, M., GRACHTCHOUK, M., SHENG, H., GRACHTCHOUK, V., WANG, A., WEI, L., LIU, J., RAMIREZ, A., METZGER, D., CHAMBON, P., JORCANO, J. & DLUGOSZ, A.A. (2003) Hedgehog Signaling Regulates Sebaceous Gland Development. *American Journal of Pathology* **163**, 2173–2178.

ANDERSEN, M.S., HANNEZO, E., ULYANCHENKO, S., ESTRACH, S., ANTOKU, Y., PISANO, S., BOONEKAMP, K.E., SENDRUP, S., MAIMETS, M., PEDERSEN, M.T., JOHANSEN, J. V., CLEMENT, D.L., FERAL, C.C., SIMONS, B.D. & JENSEN, K.B. (2019) Tracing the cellular dynamics of sebaceous gland development in normal and perturbed states. *Nature Cell Biology* **21**, 924–932.

ANSAI, S. (2017) Topics in histopathology of sweat gland and sebaceous neoplasms. *The Journal of Dermatology* **44**, 315–326.

AZZI, L., EL-ALFY, M. & LABRIE, F. (2006) Gender differences and effects of sex steroids and dehydroepiandrosterone on androgen and oestrogen alpha receptors in mouse sebaceous glands. *British Journal of Dermatology* **154**, 21–27.

BARNES, L., SAURAT, J.H. & KAYA, G. (2017) Senescent atrophic epidermis retains Lrig1+stem cells and loses Wnt signaling, a phenotype shared with CD44KO Mice. *PLOS ONE* **12**, 1–16.

BASTA, M., WILBURG, J. & HECZKO, P.B. (1980) In vitro effects of skin lipid extracts on skin bacteria in relation to age and acne changes. *Journal of Investigative Dermatology* **74**, 437–439.

BEADLE, P.C. & BURTON, J.L. (1981) Absorption of ultraviolet radiation by skin surface lipid. *British Journal of Dermatology* **104**, 549–551.

BEAR, M., CONNORS, B. & PARADISO, M. (2007a) Neurotransmitter Systems. In *Neuroscience: Exploring the Brain* pp. 133–166, 3rd edition. Lippincott Williams and Wilkins.

BEAR, M., CONNORS, B. & PARADISO, M. (2007b) Synaptic Transmission. In *Neuroscience: Exploring the Brain* pp. 101–132, 3rd edition. Lippincott Williams and Wilkins.

BERGER, J. & MOLLER, D.E. (2002) The Mechanisms of Action of PPARs. *Annual Review of Medicine* **53**, 409–435.

BILGIÇ, Ö., ALTINYAZAR, C., HIRA, H. & DOĞDU, M. (2015) Investigation of the Association of the Second-to-Fourth Digit Ratio with Skin Sebum Levels in Females with Acne Vulgaris. *American Journal of Clinical Dermatology* **16**, 559–564.

BLAIS, M., MOTTIER, L., GERMAIN, M.-A., BELLENFANT, S., CADAU, S. & BERTHOD, F. (2014) Sensory neurons accelerate skin reepithelialization via substance P in an innervated tissue-engineered wound healing model. *Tissue Engineering* **20**, 2180–2188.

BLOCH, B. (1931) Metabolism, endocrine glands and skin diseases, with special reference to acne vulgaris and xanthoma. *British Journal of Dermatology and Syphilis* **43**, 61–87.

BOEHNCKE, W.-H. (2015) Etiology and Pathogenesis of Psoriasis. *Rheumatic Disease Clinics of North America* **41**, 665–675.

BOL, D., KIGUCHI, K., BELTRÁN, L., RUPP, T., MOATS, S., GIMENEZ-CONTI, I., JORCANO, J. & DIGIOVANNI, J. (1998) Severe Follicular Hyperplasia and Spontaneous Papilloma Formation in Transgenic Mice Expressing the Neu Oncogene Under the Control of the Bovine Keratin 5 Promoter. *Molecular Carcinogenesis* **21**, 2–122.

BORLU, M., KARACA, Z., YILDIZ, H., TANRIVERDI, F., DEMIREL, B., ELBUKEN, G., CAKIR, I., DOKMETAS, H.S., COLAK, R., UNLUHIZARCI, K. & KELESTIMUR, F. (2012) Acromegaly is associated with decreased skin transepidermal water loss and temperature, and increased skin pH and sebum secretion partially reversible after treatment. *Growth Hormone & IGF Research* **22**, 82–86.

BOTCHKAREV, V.A., BOTCHKAREVA, N. V., PETERS, E.M.J. & PAUS, R. (2004) Epithelial growth control by neurotrophins: leads and lessons from the hair follicle. *Progress in Brain Research* **146**, 493–513.

BOTCHKAREV, V.A., LLER, S.E., JOHANSSON, O. & PAUS, R. (1997) Hair Cycle-Dependent Plasticity of Skin and Hair Follicle Innervation in Normal Murine Skin. *Journal of Comparative Neurology* **386**, 379–395.

BOTCHKAREV, V.A., PETERS, E.M.J., BOTCHKAREVA, N. V, MAURER, M. & PAUS, R. (1999) Hair cycle-dependent changes in adrenergic skin innervation, and hair growth modulation by adrenergic drugs. *Journal of Investigative Dermatology* **113**, 878–887.

BRANDES, D., BERTINI, F. & SMITH, E.W. (1965) Role of lysosomes in cellular lytic processes: II. Cell death during holocrine secretion in sebaceous glands. *Experimental and Molecular Pathology* **4**, 245–265.

BRONSON, F.H., DAGG, C.P. & SNELL, G.D. (1966) Reproduction. In *Biology of the Laboratory Mouse* (ed E.L. GREEN), p. Chapter 11, 2nd edition. Dover Publications, Inc, New York, NY.

BROWNELL, I., GUEVARA, E., BAI, C.B., LOOMIS, C.A. & JOYNER, A.L. (2012) Nerve-derived Sonic Hedgehog defines a niche for hair follicle stem cells capable of becoming epidermal stem cells. *Cell Stem Cell* **8**, 552–565.

BUCKLEY, G., WONG, J., METCALFE, A.D. & FERGUSON, M.W.J. (2012) Denervation affects regenerative responses in MRL/MpJ and repair in C57BL/6 ear wounds. *Journal of anatomy* **220**, 3–12.

BURKE, B.. & CUNLIFFE, W.. (1984) The assessment of acne vulgaris - the Leeds technique. *British Journal of Dermatology* **111**, 83–92.

BURTON, J.L., CARTLIDGE, M., CARTLIDGE, N.E.F. & SHUSTER, S. (1973) Sebum excretion in Parkinsonism. *British Journal of Dermatology* **88**, 263–266.

BURTON, J.L., CUNLIFFE, W.J., SAUNDERS, I.G.G. & SHUSTER, S. (1971a) The Effect of Facial Nerve Paresis on Sebum Excretion. *British Journal of Dermatology* **84**, 135–138.

BURTON, J.L., CUNLIFFE, W.J., STAFFORD, I. & SHUSTER, S. (1971b) The prevalence of acne vulgaris in adolescence. *British Journal of Dermatology* **85**, 119–126.

BURTON, J.L. & PYE, R.J. (1983) Seborrhoea is not a feature of seborrhoeic dermatitis. *British Medical Journal* **286**, 1169–1170.

BUTOVICH, I.A. (2017) Meibomian glands, meibum, and meibogenesis. *Experimental Eye Research* **163**, 2–16.

CALHOUN, M.E., JUCKER, M., MARTIN, L.J., THINAKARAN, G., PRICE, D.L. & MOUTON, P.R. (1996) Comparative evaluation of synaptophysin-based methods for quantification of synapses. *Journal of neurocytology* **25**, 821–828.

CAMERA, E., DAHLHOFF, M., LUDOVICI, M., ZOUBOULIS, C.C. & SCHNEIDER, M.R. (2014) Perilipin 3

modulates specific lipogenic pathways in SZ95 sebocytes. *Experimental Dermatology* **23**, 759–761.

CAMERA, E., LUDOVICI, M., GALANTE, M., SINAGRA, J.-L. & PICARDO, M. (2010) Comprehensive analysis of the major lipid classes in sebum by rapid resolution high-performance liquid chromatography and electrospray mass spectrometry. *Journal of Lipid Research* **51**, 3377–3388.

CAMERA, E., LUDOVICI, M., TORTORELLA, S., SINAGRA, J.-L., CAPITANIO, B., GORACCI, L. & PICARDO, M. (2016) Use of lipidomics to investigate sebum dysfunction in juvenile acne. *Journal of Lipid Research* **57**, 1051–1058.

CARTLIDGE, M., BURTON, J.L. & SHUSTER, S. (1972) The effect of prolonged topical application of an anticholinergic agent on the sebaceous glands. *British Journal of Dermatology* **86**, 61–64.

CATERINA, M.J. (2014) TRP channel cannabinoid receptors in skin sensation, homeostasis, and inflammation. *ACS Chemical Neuroscience* **5**, 1107–1116.

LO CELSO, C., BERTA, M.A., BRAUN, K.M., FRYE, M., LYLE, S., ZOUBOULIS, C.C. & WATT, F.M. (2008) Characterization of Bipotential Epidermal Progenitors Derived from Human Sebaceous Gland: Contrasting Roles of c-Myc and β-Catenin. *Stem Cells* **26**, 1241–1252.

LO CELSO, C., PROWSE, D.M. & WATT, F.M. (2004) Transient activation of beta-catenin signalling in adult mouse epidermis is sufficient to induce new hair follicles but continuous activation is required to maintain hair follicle tumours. *Development* **131**, 1787–1799.

CHAMPY, C., COUJARD, R. & COUJARD-CHAMPY, C. (1945) L'innervation Sympathique des glandes. *Cells Tissues Organs* **1**, 233–283.

CHASE, H.B., MONTAGNA, W. & MALONE, J.D. (1953) Changes in the skin in relation to the hair growth cycle. *The Anatomical record* **116**, 75–81.

CHEN, H.C., SMITH, S.J., TOW, B., ELIAS, P.M., FARESE, R. V & JR. (2002) Leptin modulates the effects of acyl CoA:diacylglycerol acyltransferase deficiency on murine fur and sebaceous glands. *Journal of Clinical Investigation* **109**, 175–181.

CHEN, W., KELLY, M.A., OPITZ-ARAYA, X., THOMAS, R.E., LOW, M.J. & CONE, R.D. (1997) Exocrine gland dysfunction in MC5-R-deficient mice: evidence for coordinated regulation of exocrine gland function by melanocortin peptides. *Cell* **91**, 789–798.

CHENG, C.-C., TSUTSUI, K., TAGUCHI, T., SANZEN, N., NAKAGAWA, A., KAKIGUCHI, K., YONEMURA, S., TANEGASHIMA, C., KEELEY, S.D., KIYONARI, H., FURUTA, Y., TOMONO, Y., WATT, F.M. & FUJIWARA, H. (2018) Hair follicle epidermal stem cells define a niche for tactile sensation. *eLife* **7**, e38883.

CHERET, J., LEBONVALLET, N., BUHE, V., CARRE, J.L., MISERY, L., LE GALL-IANOTTO, C., CHÉRET, J., LEBONVALLET, N., BUHÉ, V., CARRE, J.L., MISERY, L. & LE GALL-IANOTTO, C. (2014) Influence of sensory neuropeptides on human cutaneous wound healing process. *Journal of Dermatological Science* **74**, 193–203.

CHOI, C.W., KIM, Y., KIM, J.E., SEO, E.Y., ZOUBOULIS, C.C., KANG, J.S., YOUN, S.W. & CHUNG, J.H. (2019) Enhancement of lipid content and inflammatory cytokine secretion in SZ95 sebocytes by palmitic acid suggests a potential link between free fatty acids and acne aggravation. *Experimental Dermatology* **28**, 207–210.

CHUAH, S. & GOH, C. (2015) The impact of post-acne scars on the quality of life among young adults in Singapore. *Journal of Cutaneous and Aesthetic Surgery* **8**, 153–158.

CHUNG, S.S., LEE, J.S., KIM, M., AHN, B.Y., JUNG, H.S., LEE, H.M., KIM, J.-W. & PARK, K.S. (2012) Regulation of Wnt/β-Catenin Signaling by CCAAT/Enhancer Binding Protein β During Adipogenesis. *Obesity* **20**, 482–487.

CLAYTON, R.W., GÖBEL, K., NIESSEN, C.M., PAUS, R., STEENSEL, M.A.M. & LIM, X. (2019) Homeostasis of the sebaceous gland and mechanisms of acne pathogenesis. *British Journal of Dermatology* **181**, 677–690.

CLAYTON, R.W., LANGAN, E.A., ANSELL, D.M., VOS, I.J.H.M. DE, GÖBEL, K., SCHNEIDER, M.R., PICARDO, M., LIM, X., STEENSEL, M.A.M. VAN & PAUS, R. (2020) Neuroendocrinology and neurobiology of sebaceous glands. *Biological Reviews* (ahead of print).

COLLIER, C.N., HARPER, J.C., CAFARDI, J.A., CANTRELL, W.C., WANG, W., FOSTER, K.W., ELEWSKI, B.E. & ELEWSKI, B.E. (2008) The prevalence of acne in adults 20 years and older. *Journal of the American Academy of Dermatology* **58**, 56–59.

COLLINS, C.A. & WATT, F.M. (2008) Dynamic regulation of retinoic acid-binding proteins in developing, adult and neoplastic skin reveals roles for β-catenin and Notch signalling. *Developmental Biology*

324, 55–67.

CONNORS, B. (2009) Synaptic Transmission in the Nervous System. In *Medical Physiology* (eds W. BORON & E. BOULPAEP), pp. 323–350, 2nd edition. Elsevier.

COSSETTE, C., PATEL, P., ANUMOLU, J.R., SIVENDRAN, S., LEE, G.J., GRAVEL, S., GRAHAM, F.D., LESIMPLE, A., MAMER, O.A., ROKACH, J. & POWELL, W.S. (2008) Human Neutrophils Convert the Sebum-derived Polyunsaturated Fatty Acid Sebaleic Acid to a Potent Granulocyte Chemoattractant. *Journal of Biological Chemistry* **283**, 11234–11243.

COTTERILL, J.A., CUNLIFFE, W.J., WILLIAMSON, B. & BULUSU, L. (1972) Age and sex variation in skin surface lipid composition and sebum excretion rate. *British Journal of Dermatology* **87**, 333–340.

COTTERILL, J.A., CUNLIFFE, W.J.J. & WILLIAMSON, B. (1971) Severity of Acne and Sebum Excretion Rate. *British Journal of Dermatology* **1**, 1–10.

COTTLE, D.L., KRETZSCHMAR, K., SCHWEIGER, P.J., QUIST, S.R., GOLLNICK, H.P., NATSUGA, K., AOYAGI, S. & WATT, F.M. (2013) c-MYC-Induced Sebaceous Gland Differentiation Is Controlled by an Androgen Receptor/p53 Axis. *Cell Reports* **3**, 427–441.

COX, S.M. & NICHOLS, J.J. (2014) The Neurobiology of the Meibomian Glands. *The Ocular Surface* **12**, 167–177.

CRAVATT, B.F., DEMAREST, K., PATRICELLI, M.P., BRACEY, M.H., GIANG, D.K., MARTIN, B.R. & LICHTMAN, A.H. (2001) Supersensitivity to anandamide and enhanced endogenous cannabinoid signaling in mice lacking fatty acid amide hydrolase. *PNAS* **98**, 9371–9376.

CUNLIFFE, W.J. & COTTERILL, J. (1970) The effect of propranolol on acne vulgaris and the rate of sebum excretion. *British Journal of Dermatology* **83**, 550–551.

CUNLIFFE, W.J., COTTERILL, J.A., WILLIAMSON, B. & FORSTER, R.A. (1972) The Relevance of Skin Surface Lipids to Acne Vulgaris. *British Journal of Dermatology* **86**, 10–15.

CUNLIFFE, W.J. & GOULD, D.J. (1979) Prevalence of facial acne vulgaris in late adolescence and in adults. *British Medical Journal* **1**, 1109–1110.

DAHLHOFF, M., DE ANGELIS, M.H., WOLF, E. & SCHNEIDER, M.R. (2013a) Ligand-independent epidermal

growth factor receptor hyperactivation increases sebaceous gland size and sebum secretion in mice. *Experimental Dermatology* **22**, 667–669.

DAHLHOFF, M., CAMERA, E., PICARDO, M., ZOUBOULIS, C.C., CHAN, L., CHANG, B.H.-J. & SCHNEIDER, M.R. (2013b) PLIN2, the major perilipin regulated during sebocyte differentiation, controls sebaceous lipid accumulation in vitro and sebaceous gland size in vivo. *Biochimica et Biophysica Acta* **1830**, 4642–4649.

DAHLHOFF, M., CAMERA, E., SCHÄFER, M., EMRICH, D., RIETHMACHER, D., FOSTER, A., PAUS, R. & SCHNEIDER, M.R. (2016a) Sebaceous lipids are essential for water repulsion, protection against UVB-induced apoptosis, and ocular integrity in mice. *Development* **143**, 1823–1831.

DAHLHOFF, M., FROHLICH, T., ARNOLD, G.J., MULLER, U., LEONHARDT, H., ZOUBOULIS, C.C. & SCHNEIDER, M.R. (2015) Characterization of the sebocyte lipid droplet proteome reveals novel potential regulators of sebaceous lipogenesis. *Experimental Cell Research* **332**, 146–155.

DAHLHOFF, M., ZOUBOULIS, C.C. & SCHNEIDER, M.R. (2016b) Expression of dermcidin in sebocytes supports a role for sebum in the constitutive innate defense of human skin. *Journal of Dermatological Science* **81**, 124–126.

DANILENKO, D.M., RING, B.D., YANAGIHARA, D., BENSON, W., WIEMANN, B., STARNES, C.O. & PIERCE, G.F. (1995) Keratinocyte growth factor is an important endogenous mediator of hair follicle growth, development, and differentiation. Normalization of the nu/nu follicular differentiation defect and amelioration of chemotherapy-induced alopecia. *American Journal of Pathology* **147**, 145–154.

DEJANOVIC, B., HUNTLEY, M.A., DE MAZIÈRE, A., MEILANDT, W.J., WU, T., SRINIVASAN, K., JIANG, Z., GANDHAM, V., FRIEDMAN, B.A., NGU, H., FOREMAN, O., CARANO, R.A.D., CHIH, B., KLUMPERMAN, J., BAKALARSKI, C., ET AL. (2018) Changes in the Synaptic Proteome in Tauopathy and Rescue of Tau-Induced Synapse Loss by C1q Antibodies. *Neuron* **100**, 1322-1336.e7.

DESSINIOTI, C. & KATSAMBAS, A. (2013) Seborrheic dermatitis: Etiology, risk factors, and treatments: *Clinics in Dermatology* **31**, 343–351.

DOBROSI, N., TÓTH, B.I., NAGY, G., DÓZSA, A., GÉCZY, T., NAGY, L., ZOUBOULIS, C.C., PAUS, R., KOVÁCS, L. & BÍRÓ, T. (2008) Endocannabinoids enhance lipid synthesis and apoptosis of human

sebocytes via cannabinoid receptor-2-mediated signaling. *FASEB* **22**, 3685–3695.

DORES, G.M., CURTIS, R.E., TORO, J.R., DEVESA, S.S. & FRAUMENI, J.F. (2008) Incidence of cutaneous sebaceous carcinoma and risk of associated neoplasms: Insight into Muir-Torré syndrome. *Cancer* **113**, 3372–3381.

DOSHI, A., ZAHEER, A. & STILLER, M.J. (1997) A comparison of current acne grading systems and proposal of a novel system. *International Journal of Dermatology* **36**, 416–418.

DOWNING, D.T., STEWART, M.E., WERTZ, P.W. & STRAUSS, J.S. (1986) Essential fatty acids and acne. *Journal of the American Academy of Dermatology* **14**, 221–225.

DOWNING, D.T., STRAUSS, J.S. & POCHI, P.E. (1969) Variability in the Chemical Composition of Human Skin Surface Lipids. *Journal of Investigative Dermatology* **53**, 322–327.

DRAKE, D.R., BROGDEN, K.A., DAWSON, D. V & WERTZ, P.W. (2008) Thematic review series: skin lipids. Antimicrobial lipids at the skin surface. *Journal of Lipid Research* **49**, 4–11.

DUGAN, K.H. (1974) Ultrastructural observation of possible nerve endings in rat sebaceous gland. *Cell and Tissue Research* **150**, 9–12.

EBLING, F.J., EBLING, E. & SKINNER, J. (1969) The influence of pituitary hormones on the response of the sebaceous glands of the male rat to testosterone. *Journal of Endocrinology* **45**, 245–256.

EHRMANN, C. & SCHNEIDER, M.R. (2016) Genetically modified laboratory mice with sebaceous glands abnormalities. *Cellular and Molecular Life Sciences* **73**, 4623–4642.

ELDREDGE, L.C., GAO, X.M., QUACH, D.H., LI, L., HAN, X., LOMASNEY, J. & TOURTELLOTTE, W.G. (2008) Abnormal sympathetic nervous system development and physiological dysautonomia in Egr3-deficient mice. *Development* **135**, 2949–2957.

EMMERSON, E., MAY, A.J., BERTHOIN, L., CRUZ-PACHECO, N., NATHAN, S., MATTINGLY, A.J., CHANG, J.L., RYAN, W.R., TWARD, A.D. & KNOX, S.M. (2018) Salivary glands regenerate after radiation injury through SOX2-mediated secretory cell replacement. *EMBO Molecular Medicine* **10**, e8051.

EMMERSON, E., MAY, A.J., NATHAN, S., CRUZ-PACHECO, N., LIZAMA, C.O., MALISKOVA, L., ZOVEIN, A.C., SHEN, Y., MUENCH, M.O. & KNOX, S.M. (2017) SOX2 regulates acinar cell development in

the salivary gland. *eLife* **6**, e26620.

EPSTEIN, E.H. & EPSTEIN, W.L. (1966) New Cell Formation in Human Sebaceous Glands. *Journal of Investigative Dermatology* **46**, 453–458.

FAN, L., JIA, Y., CUI, L., LI, X. & HE, C. (2018) Analysis of sensitive skin barrier function: basic indicators and sebum composition. *International Journal of Cosmetic Science* **40**, 117–126.

FAN, Y.-Y., YU, T.-S., WANG, T., LIU, W.-W., ZHAO, R., ZHANG, S.-T., MA, W.-X., ZHENG, J.-L. & GUAN, D.-W. (2011) Nicotinic acetylcholine receptor α7 subunit is time-dependently expressed in distinct cell types during skin wound healing in mice. *Histochemistry and Cell Biology* **135**, 375–387.

FERREIRA, A. & CACERES, A. (1992) Expression of the class III beta-tubulin isotype in developing neurons in culture. *Journal of Neuroscience Research* **32**, 516–529.

FISCHER, H., FUMICZ, J., ROSSITER, H., NAPIREI, M., BUCHBERGER, M., TSCHACHLER, E. & ECKHART, L. (2017) Holocrine Secretion of Sebum Is a Unique DNase2-Dependent Mode of Programmed Cell Death. *Journal of Investigative Dermatology* **137**, 587–594.

FLOETTMANN, E., LEES, D., SEELIGER, F. & JONES, H.B. (2015) Pharmacological Inhibition of DGAT1 Induces Sebaceous Gland Atrophy in Mouse and Dog Skin While Overt Alopecia Is Restricted to the Mouse. *Toxicologic Pathology* **43**, 376–383.

FLUHR, J.W., MAO-QIANG, M., BROWN, B.E., WERTZ, P.W., CRUMRINE, D., SUNDBERG, J.P., FEINGOLD, K.R. & ELIAS, P.M. (2003) Glycerol Regulates Stratum Corneum Hydration in Sebaceous Gland Deficient (Asebia) Mice. *Journal of Investigative Dermatology* **120**, 728–737.

FONTAO, F., BARNES, L., KAYA, G., SAURAT, J.-H. & SORG, O. (2017) High Susceptibility of Lrig1 Sebaceous Stem Cells to TCDD in Mice. *Toxicological Sciences* **160**, 230–243.

FRANCES, D. & NIEMANN, C. (2012) Stem cell dynamics in sebaceous gland morphogenesis in mouse skin. *Developmental Biology* **363**, 138–146.

FRIDE, E. (2005) Endocannabinoids in the central nervous system: from neuronal networks to behavior. *Current Drug Targets. CNS and Neurological Disorders* **4**, 633–642.

FUJIE, T., SHIKIJI, T., UCHIDA, N., URANO, Y., NAGAE, H. & ARASE, S. (1996) Culture of cells derived from the human sebaceous gland under serum-free conditions without a biological feeder layer or specific matrices. *Archives of Dermatological Research* **288**, 703–708.

FÜLLGRABE, A., JOOST, S., ARE, A., JACOB, T., SIVAN, U., HAEGEBARTH, A., LINNARSSON, S., SIMONS, B.D., CLEVERS, H., TOFTGÅRD, R. & KASPER, M. (2015) Dynamics of Lgr6+ progenitor cells in the hair follicle, sebaceous gland, and interfollicular epidermis. *Stem Cell Reports* **5**, 843–855.

GAT, U., DASGUPTA, R., DEGENSTEIN, L. & FUCHS, E. (1998) De Novo hair follicle morphogenesis and hair tumors in mice expressing a truncated beta-catenin in skin. *Cell* **95**, 605–614.

GAUDILLERE, A., MISERY, L., SOUCHIER, C., CLAUDY, A. & SCHMITT, D. (1996) Intimate associations between PGP9.5-positive nerve fibres and Langerhans cells. *British Journal of Dermatology* **135**, 343–344.

GEORGEL, P., CROZAT, K., LAUTH, X., MAKRANTONAKI, E., SELTMANN, H., SOVATH, S., HOEBE, K., DU, X., RUTSCHMANN, S., JIANG, Z., BIGBY, T., NIZET, V., ZOUBOULIS, C.C. & BEUTLER, B. (2005) A Toll-Like Receptor 2-Responsive Lipid Effector Pathway Protects Mammals against Skin Infections with Gram-Positive Bacteria. *Infection and Immunity* **73**, 4512–4521.

GEYFMAN, M., PLIKUS, M. V., TREFFEISEN, E., ANDERSEN, B. & PAUS, R. (2015) Resting no more: Re-defining telogen, the maintenance stage of the hair growth cycle. *Biological Reviews* **90**, 1179–1196.

GHODSI, S.Z., ORAWA, H. & ZOUBOULIS, C.C. (2009) Prevalence, severity, and severity risk factors of acne in high school pupils: a community-based study. *Journal of Investigative Dermatology* **129**, 2136–2141.

GOETZ, J.A., SUBER, L.M., ZENG, X. & ROBBINS, D.J. (2002) Sonic Hedgehog as a mediator of long-range signaling. *BioEssays* **24**, 157–165.

GONG, X., CARMON, K.S., LIN, Q., THOMAS, A., YI, J. & LIU, Q. (2012) LGR6 Is a High Affinity Receptor of R-Spondins and Potentially Functions as a Tumor Suppressor. *PLOS ONE* **7**, e37137.

GOULDEN, V., STABLES, G.I. & CUNLIFFE, W.J. (1999) Prevalence of facial acne in adults. *Journal of the American Academy of Dermatology* **41**, 577–580.

GOYAL, R.K. & CHAUDHURY, A. (2013) Structure activity relationship of synaptic and junctional neurotransmission. *Autonomic Neuroscience* **176**, 11–31.

GRANDL, M. & SCHMITZ, G. (2009) Fluorescent high-content imaging allows the discrimination and quantitation of E-LDL-induced lipid droplets and Ox-LDL-generated phospholipidosis in human macrophages. *Cytometry Part A* **77**, 231–242.

GREENE, R.S., DOWNING, D.T., POCHI, P.E. & STRAUSS, J.S. (1970) Anatomical variation in the amount and composition of human skin surface lipid. *Journal of Investigative Dermatology* **54**, 240–247.

GU, L.-H. & COULOMBE, P.A. (2008) Hedgehog Signaling, Keratin 6 Induction, and Sebaceous Gland Morphogenesis. *American Journal of Pathology* **173**, 752–761.

GUINDON, J., GUIJARRO, A., PIOMELLI, D. & HOHMANN, A.G. (2011) Peripheral antinociceptive effects of inhibitors of monoacylglycerol lipase in a rat model of inflammatory pain. *British Journal of Pharmacology* **163**, 1464–1478.

GUINDON, J., LAI, Y., TAKACS, S.M., BRADSHAW, H.B. & HOHMANN, A.G. (2013) Alterations in endocannabinoid tone following chemotherapy-induced peripheral neuropathy: effects of endocannabinoid deactivation inhibitors targeting fatty-acid amide hydrolase and monoacylglycerol lipase in comparison to reference analgesics following c. *Pharmacological Research* **67**, 94–109.

GUO, L., LI, X. & TANG, Q.-Q. (2015) Transcriptional Regulation of Adipocyte Differentiation: A Central Role for CCAAT/Enhancer-binding Protein (C/EBP) β. *Journal of Biological Chemistry* **290**, 755–761.

GUO, M., PEGORARO, A.F., MAO, A., ZHOU, E.H., ARANY, P.R., HAN, Y., BURNETTE, D.T., JENSEN, M.H., KASZA, K.E., MOORE, J.R., MACKINTOSH, F.C., FREDBERG, J.J., MOONEY, D.J., LIPPINCOTT-SCHWARTZ, J. & WEITZ, D.A. (2017) Cell volume change through water efflux impacts cell stiffness and stem cell fate. *Proceedings of the National Academy of Sciences of the United States of America* **114**, E8618–E8627.

GUY, R., RIDDEN, C. & KEALEY, T. (1996) The improved organ maintenance of the human sebaceous gland: modeling in vitro the effects of epidermal growth factor, androgens, estrogens, 13-cis retinoic acid, and phenol red. *Journal of Investigative Dermatology* **106**, 454–460.

HAMILTON, E. (1974) Cell kinetics in the sebaceous glands of the mouse. I. The glands in resting skin. *Cell and Tissue Kinetics* **7**, 389–398.

HAMILTON, E., HOWARD, A. & POTTEN, C.S. (1974) Cell kinetics in the sebaceous glands of the mouse. II. The glands during hair growth. *Cell and Tissue Kinetics* **7**, 399–405.

HAN, X., LIU, Y., KAM, W.R. & SULLIVAN, D.A. (2018) Effect of brimonidine, an α2 adrenergic agonist, on human meibomian gland epithelial cells. *Experimental Eye Research* **170**, 20–28.

HASHIMOTO, K., OGAWA, K. & LEVER, W.F. (1963) Histochemical Studies of the Skin. *Journal of Investigative Dermatology* **40**, 15–26.

HAY, D.L. & WALKER, C.S. (2017) CGRP and its receptors. *Headache* **57**, 625–636.

HELLMANN, K. (1955) Cholinesterase and amine oxidase in the skin: a histochemical investigation. *The Journal of physiology* **129**, 454–463.

HINDE, E., HASLAM, I.S., SCHNEIDER, M.R., LANGAN, E. A., KLOEPPER, J.E., SCHRAMM, C., ZOUBOULIS, C.C. & PAUS, R. (2013) A practical guide for the study of human and murine sebaceous glands in situ. *Experimental Dermatology* **22**, 631–637.

HORSLEY, V., O'CARROLL, D., TOOZE, R., OHINATA, Y., SAITOU, M., OBUKHANYCH, T., NUSSENZWEIG, M., TARAKHOVSKY, A. & FUCHS, E. (2006) Blimp1 defines a progenitor population that governs cellular input to the sebaceous gland. *Cell* **126**, 597–609.

HOUSE, J.S., ZHU, S., RANJAN, R., LINDER, K. & SMART, R.C. (2010) C/EBPalpha and C/EBPbeta are required for Sebocyte differentiation and stratified squamous differentiation in adult mouse skin. *PLOS ONE* **5**, e9837.

HU, Y., CONVERSE, C., LYONS, M.C. & HSU, W.H. (2018) Neural control of sweat secretion: a review. *British Journal of Dermatology* **178**, 1246–1256.

HURLEY, H.J., SHELLEY, W.B. & KOELLE, G.B. (1953) The distribution cholinesterases in human skin, with special reference to eccrine and apocrine sweat glands. *Journal of Investigative Dermatology* **21**, 139–147.

ICRE, G., WAHLI, W. & MICHALIK, L. (2006) Functions of the Peroxisome Proliferator-Activated

Receptor (PPAR) α and β in Skin Homeostasis, Epithelial Repair, and Morphogenesis. *Journal of Investigative Dermatology Symposium Proceedings* **11**, 30–35.

IKAI, K. (1958) Rate of Sebum Excretion from the Glands to the Skin Surface. *Journal of Investigative Dermatology* **32**, 27–33.

JAKOB, S. & LOVELL-BADGE, R. (2011) Sex determination and the control of *Sox9* expression in mammals. *FEBS Journal* **278**, 1002–1009.

JALIAN, H.R., TAM, J., VUONG, L.N., FISHER, J., GARIBYAN, L., MIHM, M.C., ZURAKOWSKI, D., EVANS, C.L. & ANDERSON, R.R. (2015) Selective Cryolysis of Sebaceous Glands. *Journal of Investigative Dermatology* **135**, 2173–2180.

JANKOVIC, J. & DIAMOND, A. (2006) Botulinum toxin in dermatology - Beyond wrinkles and sweat. *Journal of Cosmetic Dermatology* **5**, 169.

JAWOREK, J., KONTUREK, S.J. & SZLACHCIC, A. (1997) The role of CGRP and afferent nerves in the modulation of pancreatic enzyme secretion in the rat. *International Journal of Pancreatology* **22**, 137–146.

JEJURIKAR, S.S., MARCELO, C.L. & KUZON, W.M. (2002) Skeletal muscle denervation increases satellite cell susceptibility to apoptosis. *Plastic and Reconstructive Surgery* **110**, 160–168.

JENKINS, B.A., FONTECILLA, N.M., LU, C.P., FUCHS, E. & LUMPKIN, E.A. (2019) The cellular basis of mechanosensory Merkel-cell innervation during development. *eLife* **8**, e42633.

JENSEN, A.A., ERICHSEN, M.N., NIELSEN, C.W., STENSBØL, T.B., KEHLER, J. & BUNCH, L. (2009a) Discovery of the First Selective Inhibitor of Excitatory Amino Acid Transporter Subtype 1. *Journal of Medicinal Chemistry* **52**, 912–915.

JENSEN, K.B., COLLINS, C.A., NASCIMENTO, E., TAN, D.W., FRYE, M., ITAMI, S. & WATT, F.M. (2009b) Lrig1 Expression Defines a Distinct Multipotent Stem Cell Population in Mammalian Epidermis. *Cell Stem Cell* **4**, 427–439.

JESSUP, C.J., REDSTON, M., TILTON, E. & REIMANN, J.D.R. (2016) Importance of universal mismatch repair protein immunohistochemistry in patients with sebaceous neoplasia as an initial screening tool for Muir-Torre syndrome. *Human Pathology* **49**, 1–9.

JOOST, S., ZEISEL, A., JACOB, T., SUN, X., LA MANNO, G., LÖNNERBERG, P., LINNARSSON, S. & KASPER, M. (2016) Single-Cell Transcriptomics Reveals that Differentiation and Spatial Signatures Shape Epidermal and Hair Follicle Heterogeneity. *Cell Systems* **3**, 221-237.e9.

JULIUS, D., CATERINA, M.J., ROSEN, T.A., TOMINAGA, M. & BRAKE, A.J. (1999) A capsaicin-receptor homologue with a high threshold for noxious heat. *Nature* **398**, 436–441.

JUNG, Y., TAM, J., JALIAN, H.R., ANDERSON, R.R. & EVANS, C.L. (2015) Longitudinal, 3D in vivo imaging of sebaceous glands by coherent anti-Stokes Raman scattering microscopy – normal function and response to cryotherapy. *Journal of Investigative Dermatology* **42**, 39–44.

KAKANJ, P., REUTER, K., SÉQUARIS, G., WODTKE, C., SCHETTINA, P., FRANCES, D., ZOUBOULIS, C.C., LANSKE, B. & NIEMANN, C. (2013) Indian hedgehog controls proliferation and differentiation in skin tumorigenesis and protects against malignant progression. *Cell Reports* **4**, 340–351.

KAM, W.R. & SULLIVAN, D.A. (2011) Neurotransmitter Influence on Human Meibomian Gland Epithelial Cells. *Investigative Opthalmology & Visual Science* **52**, 8543.

KARNIK, P., TEKESTE, Z., MCCORMICK, T.S., GILLIAM, A.C., PRICE, V.H., COOPER, K.D. & MIRMIRANI, P. (2009) Hair follicle stem cell-specific PPARgamma deletion causes scarring alopecia. *Journal of Investigative Dermatology* **129**, 1243–1257.

KEMPSON, S.A., ZHOU, Y. & DANBOLT, N.C. (2014) The betaine/GABA transporter and betaine: roles in brain, kidney, and liver. *Frontiers in Physiology* **5**, 159.

KESTELL, G.R., ANDERSON, R.L., CLARKE, J.N., HABERBERGER, R. V. & GIBBINS, I.L. (2015) Primary afferent neurons containing calcitonin gene-related peptide but not substance P in forepaw skin, dorsal root ganglia, and spinal cord of mice. *Journal of Comparative Neurology* **523**, 2555–2569.

KIGUCHI, K., BOL, D., CARBAJAL, S., BELTRÁN, L., MOATS, S., CHAN, K., JORCANO, J. & DIGIOVANNI, J. (2000) Constitutive expression of erbB2 in epidermis of transgenic mice results in epidermal hyperproliferation and spontaneous skin tumor development. *Oncogene* **19**, 4243–4254.

KIM, B.R., CHUN, M.Y., KIM, S.A. & YOUN, S.W. (2015) Sebum Secretion of the Trunk and the Development of Truncal Acne in Women: Do Truncal Acne and Sebum Affect Each Other? *Dermatology* **231**, 87–93.

KIM, Y.J., LEE, S.-B. & LEE, H.B. (2019) Oleic acid enhances keratinocytes differentiation via the upregulation of miR-203 in human epidermal keratinocytes. *Journal of Cosmetic Dermatology* **18**, 383–389.

KLIGMAN, A.M. (1959) The human hair cycle. *Journal of Investigative Dermatology* **33**, 307–316.

KLIGMAN, A.M. (1974) An overview of acne. *Journal of Investigative Dermatology* **62**, 268–287.

KLIGMAN, A.M. & KWONG, T. (1979) An improved rabbit ear model for assessing comedogenic substances. *British Journal of Dermatology* **100**, 699–702.

KLIGMAN, A.M. & SHELLEY, W.B. (1958) An investigation of the biology of the human sebaceous gland. *Journal of Investigative Dermatology* **30**, 99–125.

KLIGMAN, A.M. & STRAUSS, J.S. (1956) The Formation of Vellus Hair Follicles from Human Adult Epidermis. *Journal of Investigative Dermatology* **27**, 19–23.

KNOX, S.M., LOMBAERT, I.M.A., REED, X., VITALE-CROSS, L., GUTKIND, J.S. & HOFFMAN, M.P. (2010) Parasympathetic innervation maintains epithelial progenitor cells during salivary organogenesis. *Science* **329**, 1645–1647.

KOBAYASHI, T., VOISIN, B., KIM, D.Y., KENNEDY, E.A., JO, J.-H., SHIH, H.-Y., TRUONG, A., DOEBEL, T., SAKAMOTO, K., CUI, C.-Y., SCHLESSINGER, D., MORO, K., NAKAE, S., HORIUCHI, K., ZHU, J., ET AL. (2019) Homeostatic Control of Sebaceous Glands by Innate Lymphoid Cells Regulates Commensal Bacteria Equilibrium. *Cell* **176**, P982-997.e16.

KOSMADAKI, M. & KATSAMBAS, A. (2017) Topical treatments for acne. *Clinics in Dermatology* **35**, 173–178.

KRETZSCHMAR, K., WEBER, C., DRISKELL, R.R., CALONJE, E. & WATT, F.M. (2016) Compartmentalized Epidermal Activation of β-Catenin Differentially Affects Lineage Reprogramming and Underlies Tumor Heterogeneity. *Cell Reports* **14**, 269–281.

KURZEN, H., BERGER, H., JÄGER, C., HARTSCHUH, W., NÄHER, H., GRATCHEV, A., GOERDT, S. & DEICHMANN, M. (2004) Phenotypical and molecular profiling of the extraneuronal cholinergic system of the skin. *Journal of Investigative Dermatology* **123**, 937–949.

KURZEN, H. & SCHALLREUTER, K.U. (2004) Novel aspects in cutaneous biology of acetylcholine synthesis and acetylcholine receptors. *Experimental Dermatology* **13 Suppl 4**, 27–30.

KURZEN, H., WESSLER, I., KIRKPATRICK, C.J., KAWASHIMA, K. & GRANDO, S.A. (2007) The non-neuronal cholinergic system of human skin. *Hormone and Metabolic Research* **39**, 125–135.

KYLLO, R.L., BRADY, K.L. & HURST, E.A. (2015) Sebaceous carcinoma: review of the literature. *Dermatologic Surgery* **41**, 1–15.

LAW, M.P.M., CHUH, A.A.T., LEE, A. & MOLINARI, N. (2010) Acne prevalence and beyond: Acne disability and its predictive factors among Chinese late adolescents in Hong Kong. *Clinical and Experimental Dermatology* **35**, 16–21.

LAYTON, A.M. (2014) The Leeds Acne Grading Technique. In *Pathogenesis and Treatment of Acne and Rosacea.* (eds C.C. ZOUBOULIS, A.D. KATSAMBAS & A.M. KLIGMAN), pp. 317–324. Springer, Berlin, Heidelberg.

LEBONVALLET, N., BOULAIS, N., LE GALL, C., PEREIRA, U., GAUCHÉ, D., GOBIN, E., PERS, J.-O., JEANMAIRE, C., DANOUX, L., PAULY, G. & MISERY, L. (2012) Effects of the re-innervation of organotypic skin explants on the epidermis. *Experimental Dermatology* **21**, 156–158.

LEE, D.-Y., HUANG, C.-M., NAKATSUJI, T., THIBOUTOT, D., KANG, S.-A., MONESTIER, M. & GALLO, R.L. (2009) Histone H4 Is a Major Component of the Antimicrobial Action of Human Sebocytes. *Journal of Investigative Dermatology* **129**, 2489–2496.

VAN DER LEE, S. & BOOT, L.M. (1955) Spontaneous pseudopregnancy in mice. *Acta Physiologica et Pharmacologica Neerlandica* **4**, 442–444.

LEE, W.J., JUNG, H.D., LEE, H.J., KIM, B.S., LEE, S.-J.J. & KIM, D.W. (2008) Influence of substance-P on cultured sebocytes. *Archives of Dermatological Research* **300**, 311–316.

LI, C.-M., LI, W., MAN, X.-Y., LIU, Z.-G. & ZHENG, M. (2013a) Expression of pigment epithelium-derived factor in human cutaneous appendages. *Clinical and Experimental Dermatology* **38**, 652–658.

LI, L. & GINTY, D.D. (2014) The structure and organization of lanceolate mechanosensory complexes at mouse hair follicles. *eLife* **3**, e01901.

LI, Y., STOLL, S.W., SEKHON, S., TALSMA, C., CAMHI, M.I., JONES, J.L., LAMBERT, S., MARLEY, H., RITTIÉ, L., GRACHTCHOUK, M., FRITZ, Y., WARD, N.L. & ELDER, J.T. (2016) Transgenic expression of human amphiregulin in mouse skin: inflammatory epidermal hyperplasia and enlarged sebaceous glands. *Experimental Dermatology* **25**, 187–193.

LI, Z.J., PARK, S.B., SOHN, K.C., LEE, Y., SEO, Y.J., KIM, C.D., KIM, Y.S., LEE, J.H. & IM, M. (2013b) Regulation of lipid production by acetylcholine signalling in human sebaceous glands. *Journal of Dermatological Science* **72**, 116–122.

LIAKOU, A.I., NYENGAARD, J.R., BONOVAS, S., KNOLLE, J., MAKRANTONAKI, E. & ZOUBOULIS, C.C. (2016) Marked Reduction of the Number and Individual Volume of Sebaceous Glands in Psoriatic Lesions. *Dermatology* **232**, 415–424.

LIAO, X.-H. & NGUYEN, H. (2014) Epidermal expression of Lgr6 is dependent on nerve endings and Schwann cells. *Experimental Dermatology* **23**, 195–198.

LIEN, W.H., POLAK, L., LIN, M., LAY, K., ZHENG, D. & FUCHS, E. (2014) In vivo transcriptional governance of hair follicle stem cells by canonical Wnt regulators. *Nature Cell Biology* **16**, 179–190.

LOVÁSZI, M., SZEGEDI, A., ZOUBOULIS, C.C. & TÖRŐCSIK, D. (2017) Sebaceous-immunobiology is orchestrated by sebum lipids. *Dermato-Endocrinology* **1980**, e1375636.

LUDOVICI, M., KOZUL, N., MATERAZZI, S., RISOLUTI, R., PICARDO, M. & CAMERA, E. (2018) Influence of the sebaceous gland density on the stratum corneum lipidome. *Scientific Reports* **8**, 11500.

LYNN, D.D., UMARI, T., DUNNICK, C.A. & DELLAVALLE, R.P. (2016) The epidemiology of acne vulgaris in late adolescence. *Adolescent Health, Medicine and Therapeutics* **7**, 13–25.

MA, W.-X., YU, T.-S., FAN, Y.-Y., ZHANG, S.-T., REN, P., WANG, S.-B., ZHAO, R., PI, J.-B. & GUAN, D.-W. (2011) Time-dependent expression and distribution of monoacylglycerol lipase during the skin-incised wound healing in mice. *International Journal of Legal Medicine* **125**, 549–558.

MACCARRONE, M., BAB, I., BÍRÓ, T., CABRAL, G.A., DEY, S.K., DI MARZO, V., KONJE, J.C., KUNOS, G., MECHOULAM, R., PACHER, P., SHARKEY, K.A. & ZIMMER, A. (2015) Endocannabinoid signaling at the periphery: 50 years after THC. *Trends in Pharmacological Sciences* **36**, 277–296.

MAKLAD, A., NICOLAI, J.R., BICHSEL, K.J., EVENSON, J.E., LEE, T.-C., THREADGILL, D.W. & HANSEN, L.A. (2009) The EGFR is required for proper innervation to the skin. *The Journal of Investigative Dermatology* **129**, 690–698.

MAN, M.Q., XIN, S.J., SONG, S.P., CHO, S.Y., ZHANG, X.J., TU, C.X., FEINGOLD, K.R. & ELIAS, P.M. (2009) Variation of Skin Surface pH, Sebum Content and Stratum Corneum Hydration with Age and Gender in a Large Chinese Population. *Skin Pharmacology and Physiology* **22**, 190–199.

MARPLES, R.R., DOWNING, D.T. & KLIGMAN, A.M. (1971) Control of free fatty acids in human surface lipids by Corynebacterium acnes. *Journal of Investigative Dermatology* **56**, 127–131.

DI MARZO, V. & PISCITELLI, F. (2015) The Endocannabinoid System and its Modulation by Phytocannabinoids. *Neurotherapeutics* **12**, 692–698.

MAURER, M., PETERS, E.M.J., BOTCHKAREV, V.A. & PAUS, R. (1998) Intact hair follicle innervation is not essential for anagen induction and development. *Archives of Dermatological Research* **290**, 574–578.

MERRILL, B.J., GAT, U., DASGUPTA, R. & FUCHS, E. (2001) Tcf3 and Lef1 regulate lineage differentiation of multipotent stem cells in skin. *Genes & Development* **15**, 1688–1705.

MESQUITA-GUIMARÃTES, J. & COIMBRA, A. (1976) Holocrine cell Lysis in the rat preputial sebaceous gland. Evidence of autophagocytosis during cell involution. *The Anatomical Record* **186**, 49–67.

MIESCHER, G. & SCHONBERG, A. (1944) Untersuchungen über die Funktion der Talgdrusen. *Bulletin der Schweizerischen Akademie der Medizinischen Wissenschaften* **1**, 101.

MÍKOVÁ, R., VRKOSLAV, V., HANUS, R., HÁKOVA, E., HÁBOVÁ, Z., DOLEŽAL, A., PLAVKA, R., COUFAL, P. & CVAČKA, J. (2014) Newborn boys and girls differ in the lipid composition of vernix caseosa. *PLOS ONE* **9**, e99173.

MIN, P., XI, W., GRASSETTI, L., TRISLIANA PERDANASARI, A., TORRESETTI, M., FENG, S., SU, W., PU, Z., ZHANG, Y.X.Y., HAN, S., ZHANG, Y.X.Y., DI BENEDETTO, G. & LAZZERI, D. (2015) Sebum Production Alteration after Botulinum Toxin Type A Injections for the Treatment of Forehead Rhytides: A Prospective Randomized Double-Blind Dose-Comparative Clinical Investigation. *Aesthetic Surgery Journal* **35**, 600–610.

MIRSHAHPANAH, P. & MAIBACH, H.I. (2007) Models in acnegenesis. *Cutaneous and Ocular Toxicology* **26**, 195–202.

MONTAGNA, W. & ELLIS, R. (1957a) Histology and Cytochemistry of Human Skin XII Cholinesterases in the hair follicles of the scalp. *Journal of Investigative Dermatology* **37**, 145–151.

MONTAGNA, W. & ELLIS, R.A. (1957b) Cholinergic Innervation of the Meibomian Glands, *Anatomical Record* **135**,121–127.

MONTAGNA, W. & PARAKKAL, P. (1974a) The Pilary Apparatus. In *The Structure & Function of Skin* (eds W. MONTAGNA & P.F. PARAKKAL), pp. 172–258, 3rd edition. London Academic Press, Beaverton, Oregon, United States.

MONTAGNA, W. & PARAKKAL, P. (1974b) Eccrine Sweat Glands. In *The Structure & Function of Skin* (eds W. MONTAGNA & P.F. PARAKKAL), pp. 366–411, 3rd edition. London Academic Press, Beaverton, Oregon, United States.

MONTAGNA, W. & PARAKKAL, P.F. (1974c) Sebaceous Glands. In *The Structure & Function of Skin* (eds W. MONTAGNA & P.F. PARAKKAL), pp. 280–331, 3rd edition. London Academic Press, Beaverton, Oregon, United States.

MORELLINI, N., FINCH, P.M., GOEBEL, A. & DRUMMOND, P.D. (2018) Dermal nerve fibre and mast cell density, and proximity of mast cells to nerve fibres in the skin of patients with complex regional pain syndrome. *Pain* **159**, 2021–2029.

MOTOYOSHI, K. (1983) Enhanced comedo formation in rabbit ear skin by squalene and oleic acid peroxides. *British Journal of Dermatology* **109**, 191–198.

MUDIYANSELAGE, S.E., ELSNER, P., THIELE, J.J. & HAMBURGER, M. (2003) Ultraviolet A Induces Generation of Squalene Monohydroperoxide Isomers in Human Sebum and Skin Surface Lipids In Vitro and In Vivo. *Journal of Investigative Dermatology* **120**, 915–922.

MULCAHY, M.J., PAULO, J.A. & HAWROT, E. (2018) Proteomic Investigation of Murine Neuronal α7-Nicotinic Acetylcholine Receptor Interacting Proteins. *Journal of Proteome Research* **17**, 3959–3975.

MÜLLER-RÖVER, S., HANDJISKI, B., VAN DER VEEN, C., EICHMÜLLER, S., FOITZIK, K., MCKAY, I.A.,

STENN, K.S. & PAUS, R. (2001) A comprehensive guide for the accurate classification of murine hair follicles in distinct hair cycle stages. *Journal of Investigative Dermatology* **117**, 3–15.

MÜLLER, F.B., MÜLLER-RÖVER, S., KORGE, B.P., KAPAS, S., HINSON, J.P. & PHILPOTT, M.P. (2003) Adrenomedullin: Expression and possible role in human skin and hair growth. *British Journal of Dermatology* **148**, 30–38.

MUZUMDAR, M.D., TASIC, B., MIYAMICHI, K., LI, L. & LUO, L. (2007) A global double-fluorescent Cre reporter mouse. *Genesis* **45**, 593–605.

NAKATSUJI, T., KAO, M.C., ZHANG, L., ZOUBOULIS, C.C., GALLO, R.L. & HUANG, C.-M. (2010) Sebum Free Fatty Acids Enhance the Innate Immune Defense of Human Sebocytes by Upregulating β-Defensin-2 Expression. *Journal of Investigative Dermatology* **130**, 985–994.

NEDVETSKY, P.I., EMMERSON, E., FINLEY, J.K., ETTINGER, A., CRUZ-PACHECO, N., PROCHAZKA, J., HADDOX, C.L., NORTHRUP, E., HODGES, C., MOSTOV, K.E., HOFFMAN, M.P. & KNOX, S.M. (2014) Parasympathetic innervation regulates tubulogenesis in the developing salivary gland. *Developmental Cell* **30**, 449–462.

NEWTON, R. (2000) Molecular mechanisms of glucocorticoid action: what is important? *Thorax* **55**, 603–613.

NICOLAIDES, N. (1974) Skin lipids: their biochemical uniqueness. *Science* **186**, 19–26.

NICOLAIDES, N., ANSARI, M.N.A., FU, H.C. & LINDSAY, D.G. (1970) Lipid composition of comedones compared with that of human skin surface in acne patients. *Journal of Investigative Dermatology* **54**, 487–495.

NIEMANN, C. & HORSLEY, V. (2012) Development and homeostasis of the sebaceous gland. *Seminars in Cell and Developmental Biology* **23**, 928–936.

NIEMANN, C., OWENS, D.M., HÜLSKEN, J., BIRCHMEIER, W., WATT, F.M. & WATT, F.M. (2002) Expression of DeltaNLef1 in mouse epidermis results in differentiation of hair follicles into squamous epidermal cysts and formation of skin tumours. *Development* **129**, 95–109.

NIEMANN, C., OWENS, D.M., SCHETTINA, P. & WATT, F.M. (2007) Dual Role of Inactivating Lef1 Mutations in Epidermis: Tumor Promotion and Specification of Tumor Type. *Cancer Research* **67**,

2916–2921.

NIEMANN, C., UNDEN, A.B., LYLE, S., ZOUBOULIS, C.C., TOFTGÅRD, R. & WATT, F.M. (2003) Indian hedgehog and beta-catenin signaling: role in the sebaceous lineage of normal and neoplastic mammalian epidermis. *PNAS* **100 Suppl**, 11873–11880.

NOLANO, M., PROVITERA, V., CAPORASO, G., STANCANELLI, A., LEANDRI, M., BIASIOTTA, A., CRUCCU, G., SANTORO, L. & TRUINI, A. (2013) Cutaneous innervation of the human face as assessed by skin biopsy. *Journal of Anatomy* **222**, 161–169.

NORRIS, D.O. & CARR, J.A. (2013) The Endocrinology of Mammalian Reproduction. In *Vertebrate Endocrinology* pp. 317–374. Elsevier.

NOWAK, J.A., POLAK, L., PASOLLI, H.A. & FUCHS, E. (2008) Hair Follicle Stem Cells are Specified and Function in Early Skin Morphogenesis. *Cell Stem Cell* **3**, 33–43.

O'BRIEN, S., LEWIS, J. & CUNLIFFE, W. (1998) The Leeds revised acne grading system. *Journal of Dermatologic Treatment* **9**, 215–220.

OHSAWA, K., WATANABE, T., MATSUKAWA, R., YOSHIMURA, Y. & IMAEDA, K. (1984) The possible role of squalene and its peroxide of the sebum in the occurrence of sunburn and protection from the damage caused by U.V. irradiation. *The Journal of Toxicological Sciences* **9**, 151–159.

OKORO, E.O., BULUS, N.G. & ZOUBOULIS, C.C. (2016) Study of Facial Sebum Levels and Follicular Red Fluorescence in Patients with Acne Vulgaris in Nigeria. *Dermatology* **232**, 156–161.

OLÁH, A., MARKOVICS, A., SZABÓ-PAPP, J., SZABÓ, P.T., STOTT, C., ZOUBOULIS, C.C. & BÍRÓ, T. (2016) Differential effectiveness of selected non-psychotropic phytocannabinoids on human sebocyte functions implicates their introduction in dry/seborrheic skin and acne treatment. *Experimental Dermatology* **25**, 701–707.

OLÁH, A., TÓTH, B.I., BORBÍRÓ, I., SUGAWARA, K., SZÖLLŐSI, A.G., CZIFRA, G., PÁL, B., AMBRUS, L., KLOEPPER, J., CAMERA, E., LUDOVICI, M., PICARDO, M., VOETS, T., ZOUBOULIS, C.C., PAUS, R., ET AL. (2014) Cannabidiol exerts sebostatic and antiinflammatory effects on human sebocytes. *Journal of Clinical Investigation* **124**, 3713–3724.

ORO, A.E. & HIGGINS, K. (2003) Hair cycle regulation of Hedgehog signal reception. *Developmental*

Biology **255**, 238–248.

OULÈS, B., ROGNONI, E., HOSTE, E., GOSS, G., FIEHLER, R., NATSUGA, K., QUIST, S., MENTINK, R., DONATI, G. & WATT, F.M. (2019) Mutant Lef1 controls Gata6 in sebaceous gland development and cancer. *The EMBO journal* **38**, e100526.

OUSPENSKAIA, T., MATOS, I., MERTZ, A.F., FIORE, V.F. & FUCHS, E. (2016) WNT-SHH Antagonism Specifies and Expands Stem Cells prior to Niche Formation. *Cell* **164**, 156–169.

PAGE, M.E., LOMBARD, P., NG, F., GÖTTGENS, B. & JENSEN, K.B. (2013) The Epidermis Comprises Autonomous Compartments Maintained by Distinct Stem Cell Populations. *Cell Stem Cell* **13**, 471–482.

PAN, J., WANG, Q. & TU, P. (2017) A Topical Medication of All-Trans Retinoic Acid Reduces Sebum Excretion Rate in Patients With Forehead Acne. *American Journal of Therapeutics* **24**, e207–e212.

PAPPAS, A., JOHNSEN, S., LIU, J.-C. & EISINGER, M. (2009) Sebum analysis of individuals with and without acne. *Dermato-Endocrinology* **1**, 157–161.

PARFITT, G.J., LEWIS, P.N., YOUNG, R.D., RICHARDSON, A., LYONS, J.G., DI GIROLAMO, N. & JESTER, J. V. (2016) Renewal of the Holocrine Meibomian Glands by Label-Retaining, Unipotent Epithelial Progenitors. *Stem Cell Reports* **7**, 399–410.

PARK, J.-H., PARK, Y.J., KIM, S.K., KWON, J.E., KANG, H.Y., LEE, E.-S., CHOI, J.H. & KIM, Y.C. (2016) Histopathological Differential Diagnosis of Psoriasis and Seborrheic Dermatitis of the Scalp. *Annals of Dermatology* **28**, 427–432.

PASSI, S., DE PITÀ, O., PUDDU, P. & LITTARRU, G.P. (2002) Lipophilic antioxidants in human sebum and aging. *Free Radical Research* **36**, 471–477.

PAUS, R., MÜLLER-RÖVER, S., VAN DER VEEN, C., MAURER, M., EICHMÜLLER, S., LING, G., HOFMANN, U., FOITZIK, K., MECKLENBURG, L. & HANDJISKI, B. (1999) A Comprehensive Guide for the Recognition and Classification of Distinct Stages of Hair Follicle Morphogenesis. *Journal of Investigative Dermatology* **113**, 523–532.

PAUS, R., PETERS, E.M.J., EICHMÜLLER, S. & BOTCHKAREV, V.A. (1997) Neural mechanisms of hair growth control. *Journal of Investigative Dermatology Symposium Proceedings* **2**, 61–68.

PAUS, R., THEOHARIDES, T.C. & ARCK, P.C. (2006) Neuroimmunoendocrine circuitry of the 'brain-skin connection'. *Trends in Immunology* **27**, 32–39.

PAWLOWSKI, A. & WEDDELL, G. (1967) The lability of cutaneous neural elements. *British Journal of Dermatology* **79**, 14–19.

PETERS, E.M.J., BOTCHKAREV, V.A., BOTCHKAREVA, N. V., TOBIN, D.J. & PAUS, R. (2001) Hair-Cycle-Associated Remodeling of the Peptidergic Innervation of Murine Skin, and Hair Growth Modulation by Neuropeptides. *Journal of Investigative Dermatology* **116**, 236–245.

PETERS, E.M.J., BOTCHKAREV, V.A., MÜLLER-RÖVER, S., MOLL, I., RICE, F.L. & PAUS, R. (2002) Developmental timing of hair follicle and dorsal skin innervation in mice. *Journal of Comparative Neurology* **448**, 28–52.

PETERS, E.M.J., HENDRIX, S., GÖLZ, G., KLAPP, B.F., ARCK, P.C. & PAUS, R. (2006) Nerve Growth Factor and its Precursor Differentially Regulate Hair Cycle Progression in Mice. *Journal of Histochemistry and Cytochemistry* **54**, 275–288.

PETERSEN, M.J., ZONE, J.J. & KRUEGER, G.G. (1984) Development of a nude mouse model to study human sebaceous gland physiology and pathophysiology. *Journal of Clinical Investigation* **74**, 1358–1365.

PETERSON, S.C., BROWNELL, I. & WONG, S.Y. (2016) Cutaneous Surgical Denervation: A Method for Testing the Requirement for Nerves in Mouse Models of Skin Disease. *Journal of Visualized Experiments* **112**, e54050–e54050.

PETERSSON, M., BRYLKA, H., KRAUS, A., JOHN, S., RAPPL, G., SCHETTINA, P. & NIEMANN, C. (2011) TCF/Lef1 activity controls establishment of diverse stem and progenitor cell compartments in mouse epidermis. *EMBO Journal* **30**, 3004–3018.

PETROFF, O.A.C. (2002) GABA and Glutamate in the Human Brain. *The Neuroscientist* **8**, 562–573.

PICARDO, M., OTTAVIANI, M., CAMERA, E. & MASTROFRANCESCO, A. (2009) Sebaceous gland lipids. *Dermatoendocrinol* **1**, 68–71.

PINKUS, H. & MEHREGAN, A.H. (1966) The Primary Histologic Lesion of Seborrheic Dermatitis and Psoriasis. *Journal of Investigative Dermatology* **46**, 109–116.

PLIKUS, M. V & CHUONG, C.-M. (2008) Complex hair cycle domain patterns and regenerative hair waves in living rodents. *Journal of Investigative Dermatology* **128**, 1071–1080.

POBLET, E., JIMÉNEZ, F. & ORTEGA, F. (2004) The contribution of the arrector pili muscle and sebaceous glands to the follicular unit structure. *Journal of the American Academy of Dermatology* **51**, 217–222.

POCHI, P.E., STRAUSS, J.S. & DOWNING, D.T. (1977) Skin surface lipid composition, acne, pubertal development, and urinary excretion of testosterone and 17-ketosteroids in children. *Journal of Investigative Dermatology* **69**, 485–489.

POCHI, P.E., STRAUSS, J.S. & MESCON, H. (1962) Sebum secretion and urinary fractional 17-ketosteroid and total 17-hydroxycorticoid excretion in male castrates. *Journal of Investigative Dermatology* **39**, 475–483.

POLAK, J.M. & BLOOM, S.R. (1981) The peripheral substance P-ergic system. *Peptides* **2 Suppl 2**, 133–148.

POLI, F., DRENO, B. & VERSCHOORE, M. (2001) An epidemiological study of acne in female adults: results of a survey conducted in France. *Journal of the European Academy of Dermatology and Venereology* **15**, 541–545.

POTENZIERI, C., BRINK, T.S. & SIMONE, D.A. (2009) Excitation of cutaneous C nociceptors by intraplantar administration of anandamide. *Brain Research* **1268**, 38–47.

POWELL, A.E., WANG, Y., LI, Y., POULIN, E.J., MEANS, A.L., WASHINGTON, M.K., HIGGINBOTHAM, J.N., JUCHHEIM, A., PRASAD, N., LEVY, S.E., GUO, Y., SHYR, Y., ARONOW, B.J., HAIGIS, K.M., FRANKLIN, J.L., ET AL. (2012) The pan-ErbB negative regulator Lrig1 is an intestinal stem cell marker that functions as a tumor suppressor. *Cell* **149**, 146–158.

PROSE, P. (1965) Pathologic changes in eczema. *The Journal of Pediatrics* **66**, 178–199.

PUHVEL, S.M., REISNER, R.M. & SAKAMOTO, M. (1975) Analysis of lipid composition of isolated human sebaceous gland homogenates after incubation with cutaneous bacteria. Thin-layer chromatography. *Journal of Investigative Dermatology* **64**, 406–411.

PÜNCHERA, J., BARNES, L. & KAYA, G. (2016) Lrig1 Expression in Human Sebaceous Gland Tumors.

Dermatopathology **3**, 44–54.

QUIST, S.R., ECKARDT, M., KRIESCHE, A. & GOLLNICK, H.P. (2016) Expression of epidermal stem cell markers in skin and adnexal malignancies. *British Journal of Dermatology* **175**, 520–530.

RADEMAKER, M., GARIOCH, J.J. & SIMPSON, N.B. (1989) Acne in schoolchildren: no longer a concern for dermatologists. *BMJ (Clinical research ed.)* **298**, 1217–1219.

RAY, R., NOVOTNY, N.M., CRISOSTOMO, P.R., LAHM, T., ABARBANELL, A. & MELDRUM, D.R. (2008) Sex steroids and stem cell function. *Molecular Medicine* **14**, 493–501.

REAMS, W.M. (1967) Effects of nerve-growth promoting protein on murine integument. *Journal of Investigative Dermatology* **49**, 552–558.

REICHENBACH, B., CLASSON, J., AIDA, T., TANAKA, K., GENANDER, M. & GÖRITZ, C. (2018) Glutamate transporter Slc1a3 mediates inter-niche stem cell activation during skin growth. *EMBO Journal* **37**, e98280.

RICHERSON, G.B. (2009) The Autonomic Nervous System. In *Medical Physiology* (eds W. BORON & E. BOULPAEP), pp. 351–370, 2nd edition. Elsevier.

RIDDEN, J., FERGUSON, D. & KEALEY, T. (1990) Organ maintenance of human sebaceous glands: in vitro effects of 13-cis retinoic acid and testosterone. *Journal of Cell Science* **95 (Pt 1)**, 125–136.

RISSMANN, R., GROENINK, H.W.W., WEERHEIM, A.M., HOATH, S.B., PONEC, M. & BOUWSTRA, J. A (2006) New insights into ultrastructure, lipid composition and organization of vernix caseosa. *Journal of Investigative Dermatology* **126**, 1823–1833.

RITTIÉ, L., TEJASVI, T., HARMS, P.W., XING, X., NAIR, R.P., GUDJONSSON, J.E., SWINDELL, W.R. & ELDER, J.T. (2016) Sebaceous Gland Atrophy in Psoriasis: An Explanation for Psoriatic Alopecia? *Journal of Investigative Dermatology* **136**, 1792–1800.

ROCHA, M.A. & BAGATIN, E. (2018) Adult-onset acne: prevalence, impact, and management challenges. *Clinical, Cosmetic and Investigational Dermatology* **11**, 59–69.

ROSIGNOLI, C., NICOLAS, J.C., JOMARD, A. & MICHEL, S. (2003) Involvement of the SREBP pathway in the mode of action of androgens in sebaceous glands in vivo. *Experimental Dermatology* **12**, 480–

489.

ROSSITER, H., STÜBIGER, G., GRÖGER, M., KÖNIG, U., GRUBER, F., SUKSEREE, S., MLITZ, V., BUCHBERGER, M., OSKOLKOVA, O., BOCHKOV, V., ECKHART, L. & TSCHACHLER, E. (2018) Inactivation of autophagy leads to changes in sebaceous gland morphology and function. *Experimental Dermatology* **27**, 1142–1151.

RUOCCO, I., CUELLO, A.C., SHIGEMOTO, R. & RIBEIRO-DA-SILVA, A. (2001) Light and electron microscopic study of the distribution of substance P-immunoreactive fibers and neurokinin-1 receptors in the skin of the rat lower lip. *Journal of Comparative Neurology* **432**, 466–480.

RYU, A., ARAKANE, K., KOIDE, C., ARAI, H. & NAGANO, T. (2009) Squalene as a target molecule in skin hyperpigmentation caused by singlet oxygen. *Biological & pharmaceutical bulletin* **32**, 1504–1509.

SAHBAIE, P., SHI, X., GUO, T.-Z., QIAO, Y., YEOMANS, D.C., KINGERY, W.S. & CLARK, D.J. (2009) Role of substance P signaling in enhanced nociceptive sensitization and local cytokine production after incision. *Pain* **145**, 341–349.

SAITOH, M., UZUKA, M. & SAKAMOTO, M. (1970) Human hair cycle. *Journal of Investigative Dermatology* **54**, 65–81.

SAMPATH, H., FLOWERS, M.T., LIU, X., PATON, C.M., SULLIVAN, R., CHU, K., ZHAO, M. & NTAMBI, J.M. (2009) Skin-specific Deletion of Stearoyl-CoA Desaturase-1 Alters Skin Lipid Composition and Protects Mice from High Fat Diet-induced Obesity. *Journal of Biological Chemistry* **284**, 19961–19973.

SARDELLA, C., WINKLER, C., QUIGNODON, L., HARDMAN, J.A., TOFFOLI, B., MARIA, G., ATTIANESE, P.G., HUNDT, J.E., MICHALIK, L., VINSON, C.R., PAUS, R., DESVERGNE, B., GILARDI, F., GIORDANO ATTIANESE, G.M.P., HUNDT, J.E., ET AL. (2017) Delayed Hair Follicle Morphogenesis and Hair Follicle Dystrophy in a Lipoatrophy Mouse Model of Pparg Total Deletion. *Journal of Investigative Dermatology* **138**, 500–510.

SATO, T., IMAI, N., AKIMOTO, N., ITO, A., SAKIGUCHI, T. & KITAMURA, K. (2001) Epidermal Growth Factor and 1α,25-Dihydroxyvitamin D3 Suppress Lipogenesis in Hamster Sebaceous Gland Cells In Vitro. *Journal of Investigative Dermatology* **117**, 965–970.

SAURAT, J.-H. (2015) Strategic Targets in Acne: The Comedone Switch in Question. *Dermatology* **231**, 105–111.

SAXOD, R. (1978) Combination of cholinesterase staining of nerves and stereoscopic viewing for three-dimensional study of skin innervation on whole mounts. *Journal of Investigative Dermatology* **70**, 95–97.

SCHAFER, T., NIENHAUS, A., VIELUF, D., BERGER, J. & RING, J. (2001) Epidemiology of acne in the general population: the risk of smoking. *British Journal of Dermatology* **145**, 100–104.

SCHANK, J.R. & HEILIG, M. (2017) Substance P and the Neurokinin-1 Receptor: The New CRF. *International Review of Neurobiology* **136**, 151–175.

SCHEPELER, T., PAGE, M.E. & JENSEN, K.B. (2014) Heterogeneity and plasticity of epidermal stem cells. *Development* **141**, 2559–2567.

SCHNEIDER, M.R. (2015) Lipid droplets and associated proteins in sebocytes. *Experimental Cell Research* **340**, 205–208.

SCHNEIDER, M.R. & PAUS, R. (2014) Deciphering the functions of the hair follicle infundibulum in skin physiology and disease. *Cell and Tissue Research* **358**, 697–704.

SCHNEIDER, M.R., ZHANG, S. & LI, P. (2016) Lipid droplets and associated proteins in the skin: basic research and clinical perspectives. *Archives of Dermatological Research* **308**, 1–6.

SCHNEIDER, M.R. & ZOUBOULIS, C.C. (2018) Primary sebocytes and sebaceous gland cell lines for studying sebaceous lipogenesis and sebaceous gland diseases. *Experimental Dermatology* **27**, 484–488.

SCHOLZ, C.F.P. & KILIAN, M. (2016) The natural history of cutaneous propionibacteria, and reclassification of selected species within the genus Propionibacterium to the proposed novel genera Acidipropionibacterium gen. nov., Cutibacterium gen. nov. and Pseudopropionibacterium gen. nov. *International Journal of Systematic and Evolutionary Microbiology* **66**, 4422–4432.

SCHULZE, E., WITT, M., FINK, T., HOFER, A. & FUNK, R.H.W. (1997) Immunohistochemical detection of human skin nerve fibers. *Acta Histochemica* **99**, 301–309.

VAN SCOTT, E.J., REINERTSON, R.P. & STEINMULLER, R. (1957) The growing hair roots of the human scalp and morphologic changes therein following amethopterin therapy. *Journal of Investigative Dermatology* **29**, 197–204.

SEGAL, S.S. (2009) Exercise Physiology and Sports Science. In *Medical Physiology* (eds W. BORON & E. BOULPAEP), pp. 1249–1268, 2nd edition. Elsevier.

SEIFERT, P. & SPITZNAS, M. (1996) Immunocytochemical and ultrastructural evaluation of the distribution of nervous tissue and neuropeptides in the meibomian gland. *Graefe's Archive for Clinical and Experimental Ophthalmology* **234**, 648–656.

SHAH, A.R. (2008) Use of intradermal botulinum toxin to reduce sebum production and facial pore size. *Journal of Drugs in Dermatology* **7**, 847–850.

SHI, V.Y., LEO, M., HASSOUN, L., CHAHAL, D.S., MAIBACH, H.I. & SIVAMANI, R.K. (2015) Role of sebaceous glands in inflammatory dermatoses. *Journal of the American Academy of Dermatology* **73**, 856–863.

SHUSTER, S. & THODY, A.J. (1974) The control and measurement of sebum secretion. *Journal of Investigative Dermatology* **62**, 172–190.

SILMAN, I. & SUSSMAN, J.L. (2017) Recent developments in structural studies on acetylcholinesterase. *Journal of Neurochemistry* **142**, 19–25.

SKAPER, S.D. (2012) The Neurotrophin Family of Neurotrophic Factors: An Overview. In *Neurotrophic Factors. Methods in Molecular Biology (Methods and Protocols)* (eds S. SKAPER) pp. 1–12. Humana press.

VAN SMEDEN, J., JANSSENS, M., KAYE, E.C.J., CASPERS, P.J., LAVRIJSEN, A.P., VREEKEN, R.J. & BOUWSTRA, J. A (2014) The importance of free fatty acid chain length for the skin barrier function in atopic eczema patients. *Experimental Dermatology* **23**, 45–52.

SMITH, K.R. & THIBOUTOT, D.M. (2008) Thematic review series: Skin Lipids. Sebaceous gland lipids: friend or foe? *Journal of Lipid Research* **49**, 271–281.

SMITHARD, A., GLAZEBROOK, C. & WILLIAMS, H.C. (2001) Acne prevalence, knowledge about acne and psychological morbidity in mid-adolescence: A community-based study. *British Journal of*

Dermatology **145**, 274–279.

SOMMER, B., OVERY, D.P., HALTLI, B. & KERR, R.G. (2016) Secreted lipases from Malassezia globosa: recombinant expression and determination of their substrate specificities. *Microbiology* **162**, 1069–1079.

SORRELLS, S., TORUNO, C., STEWART, R.A. & JETTE, C. (2013) Analysis of apoptosis in zebrafish embryos by whole-mount immunofluorescence to detect activated caspase 3. *Journal of Visualized Experiments* **82**, e51060.

STÄNDER, S., SCHMELZ, M., METZE, D., LUGER, T. & RUKWIED, R. (2005) Distribution of cannabinoid receptor 1 (CB1) and 2 (CB2) on sensory nerve fibers and adnexal structures in human skin. *Journal of Dermatological Science* **38**, 177–188.

STEINKRAUS, V., MAK, J.C., PICHLMEIER, U., MENSING, H., RING, J. & BARNES, P.J. (1996) Autoradiographic mapping of beta-adrenoceptors in human skin. *Archives of Dermatological Research* **288**, 549–553.

STENN, K.S. (2001) Insights from the asebia mouse: a molecular sebaceous gland defect leading to cicatricial alopecia. *Journal of Cutaneous Pathology* **28**, 445–447.

STOFFEL, W., SCHMIDT-SOLTAU, I., JENKE, B., BINCZEK, E. & HAMMELS, I. (2017) Hair Growth Cycle Is Arrested in SCD1 Deficiency by Impaired Wnt3a-Palmitoleoylation and Retrieved by the Artificial Lipid Barrier. *Journal of Investigative Dermatology* **137**, 1424–1433.

SUDY, E. & URBINA, F. (2018) Unilateral acne after facial palsy. *Anais Brasileiros de Dermatologia* **93**, 441–442.

SUMMERLY, R. & WOODBURY, S. (1971) The in vitro incorporation of 14 C-acetate into the isolated sebaceous glands and appendage-freed epidermis of human skin. A technique for the study of lipid synthesis in the isolated sebaceous gland. *British Journal of Dermatology* **85**, 424–431.

SUMMERLY, R. & WOODBURY, S. (1972) Lipid synthesis (14C-Acetate incorporation) in the isolated human sebaceous gland, the appendage-freed epidermis, the sebocytes (Steatocystoma) and the wen (Keratinous cyst of skin). *British Journal of Dermatology* **86**, 614–620.

SUMMERLY, R., WOODBURY, S. & BODDIE, H.G. (1971) The effect of facial nerve paresis on sebum

production. *British Journal of Dermatology* **84**, 602–604.

SUMMERLY, R., YARDLEY, H.J., RAYMOND, M., TABIOWO, A. & ILDERTON, E. (1976) The lipid composition of sebaceous glands as a reflection of gland size. *British Journal of Dermatology* **94**, 45–53.

SUNDBERG, J.P., BOGGESS, D., SUNDBERG, B.A., EILERTSEN, K., PARIMOO, S., FILIPPI, M. & STENN, K. (2000) Asebia-2J (Scd1ab2J): A New Allele and a Model for Scarring Alopecia. *American Journal of Pathology* **156**, 2067–2075.

SZÁNTÓ, M., OLÁH, A., SZÖLLŐSI, A.G., TÓTH, K.F., PÁYER, E., CZAKÓ, N., PÓR, Á., KOVÁCS, I., ZOUBOULIS, C.C., KEMÉNY, L., BÍRÓ, T. & TÓTH, B.I. (2019) Activation of TRPV3 Inhibits Lipogenesis and Stimulates Production of Inflammatory Mediators in Human Sebocytes-A Putative Contributor to Dry Skin Dermatoses. *Journal of Investigative Dermatology* **139**, 250–253.

TAGAMI, H. (1983) Unilateral steroid acne on the paralyzed side of the face. *The Journal of Dermatology* **10**, 281–282.

TAHA, A.A.M. (1988) Ultrastructure of the sebaceous glands of the camel (Camelus dromedarius). *Journal of Anatomy* **156**, 157–168.

TAKAHASHI, H., TSUJI, H., MINAMI-HORI, M., MIYAUCHI, Y. & IIZUKA, H. (2014) Defective barrier function accompanied by structural changes of psoriatic stratum corneum. *Journal of Dermatology* **41**, 144–148.

TALAGAS, M., LEBONVALLET, N., LESCHIERA, R., MARCORELLES, P. & MISERY, L. (2018) What about physical contacts between epidermal keratinocytes and sensory neurons? *Experimental Dermatology* **27**, 9–13.

TAN, H.H., TAN, A.W.H., BARKHAM, T., YAN, X.Y. & ZHU, M. (2007) Community-based study of acne vulgaris in adolescents in Singapore. *British Journal of Dermatology* **157**, 547–551.

TAN, J.K.L. & BHATE, K. (2015) A global perspective on the epidemiology of acne. *British Journal of Dermatology* **172 Suppl**, 3–12.

TANGHETTI, E.A. (2013) The role of inflammation in the pathology of acne. *The Journal of Clinical and Aesthetic Dermatology* **6**, 27–35.

THAPPA, D.M., ADITYAN, B. & KUMARI, R. (2009) Scoring systems in acne vulgaris. *Indian Journal of Dermatology, Venereology and Leprology* **75**, 323.

THODY, A.J. & SHUSTER, S. (1989) Control and function of sebaceous glands. *Physiological Reviews* **69**, 383–416.

THOMAS, S.E., CONWAY, J., EBLING, F.J. & HARRINGTON, C.I. (1985) Measurement of sebum excretion rate and skin temperature above and below the neurological lesion in paraplegic patients. *British Journal of Dermatology* **112**, 569–573.

TILLES, G. (2014) Acne pathogenesis: History of concepts. *Dermatology* **229**, 1–46.

TÖRŐCSIK, D., KOVÁCS, D., PÓLISKA, S., SZENTKERESZTY-KOVÁCS, Z., LOVÁSZI, M., HEGYI, K., SZEGEDI, A., ZOUBOULIS, C.C. & STÅHLE, M. (2018) Genome wide analysis of TLR1/2- and TLR4-activated SZ95 sebocytes reveals a complex immune-competence and identifies serum amyloid A as a marker for activated sebaceous glands. *PLOS ONE* **13**, e0198323.

TORRE, D. (1968) Multiple sebaceous tumors. *Archives of dermatology* **98**, 549–551.

TÓTH, B.I., GÉCZY, T., GRIGER, Z., DÓZSA, A., SELTMANN, H., KOVÁCS, L., NAGY, L., ZOUBOULIS, C.C., PAUS, R. & BÍRÓ, T. (2009) Transient Receptor Potential Vanilloid-1 Signaling as a Regulator of Human Sebocyte Biology. *Journal of Investigative Dermatology* **129**, 329–339.

TOYODA, M. & MOROHASHI, M. (2001) Pathogenesis of acne. *Medical Electron Microscopy* **34**, 29–40.

TOYODA, M. & MOROHASHI, M. (2003) New aspects in acne inflammation. *Dermatology* **206**, 17–23.

TOYODA, M., NAKAMURA, M., MAKINO, T., KAGOURA, M. & MOROHASHI, M. (2002a) Sebaceous glands in acne patients express high levels of neutral endopeptidase. *Experimental Dermatology* **11**, 241–247.

TOYODA, M., NAKAMURA, M. & MOROHASHI, M. (2002b) Neuropeptides and sebaceous glands. *European Journal of Dermatology* **12**, 422–427.

TRIVEDI, M.K., BOSANAC, S.S., SIVAMANI, R.K. & LARSEN, L.N. (2018) Emerging Therapies for Acne Vulgaris. *American Journal of Clinical Dermatology* **19**, 505–516.

TRIVEDI, N.R., CONG, Z., NELSON, A.M., ALBERT, A.J., ROSAMILIA, L.L., SIVARAJAH, S., GILLILAND,

K.L., LIU, W., MAUGER, D.T., GABBAY, R.A., THIBOUTOT, D.M., ALESTAS, T., GANCEVICIENE, R., FIMMEL, S., MULLER-DECKER, K., ET AL. (2006) Peroxisome proliferator-activated receptors increase human sebum production. *Journal of Investigative Dermatology* **126**, 2002–2009.

VILLAVICENCIO, E.H., WALTERHOUSE, D.O. & IANNACCONE, P.M. (2000) The sonic hedgehog-patched-gli pathway in human development and disease. *American journal of human genetics* **67**, 1047–1054.

VOGEL, C. & MARCOTTE, E.M. (2013) Insights into regulation of protein abundance from proteomics and transcriptomis analyses. *Nature Reviews Genetics* **13**, 227–232.

WANG, Y., POULIN, E.J. & COFFEY, R.J. (2013) LRIG1 is a triple threat: ERBB negative regulator, intestinal stem cell marker and tumour suppressor. *British Journal of Cancer* **108**, 1765–1770.

WARSHAW, T.G. (1973) Thermal Studies in Psoriasis. *Journal of Investigative Dermatology* **60**, 91–93.

WEI, T., GUO, T.-Z., LI, W.-W., HOU, S., KINGERY, W.S. & CLARK, J.D. (2012) Keratinocyte expression of inflammatory mediators plays a crucial role in substance P-induced acute and chronic pain. *Journal of Neuroinflammation* **9**, 676.

WERNER, B., BRENNER, F.M. & BÖER, A. (2008) Histopathologic study of scalp psoriasis: peculiar features including sebaceous gland atrophy. *American Journal of Dermatopathology* **30**, 93–100.

WESSLER, I., KILBINGER, H., BITTINGER, F., UNGER, R. & KIRKPATRICK, C.J. (2003) The non-neuronal cholinergic system in humans: Expression, function and pathophysiology. *Life Sciences* **72**, 2055–2061.

WESSLER, I. & KIRKPATRICK, C.J. (2008) Acetylcholine beyond neurons: the non-neuronal cholinergic system in humans. *British Journal of Pharmacology* **154**, 1558–1571.

WESTERBERG, R., TVRDIK, P., UNDÉN, A.-B., MÅNSSON, J.-E., NORLÉN, L., JAKOBSSON, A., HOLLERAN, W.H., ELIAS, P.M., ASADI, A., FLODBY, P., TOFTGÅRD, R., CAPECCHI, M.R. & JACOBSSON, A. (2004) Role for ELOVL3 and Fatty Acid Chain Length in Development of Hair and Skin Function. *Journal of Biological Chemistry* **279**, 5621–5629.

WHEATLEY (1965) Secretions of the skin in eczema. *The Journal of Pediatrics* **66**, 200–202.

WILLE, J.J. & KYDONIEUS, A. (2003) Palmitoleic Acid Isomer (C16:1Δ6) in Human Skin Sebum Is Effective against Gram-Positive Bacteria. *Skin Pharmacology and Physiology* **16**, 176–187.

WINKELMANN, R.K. & SCHMIT, R.W. (1959) Cholinesterase in the Skin of the Rat, Dog, Cat, Guinea Pig and Rabbit. *Journal of Investigative Dermatology* **33**, 185–190.

WIRTH, H., GLOOR, M. & STOIKA, D. (1981) Sebaceous Glands in Uninvolved Skin of Patients Suffering from Atopic Dermatitis. *Archives of Dermatological Research* **270**, 167–169.

WU, W., WANG, S., XU, Z., WANG, X., FENG, J., SHAN, T. & WANG, Y. (2018) Betaine promotes lipid accumulation in adipogenic-differentiated skeletal muscle cells through ERK/PPARγ signalling pathway. *Molecular and Cellular Biochemistry* **447**, 137–149.

XIAO, Y., THORESEN, D.T., WILLIAMS, J.S., WANG, C., PERNA, J., PETROVA, R. & BROWNELL, I. (2015) Neural Hedgehog signaling maintains stem cell renewal in the sensory touch dome epithelium. *PNAS* **112**, 7195–7200.

XU, Z., WANG, W., JIANG, K., YU, Z., HUANG, H., WANG, F., ZHOU, B. & CHEN, T. (2015) Embryonic attenuated Wnt/β-catenin signaling defines niche location and long-term stem cell fate in hair follicle. *eLife* **4**, e10567.

YAHYA, H. (2009) Acne vulgaris in Nigerian adolescents - Prevalence, severity, beliefs, perceptions, and practices. *International Journal of Dermatology* **48**, 498–505.

YEADON, J. (2014) 6 steps for setting up timed pregnant mice. Https://www.jax.org/news-and-insights/jax-blog/2014/september/six-steps-for-setting-up-timed-pregnant-mice# [accessed 5 February 2020].

YOSEFZON, Y., SOTERIOU, D., FELDMAN, A., KOSTIC, L., KOREN, E., BROWN, S., ANKAWA, R., SEDOV, E., GLASER, F. & FUCHS, Y. (2018) Caspase-3 Regulates YAP-Dependent Cell Proliferation and Organ Size. *Molecular Cell* **70**, 573-587.e4.

YOUN, S.W., NA, J.I., CHOI, S.Y., HUH, C.H. & PARK, K.C. (2005a) Regional and seasonal variations in facial sebum secretions: a proposal for the definition of combination skin type. *Skin Research and Technology* **11**, 189–195.

YOUN, S.W., PARK, E.-S., LEE, D.-H., HUH, C.-H. & PARK, K.-C. (2005b) Does facial sebum excretion

really affect the development of acne? *British Journal of Dermatology* **153**, 919–924.

ZÁKÁNY, N., OLÁH, A., MARKOVICS, A., TAKÁCS, E., ARANYÁSZ, A., NICOLUSSI, S., PISCITELLI, F., ALLARÀ, M., PÓR, Á., KOVÁCS, I., ZOUBOULIS, C.C., GERTSCH, J., DI MARZO, V., BÍRÓ, T. & SZABÓ, T. (2018) Endocannabinoid tone regulates human sebocyte biology. *Journal of Investigative Dermatology* **138**, 1699–1706.

ZEICHNER, J. (2017) Emerging Issues in Adult Female Acne. *Journal of Clinical and Aesthetic Dermatology* **10**, 37–46.

ZHANG, B., MA, S., RACHMIN, I., HE, M., BARAL, P., CHOI, S., GONÇALVES, W.A., SHWARTZ, Y., FAST, E.M., SU, Y., ZON, L.I., REGEV, A., BUENROSTRO, J.D., CUNHA, T.M., CHIU, I.M., ET AL. (2020) Hyperactivation of sympathetic nerves drives depletion of melanocyte stem cells. *Nature* **577**, 1–6.

ZHANG, M., LI, H., CHEN, L., FANG, S., XIE, S. & LIN, C. (2018) Three-dimensional reconstructed eccrine sweat glands with vascularization and cholinergic and adrenergic innervation. *Journal of Molecular Histology* **49**, 339–345.

ZHANG, Y., KAM, W.R., LIU, Y., CHEN, X. & SULLIVAN, D.A. (2017) Influence of Pilocarpine and Timolol on Human Meibomian Gland Epithelial Cells. *Cornea* **36**, 719–724.

ZHAO, H., FENG, J., SEIDEL, K., SHI, S., KLEIN, O., SHARPE, P. & CHAI, Y. (2014) Secretion of shh by a neurovascular bundle niche supports mesenchymal stem cell homeostasis in the adult mouse incisor. *Cell Stem Cell* **14**, 160–173.

ZHENG, J.-L., YU, T.-S., LI, X.-N., FAN, Y.-Y., MA, W.-X., DU, Y., ZHAO, R. & GUAN, D.-W. (2012) Cannabinoid receptor type 2 is time-dependently expressed during skin wound healing in mice. *International Journal of Legal Medicine* **126**, 807–814.

ZHENG, Y., EILERTSEN, K.J., GE, L., ZHANG, L., SUNDBERG, J.P., PROUTY, S.M., STENN, K.S. & PARIMOO, S. (1999) SCD1 is expressed in sebaceous glands and is disrupted in the asebia mouse. *Nature Genetics* **23**, 268–270.

ZHOU, Z., KAWANA, S., AOKI, E., KATAYAMA, M., NAGANO, M. & SUZUKI, H. (2006) Dynamic changes in nerve growth factor and substance P in the murine hair cycle induced by depilation. *Journal of Dermatology* **33**, 833–841.

ZOUBOULIS, C.C. (2017) Further Evidence of Sebaceous Differentiation Uniqueness: Holocrine Secretion of Sebocytes Is a Multistep, Cell-Specific Lysosomal DNase2-Mediated Mode of Programmed Cell Death. *Journal of Investigative Dermatology* **137**, 537–539.

ZOUBOULIS, C.C., JOURDAN, E. & PICARDO, M. (2014) Acne is an inflammatory disease and alterations of sebum composition initiate acne lesions. *Journal of the European Academy of Dermatology and Venereology* **28**, 527–532.